ESTUDIO DE LA BIODISPONIBILIDAD Y ALTERACIONES METABÓLICAS Y DEL ESTADO OXIDATIVO OCASIONADAS POR LA EXPOSICIÓN A NANOPARTÍCULAS DE ORO

TESIS DOCTORAL

Carlos López Chaves

UNIVERSIDAD DE GRANADA

DEPARTAMENTO DE FISIOLOGÍA

GRANADA, 2018

El doctorando / The *doctoral candidate* [**Carlos López Chaves**] y los directores de la tesis / and the thesis supervisor/s: [**Cristina Sánchez González y Jörg Bettmer**]

Garantizamos, al firmar esta tesis doctoral, que el trabajo ha sido realizado por el doctorando bajo la dirección de los directores de la tesis y hasta donde nuestro conocimiento alcanza, en la realización del trabajo, se han respetado los derechos de otros autores a ser citados, cuando se han utilizado sus resultados o publicaciones.

/

Guarantee, by signing this doctoral thesis, that the work has been done by the doctoral candidate under the direction of the thesis supervisor/s and, as far as our knowledge reaches, in the performance of the work, the rights of other authors to be cited (when their results or publications have been used) have been respected.

Lugar y fecha / Place and date:

Director/es de la Tesis / *Thesis supervisor/s;*   Doctorando / *Doctoral candidate:*

Firma / Signed   Firma / Signed

Oviedo, 26 de Enero de 2018   Granada, 01 Febrero 2018

JÖRG BETTMER   CARLOS LÓPEZ CHAVES

Granada, 01 de Febrero de 2018

CRISTINA SANCHEZ GONZALEZ

La inmortalidad reside en emparentar con la Sabiduría (Sb 8, 17)

INDEX

SUMMARY

INTRODUCTION

The use of nanomaterials (natural, incidental or manufactured material containing particles, in an unbound state or as an aggregate or as an agglomerate and where, for 50 % or more of the particles in the number size distribution, one or more external dimensions is in the size range 1 nm - 100 nm), has exponentially increased last decades thanks to their unique physicochemical properties such as large surface area, size, shape, charge…Thus, nanotechnology (defined as the design, synthesis and application of materials and devices whose size and shape have been engineered at the nanoscale), is recognized as one of the most emerging field in science. In this sense, the development of products with nanomaterials reaches almost every area. For example, electronics, textiles, cosmetics or materials have been made with nanocomponents that allow them to storage data in smaller spaces, repel oil and/or water, absorb ultraviolet light or increase materials resistance, to name some of them. Among them, biomedicine has enormously benefited from nanomaterials. Imaging techniques such as magnetic resonance imaging, computed tomography or positron emission tomography; sensing systems like photoluminescence or sensing based on localized surface plasmon resonance have vastly improved due to the use of nanomaterials. Furthermore, nanotechnology in biomedicine has allowed to develop new therapies in the treatment of multiple diseases such as cancer, diabetes, Parkinson, etc.

In addition to the main properties of nanomaterials previously described, Au has a diversity of inherent attributes that makes its nanostructures an attractive platform for several purposes, including biomedical applications: resistance against oxidation and corrosion, bioinert nature, good range of coordination, etc.

Nevertheless, despite the huge potential benefit of nanomaterials in the biomedical and industrial applications, nanotoxicology was developed in order to give answer to the increased interest in studying the possible deleterious effects of the nanostructures in biological systems and how these effects might be mitigated.

AIMS

The main aim of the present doctoral thesis will be to address the study of the metabolic alterations derived from the exposure to gold nanoparticles, as well as their biodistribution and repercussion on the oxidative status.

MATERIALS & METHODS

Citrate-stabilised gold nanoparticles with 10, 30 or 60 nm of diameter size suspended in ultrapure water at 50 mg·L^{-1} were used in our *in vitro* and *in vivo* studies.

In vitro: Hepatocellular carcinoma (Hep G2) and colorectar carcinoma (HT-29) cell lines were exposed to 10 µg·kg^{-1} or 10 mg·kg^{-1} of gold nanoparticles for 16 or 32 h to determine the cell viability and ROS production. Furthermore, DNA breaks were determined by Comet Assay after exposing Hep G2 cells to 10 mg·kg^{-1} AuNPs for 16 h. HT-29 cells were employed to conduct a longitudinal study to determine the intracellular location of the nanomaterials by TEM. These cells were treated with 10 mg·kg^{-1} AuNPs for 2, 4 or 16 h.

In vivo: male Wistar rats weighing 190-220 g were divided into four groups: Control group: eight rats were injected 0.4 mL ultrapure water·day^{-1}. AuC 10 group: eight rats were injected 0.4 mL·day^{-1} 10 nm size gold nanoparticles solution. AuC 30 group: eight rats were injected 0.4 mL·day^{-1} 30 nm size gold nanoparticles solution. AuC 60 group: eight rats were injected 0.4 mL·day^{-1} 60 nm size gold nanoparticles solution. In all cases, the administration route was intraperitoneal. On day 9, rats were sacrificed and blood was collected for quantification of blood parameters and subsequently centrifuged to separate the serum. The liver, kidney, spleen, brain, lung, testicle, femur, heart, intestine and gastrocnemius muscle were removed in order to determine their gold content by ICP-MS. Liver were also used to assess the lipid peroxidation and protein carbonylation (by measuring the TBARS and protein carbonyl groups), as well as the inflammatory status (after quantifying the levels of TNF-α, IL-1ß, IL-6 and IL-10) and the intracellular location of the gold nanoparticles (by TEM). Some biochemical parameters like glucose, urea, uric acid, triglycerides, albumin, cholesterol, gamma glutamyl transpeptidase, alkaline phosphatase, glutamic oxaloacetic transaminase and glutamic pyruvic transaminase were determined in serum.

RESULTS & DISCUSSION

In vitro: There was a proportional decrease in cell viability as ROS production increase. This relation also showed a dose and time-dependency, thus showing greater damage at 16 h and 10 mg·kg^{-1}. In our opinion, cells managed to control the ROS overproduction after 32 h of exposure, probably by means of the increase in the antioxidant activity, thus restoring the cell viability index.

Furthermore, the study of the comet assay proved that AuNPs induce DNA breaks in a size-dependent manner. In fact, 10 nm gold nanoparticles provoked damage similar to the positive control cells, while 60 nm AuNPs did not affect the integrity of the DNA. Taking into account that the effective diameter of the nucleus pore is around 35 nm, it is probable that the 10 and 30 nm nanoparticles were able to cross the nucleus membrane, thus favouring the DNA breaks by the ROS overproduction. This fact was lately confirmed by the TEM images, which revealed the presence of gold nanoparticles in the nucleus of the cells exposed to 10 nm AuNPs after 16 h. Additionally, the localization of the AuNPs inside the cell changed along time. The nanostructures were mainly found as individual particles throughout the cytosol after 2 and 4 h; while most of them were gradually digested and accumulated in lipid drops after 16 h; probably in an attempt to neutralise and reduce their toxicity inside the cell.

In vivo: In concordance with what was found in cells, the exposure to gold nanoparticles caused damage in the lipid and protein components. These results indicate the increased production of free radicals in this organ, which became concomitant with the increased production of TBARS and protein carbonyl groups. The fact that lipids and proteins are not only placed in a barrier-restricted area may explain the absence of differences among exposed rats regarding the toxic effects on these components.

The study of the gold concentration in the different organs, showed an unequal distribution. Liver, kidney and intestine show the same pattern, where 10 and 30 nm AuNPs seem to accumulate more than 60 nm AuNPs; that mostly accumulates in spleen. In our view, biggest nanoparticles are eliminated from the blood by the reticuloendothelial system and thus accumulated in the spleen and liver, as their size is larger than the renal filtration cut off, which blocks the urine to be the excretion route.

Similarly, the high levels of gold in intestine of rats treated with 10 and 30 nm, together with the increase in gold concentration measured in faeces, and taking into account that the administration route of the nanoparticles was intraperitoneal, probes that faecal is the main endogenous route of elimination of the smallest nanoparticles. Other organs like muscle, heart or bone also seem to be important storage tissues, although in a lesser extent.

Interestingly, the administration of AuNPs affected the function of the bone marrow, in light of the decreased levels of mean corpuscular haemoglobin, mean corpuscular haemoglobin concentration and haematocrit; which definitely defines an incipient anaemia.

Regarding the biochemical and inflammatory parameters, no changes were observed among groups. In our view, although the exposure to gold nanoparticles induces an increase in the ROS production that affects the integrity of the cellular components and provokes an initial anaemia, it is insufficient to trigger an inflammatory or biochemical response.

CONCLUSIONS

The obtained results led us to conclude that the size of the nanoparticles determine differences in their metabolic fate and in the formation of deposits in the different biological systems. The size of the nanoparticles also determines their excretion route, being the main via of elimination of the nanoparticles with the highest diameter the reticuloendothelial system of the spleen, and the intestinal endogenous via the main route of excretion of the nanoparticles with the smallest size. Furthermore, we have proved that gold nanoparticles provoke an imbalance in the oxidative status of the cells, which is accompanied by damage in the genetic, lipid and protein structures. These alterations presented a clear size-dependence, as the 10 nm AuNPs showed more injurious effects, detected by their nuclear location and their higher DNA damage. The exposure to gold nanoparticles also affected the normal function of the bone marrow and an incipient anaemic state was observed. In spite of these oxidative induced deleterious structural effects, it was not found alterations on the inflammatory status nor tissue damage after this short period of exposure to AuNPs.

RESUMEN

INTRODUCCIÓN

El uso de nanomateriales (material natural o manufacturado que contiene partículas individuales o en estado de agregación o aglomeración, y donde al menos el 50% de las nanopartículas presentan una o más dimensiones en el rango de 1 a 100 nm), ha crecido exponencialmente en las últimas décadas gracias a sus propiedades fisicoquímicas únicas tales como gran área superficial, tamaño, forma o carga. Así, la nanotecnología (definida como el diseño, síntesis y aplicación de materiales y dispositivos cuyo tamaño y forma ha sido diseñado en la nanoescala), es reconocido como uno de los campos más emergentes en el ámbito científico. En este sentido, el desarrollo de productos con nanomateriales alcanza casi todos los áreas. Por ejemplo, productos electrónicos, textiles, cosméticos o diferentes materiales de construcción han sido diseñados con nanocomponentes que les permiten almacenar información en espacios más pequeños, repeler aceite o agua, absorber luz ultravioleta o aumentar su resistencia.

Entre las distintas áreas, la biomedicina se ha beneficiado enormemente de estos nanomateriales. Como referencia, técnicas de imagen como la resonancia magnética, tomografía computerizada o tomografía de emisión de positrones; sistemas de detección como la fotoluminiscencia o la resonancia de plasmón superficial han mejorado considerablemente debido al uso de nanomateriales. Además, la nanotecnología en biomedicina ha permitido desarrollar novedosas terapias en el tratamiento de diferentes patologías como el cáncer, la diabetes o el Parkinson.

Junto con las principales propiedades de los nanomateriales previamente descritas, el oro posee una serie de atributos inherentes que hacen de sus nanoestructuras una plataforma atractiva para diversos ámbitos, incluyendo las aplicaciones biomédicas: resistencia contra la oxidación y corrosión, toxicidad más baja, buen rango de coordinación, etc.

No obstante, y pese a los amplios beneficios de los nanomateriales en biomedicina e industria, la nanotoxicología ha nacido como un nuevo campo de estudio en un intento de dar respuesta al interés de conocer los posibles efectos secundarios que las

11

nanoestructuras pueden ocasionar en los sistemas biológicos y cómo esos efectos podrían ser mitigados.

OBJETIVOS

El principal objetivo de la presente tesis doctoral será estudiar las alteraciones metabólicas derivadas de la exposición a nanopartículas de oro, así como su biodistribución y repercusión en el estado oxidativo.

MATERIALES & MÉTODOS

Para los estudios *in vitro* e *in* vivo se utilizaron nanopartículas de oro estabilizadas con citrato de 10, 30 y 60 nm; suspendidas en agua ultrapura en una concentración de 50 $mg·L^{-1}$.

In vitro: para los estudios con células, se emplearon las líneas de carcinoma hepatocelular (Hep G2) y carcinoma colorectal (HT-29). Éstas fueron expuestas a las nanopartículas en concentraciones de 10 $\mu g·kg^{-1}$ o 10 $mg·kg^{-1}$ durante 16 o 32 horas para determinar la viabilidad celular y la producción de especies reactivas de oxígeno. Además, se empleó el ensayo del cometa para evaluar las posibles roturas en ADN. Para ello se trataron los células Hep G2 con 10 $mg·kg^{-1}$ de nanopartículas de oro durante 16 horas.

Finalmente, la línea celular HT-29 fue utilizada para llevar a cabo un estudio longitudinal que determinase la localización intracelular de estos nanomateriales mediante microscopía electrónica de transmisión. Estas células fueron tratadas con 10 $mg·kg^{-1}$ de dichas nanopartículas durante 2, 4 o 16 horas.

In vivo: ratas macho Wistar con un peso inicial de 190-220 g fueron divididas en 4 grupos: Grupo control: ocho ratas que fueron inyectadas con 0.4 mL de agua ultrapura por día. Grupo AuC 10: ocho ratas que fueron inyectadas con 0.4 mL de nanopartículas de 10 nm por día. Grupo AuC 30: ocho ratas que fueron inyectadas con 0.4 mL de nanopartículas de 30 nm por día. Grupo AuC 60: ocho ratas que fueron inyectadas con 0.4 mL de nanopartículas de 60 nm por día. En todos los casos, la administración fue intraperitoneal. El día 9, los animales fueron sacrificados y la sangre fue recogida para determinar los diferentes parámetros hematológicos y posteriormente centrifugada para separar el suero. El hígado, riñón, bazo, encéfalo, pulmones, testículos, fémur,

corazón, intestino y músculo gastronemio se extrajeron para determinar el contenido en oro mediante ICP-MS. El hígado también se empleó para evaluar la peroxidación lipídica y la carbonilación proteica (mediante la medición de los niveles de TBARS y de los grupos carbonilo); así como el estado inflamatorio (tras cuantificar los valores de TNF-α, IL-1ß, IL-6 e IL-10) y la localización intracelular de las nanopartículas mediante TEM. Finalmente, se determinaron algunos parámetros bioquímicos en suero como glucosa, urea, ácido úrico, triglicéridos, albúmina, colesterol, gamma glutamil transpeptidasa, fosfatasa alcalina, GOT y GPT.

RESULTADOS & DISCUSIÓN

In vitro: Se observó un descenso proporcional en la viabilidad celular a medida que la producción en ROS aumentaba. Estos parámetros mostraron una relación dosis y tiempo dependiente, exhibiendo mayor daño a 16 horas y con una dosis de nanopartículas de 10 mg·kg^{-1}. En nuestra opinión, las células son capaces de controlar la sobreproducción de ROS tras 32 horas de exposición, probablemente gracias al incremento en la actividad antioxidante; lo que permite restaurar el índice de viabilidad celular.

Además, el estudio del ensayo del cometa probó que las nanopartículas de oro inducen roturas en el ADN de una manera tamaño dependiente. De hecho, las nanopartículas de 10 nm provocaron un daño similar al encontrado en las células control positivas; mientras que las nanopartículas de 60 nm no afectaron a la integridad del DNA. Teniendo en cuenta que el diámetro efectivo del poro del núcleo es alrededor de 35 nm, es probable que las nanopartículas de 10 y 30 nm pudieron acceder al núcleo, favoreciendo por tanto las roturas de DNA mediante la producción de ROS. Este hecho fue posteriormente confirmado mediante las imágenes de TEM, que revelaron la presencia de nanopartículas de oro de 10 nm en el núcleo tras 16 horas de exposición. Adicionalmente, este estudio longitudinal demostró la variación de la localización celular de estos nanomateriales a lo largo del tiempo. De hecho, las nanoestructuras fueron encontradas principalmente como partículas individuales por el citosol tras 2 y 4 horas; mientras que la mayoría de ellas fueron gradualmente digeridas y almacenadas en el interior de gotas lipídicas; probablemente en un intento de neutralizar y reducir su toxicidad en el interior celular.

In vivo: en concordancia con lo establecido en los cultivos celulares, la exposición a nanopartículas de oro provocó un daño en los componentes lipídicos y proteicos celulares, como atestiguan los incrementos en los niveles de TBARS y grupos carbonilo. El hecho de que los lípidos y proteínas no se encuentran en una zona restringida mediante una membrana dentro de la célula, podría explicar la ausencia de diferencias significativas entre las ratas tratadas.

El estudio de la concentración de oro en los diferentes órganos, mostró una distribución desigual. El hígado, riñón e intestino presentan el mismo patrón, donde las nanopartículas de 10 y 30 nm se acumularon en mayor medida que las de 60 nm, que tendieron a almacenarse en bazo. En nuestra opinión, las nanopartículas más grandes fueron rápidamente eliminadas de la sangre mediante el sistema reticuloendotelial y así se acumularon en hígado y bazo. Dado que su diámetro es mayor al necesario para poder filtrarse mediante el riñón, su excreción mediante la orina fue bloqueada, como acreditan los bajos niveles de oro en orina. En este sentido, los elevados valores de concentración de oro en intestino de las nanopartículas de 10 y 30 nm, junto con el incremento en el contenido de este elemento en heces; y teniendo en cuenta que la vía de administración fue intraperitoneal (no enteral), consideramos que la principal ruta de eliminación endógena de las nanopartículas más pequeñas es la fecal. Otros órganos como el músculo, corazón o hueso también parecen ser importantes órganos de almacenamiento de estos nanocompuestos, aunque en menor medida a tenor de las concentraciones de oro encontradas en estos tejidos.

La administración de las nanopartículas afectó la correcta función de la médula ósea, como demuestran los valores bajos de hemoglobina corpuscular media, concentración media de hemoglobina corpuscular y hematocrito; lo que definitivamente define una anemia incipiente.

En relación con los parámetros bioquímicos e inflamatorios, no se observaron cambios significativos entre los diferentes grupos. Bajo nuestro punto de vista, si bien la exposición a nanopartículas de oro induce un incremento en la producción de ROS que afecta a la integridad de los componentes celulares y provoca una anemia inicial, estos daños fueron insuficientes para disparar una respuesta inflamatoria o bioquímica.

CONCLUSIONES

Los resultados obtenidos nos permiten concluir que el tamaño de las nanopartículas determina sus destinos metabólicos y la formación de depósitos en los diferentes sistemas biológicos. El diámetro de las nanopartículas también determina su ruta de eliminación, siendo la principal vía de eliminación de las nanopartículas más grandes el sistema reticuloendotelial del bazo, y la vía endógena intestinal la principal ruta de excreción de las nanoestructuras con menor tamaño. Además, hemos probado que las nanopartículas de oro provocan un desequilibrio en el estado oxidativo de las células, lo que consecuentemente causa un daño en las estructuras proteicas, lipídicas y genéticas. Estas alteraciones presentaron una clara dependencia del tamaño, ya que las nanopartículas de 10 nm mostraron mayores daños, detectados por su localización nuclear y su mayores roturas de ADN. El tratamiento con nanopartículas de oro también afectó la función normal de la médula ósea y se observó una anemia incipiente. A pesar de estos efectos dañinos, no se alteró el estado inflamatorio ni se determinaron daños tisulares tras este periodo de exposición.

1. INTRODUCTION

INTRODUCTION

Nanomaterials have been defined by the European Union as a natural, incidental or manufactured material containing particles, in an unbound state or as an aggregate or as an agglomerate and where, for 50 % or more of the particles in the number size distribution, one or more external dimensions is in the size range 1 nm - 100 nm.[1] Although initially the upper size was stablished in 1000 nm, the fact that some physical properties of nanoparticles approach those of the bulk when their size reaches 100 nm finally justified the choice of this upper limit. Taking into account that the nanometer denotes one-billionth of a meter (10^{-9} m), comparing a nanometer to a meter could be equivalent to comparing the size of a marble to the size of the Earth.

Figure 1. Graphic comparison of the nanoparticles size

As a result of the use of these materials in the nanometer scale, a new field has emerged during last decades: Nanotechnology. It can be defined as the design, synthesis and application of materials and devices whose size and shape have been engineered at the nanoscale. Their reduced size offers some new physical and chemical properties in terms of conductivity, heat transfer, fusion temperature, electronic, magnetic and optical properties, etc. which are different in a larger scale. In this sense, nanotechnology offers benefits for the industrial and energy sectors, as we will discuss later. To name some practical examples, nanoscale coatings can be used for weather proofing, thus increasing durability and cleaning. Nanomaterials can also be used to create coatings that prevent corrosion and withstand high heat, enhancing the durability of the infrastructure of nuclear power plants. Nanotechnology can also

be applied to the production of photovoltaic cells used for solar power devices and to improve turbines used employed in wind energy sources.

It is often believed that nanomaterials have been created during last decades and they are completely man-made. Nevertheless, natural nanomaterials existed in the environment long before the nanotechnology era started. In fact, they are present as volcanic ashes, marine aerosols, fine sand, virus, etc. Moreover, mankind has been working with nanoparticles for several centuries without being aware of it. Actually, gold, copper and silver nanoparticles were used during the Middle Age to obtain different colours (from yellow to red) when painting the stained glasses in churches and cathedrals. Furthermore, there are evidences of the use of these nanoparticles as element to paint in the antique Egypt and the Roman Empire.[2,3]

Figure 2. Licurgo cup and gothic stained glass, both of them decorated with nanoparticles

Despite the presence of nanoparticles in nature and their use since centuries ago, it is true that the human exposure has noticeably increased due to the use of nanotechnology in a variety of products in recent years. The current insecurity is that it is mainly unknown whether nanoparticles present any risks to the environment and human health. As more and more common household products contain nanomaterials,[4] public exposure to products based on nanotechnology is rapidly increasing. In fact, most consumers are unaware or unconcerned that many common

products they use contain nanoscale materials, including food, sunscreen, hair straighteners, clothing, computer hardware, bicycles, wound dressings, air sanitizing spray, health supplements, bricks, toothpaste, baby products or automotive lubricants among others. Thus, nanotoxicology is an emerging area of study that explores the effects of nanoparticles within the body. Nanoparticles can enter the human body through several types of exposure, including ingestion, inhalation, injection, and skin absorption; therefore, this increasing human exposure indicates an urgent need for risk assessment.

1.1 NANOMATERIALS

1.1.1 NANOMATERIALS PROPERTIES

As previously described, the use of nanomaterials has exponentially increased during last years due to their unique properties, among which highlight their optical and physico-chemical properties.

1.1.1.1 Optical properties

Some metallic nanoparticles, like silver or gold nanoparticles, show a phenomenon that is commonly known as **localized surface plasmon resonance (LSPR)**. Basically, when light impinges on a nanoparticle, the free electrons of the metal will immediately sense the electromagnetic field and begin to oscillate collectively relative to the lattice of positive ions at the same frequency as the incident light.
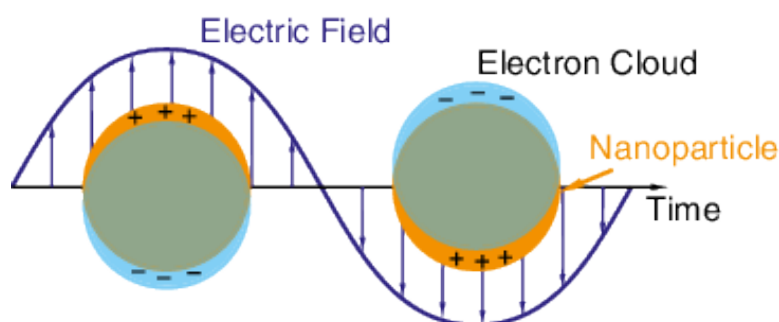
Figure 3. Representation of the localized surface plasmon effect

This phenomenon may occur in any nanomaterial with an adequately high density of free electrons[5–8]. Thus, surface resonance is highly dependent on the nanoparticle size. For instance, gold nanoparticles modify their LSPR between 405 and 516 nm, which cause a change in their colour (from red to purple and to black) when modifying the size. In general, this process can be divided into two types of light-matter interactions: scattering, in which the incident light is re-radiated at the same frequency but into all directions, and absorption, in which the light is converted to heat. Together, these two processes lead to extinction or attenuation in intensity for the incident light. In addition, strong electric fields are generated on the surface of the nanostructure, which can be used to greatly enhance the optical signals. These light–matter interactions can be harnessed to develop new probes or tools for biomedical applications[9].

Some materials show size-dependent electronic properties when reduced to nanoscale. The electronic conduction band in a spherical semiconductor material is inversely related to its mass and radius. Furthermore, the confinement of the electrons in quantum dots in all three spatial directions results in a quantized energy spectrum. For instance, quantum dots are 1-100 nm size (usually 2 nm to 10 nm) nanoparticles with wide absorption bands, narrow emission bands and fluorescence times longer than organic molecules. Thus, these materials have been employed as biosensors or nucleic acids detectors.

Another result of **quantum confinement** effect is the appearance of magnetic moments in nanoparticles of materials that are nonmagnetic in bulk, such as gold, platinum, or palladium.

TiO_2/SiO_2 nanocrystals (also known as Bragg Stacks) are sensitive to changes in temperature and humidity. Consequently, the thickness of the stacks can be modified, thus revealing different reflection bands across the visible spectrum[10].

Therefore, these materials are applied as sensors for trace amounts of solvent vapour or as observable drug-delivery systems.

Other nanomaterials (such as TiO_2 or ZnO nanoparticles) are able to absorb ultraviolet light, which makes them suitable for sunscreen creams or plastics. [11]

1.1.1.2 Physico-chemical properties

Compared to microparticles, nanoparticles have a very large **surface area** and high particle number per unit mass. For illustration, one carbon microparticle with a diameter of 60 μm has a mass of 0.3 μg and a surface area of 0.01 mm^2. The same mass of carbon in nanoparticulate form, with each particle having a diameter of 60 nm, has a surface area of 11.3 mm^2 and consists of 1×10^9 nanoparticles. As the material in nanoparticulate form presents a much larger surface area for chemical reactions, reactivity is enhanced roughly 1000-fold.

The atoms situated at the surface have less neighbours than bulk atoms, resulting in lower binding energy per atom with decreasing particle size. A consequence of reduced binding energy per atom is a melting point reduction with particle radius. For example, the melting temperature of 3 nm gold nanoparticles is more than 300 degrees lower than the melting temperature of bulk gold.

In this sense, it has been proven that **size** is also a critical parameter regarding the uptake, toxicity, bioaccumulation or route of elimination of the nanomaterials. For example, after exposing human pulmonary fibroblasts to two different silver nanoparticles, Ávalos et al. observed that 4.7 nm Ag nanoparticles were much more toxic than those with 42 nm.[12] Analogously, Öberdorster et al. demonstrated that 20 nm nanoparticles of titanium dioxide were characterized by longer retention time in the lungs and increased translocation to interstitial sites than larger nanoparticles (250 nm) of the same material, after 12 weeks of exposure[13]

In addition to size, the **shape** of these nanostructures is also a key feature. These materials can be presented as spheres, fibres, discs, squares, triangles, helices, belts, etc. Size has an important implication at biological level. In this way, the effect of the nanomaterials shape on toxicity has been extensively studied. Grabinski et al.

investigated the cellular effects of different carbon-based materials using mouse keratinocytes [14] They concluded that carbon nanofibers did not significantly affect cell viability; whereas carbon nanotubes (CNTs) reduced cell viability in a time-dependent manner. Similarly, Zhang et al. conducted a study comparing toxicity of graphene and carbon nanotubes[15]. They concluded that graphene induced a stronger metabolic activity than that of carbon nanotubes at low concentrations, indicating the effect of shape on cellular toxicity.

Therefore, shape can interfere in the optical properties of the nanoparticles, thus affecting their LSPR. This fact was observed by Haes et al., who assessed the variation on absorption band of silver nanoparticles when varying from spheres to pyramid or prism[16]

Regarding the nanostructures surface, its **charge** is an important feature. It is a major determinant of colloidal behaviour, which influences the organism response by changing the shape and size of nanoparticles through aggregate or agglomerate formation. Therefore, it influences the internalization to cells throughout the membranes. Generally, it depends on its functionalization (for example, ligands on the surface of metallic nanoparticles) and the pH. In this sense, it is widely accepted that those nanoparticles with positive charge show a higher toxicity than those negatively charged, probably because of their higher internalization. [17–19] For example, Shahbazi et al. assess the impact of silicon nanoparticles surface chemistry on immune cells.[20] It was concluded that negatively charged hydrophilic and hydrophobic silicon nanoparticles caused less genotoxicity than those with positive charge. An additional interesting study developed by Calatayud et al. proved that the functional groups on iron nanoparticles surface determined the formation of protein-magnetic nanoparticles cluster.[21]

Another change in nanomaterials when comparing with bulk form is their higher **reactivity**. For example, metallic gold is thought to be inert. However, gold nanoparticles show higher chemical reactivity, being able to create covalent bonds with organic substances, proteins and several biomolecules.

INTRODUCTION

1.1.2 NANOMATERIALS CLASSIFICATION

To better comprehend the properties and possible applications of the nanostructures, several classifications have been proposed regarding different parameters such as their origin, morphology, composition, etc.

1.1.2.1 Dimensionality

It is useful to classify the nanomaterials based on their number of dimensions:

One-dimensional nanomaterials: materials with one dimension in the nanometer scale are typically thin films or surface coatings (commonly known as monolayers). They have been used in electronic, chemistry and engineering for decades. They are a useful tool as biochemical sensors, optic fibre or solar panels.[22]

Two-dimensional nanomaterials: these structures present two dimensions in the nanometer scale. These include 2D nanostructured films or free particles with a large aspect ratio. Among these nanomaterials, carbon nanotubes are extensively used. They are made of a hexagonal net of carbon atoms that is wrapped as a cylinder. Single-walled carbon nanotubes (SWCNT) are arranged as a single net, while multi-walled carbon nanotube (MWCNT) have several walls.
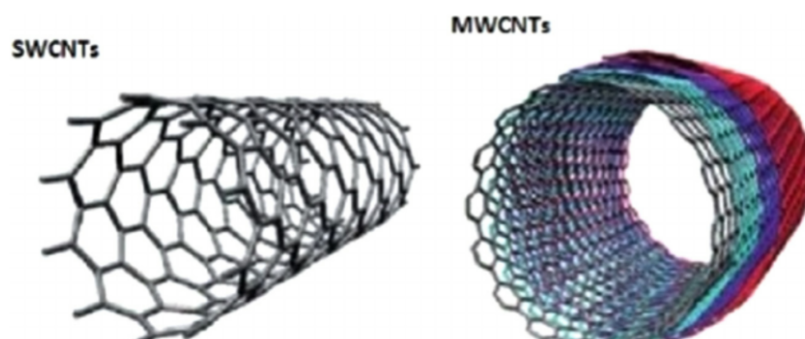
Figure 4. Graphic representations of Single-walled carbon nanotubes (SWCNTs) and Multi-walled carbon nanotubes (MWCNTs)

Thus, carbon nanotubes are promising alternatives to conventional doped

semiconductor crystals due to their varied electronic properties, ranging from metallic, to semiconducting and superconducting. Furthermore, carbon nanotubes are known for being extremely lightweight and enormously strong, having the highest tensile strength of any material tested. This is the reason why they are used in sport products as trainers, racquets, golf clubs and they are increasingly employed in electronic applications such as lithium batteries or smartphones and in biomedical research to enhance water filtration systems or in cancer therapies[11,23]

Three-dimensional nanomaterials: materials that are nanoscaled in all three dimensions are considered 3D nanomaterials. These include thin films, colloids and free nanoparticles with various morphologies.

1.1.2.2 Morphology

There are multiple morphological characteristics that can be taken into account in order to classify nanomaterials. Among them, aspect ratio, sphericity or flatness are classically employed. A general classification exists between high- and low-aspect-ratio particles. Consequently, high-aspect-ratio nanoparticles include nanotubes and nanowires, with various shapes, such as helices, zigzags, belts, etc. Low-aspect-ratio morphologies include spherical, cubic, helical or cubic.

Au nanostructures	Schematic drawing	LSPR peak positions	Size range
Clusters			<2 nm
Conventional particles		520–650 nm	1.5–180 nm
Spheres		520–650 nm	5–150 nm
Rods		600–1800 nm, for the longitudinal mode	20 nm to several µm
Plates, prisms, and disks		700–1300 nm, for the in-plane mode	40–1000 nm (edge length) and 5–50 nm (thickness)
Shells		520–900 nm	10–400 nm
Boxes, cages, frames, and related hollow structures		400–1200 nm	20–200 nm (edge length)
Polyhedra		560–1000 nm	20–270 nm
Structures with branched arms		550–800 nm	45–300 nm

Figure 5. Shapes and features of different nanostructures

1.1.2.3 Composition

Nanoparticles can be composed of a single constituent material or be a composite of several materials. Thus, natural nanostructures are often agglomerations of materials with multiple compositions, whereas nanotechnology offers the possibility to synthetize pure single-composition materials.

Organic nanoparticles: even though many organic nanoparticles exist, here we will talk about those with special significance. These nanomaterials are mainly composed by carbon atoms; and their properties vary depending on the shape they have. Among them, fullerenes are the most important ones. They are shaped as spherical capsules with several hundreds of carbon atoms. They have been widely studied due to their photochemical characteristics or their physical and electrochemical properties. They can be exposed to extreme pressure and recover their original shape once the pressure has ceased. This is one of the properties why they have been used as organic solar cells.[24] The fact that the size of certain fullerenes is similar to some biomolecules and that they can penetrate the skin has led researchers to use them as drug delivery

systems or sunscreens.[23,25]

Liposomes are also spherical organic nanoparticles composed by a lipid bilayer, acting as vesicles. Their amphiphilic nature together with their biocompatibility and stability, allow them to encapsulate medicines, genes or other active molecules and act as drug carriers.[26–28]

Inorganic nanoparticles: there is a huge variety of inorganic nanoparticles with different properties. In consequence, their possible applications are multiple. Here, we will discuss about the most representative ones, those that have been widely used in industry and research.

Quantum dots: semiconducting inorganic nanoparticles generally composed by sulphur, selenide and telluride of zinc, cadmium, lead or mercury with sizes from 2 to 10 nm. As previously described, the quantic confinement confers electric properties to these nanoparticles that imply wide absorption bands, narrow emission bands, high photo-stability, strong resistance to chemical degradation and long fluorescence times. Thus, by modifying sizes and chemical composition of the quantum dots, we will modulate the emission energy, ranging from ultraviolet to infrared region. Therefore, a single wavelength can excite various quantum dots with different emission bands. Hence, their main applications are focused on immunoassays as luminescent markers or bioimaging.

Metal nanoparticles: Metallic NPs with a core made of Ag, Cu, Pt or Au. The positively charged ions on the surface of the nucleus allow them to be joined to organic molecules such as PEG, thiols or citrate by covalent bonds. They are widely used in biomedicine due to their antimicrobial and antitumor properties.

Non-metal and metal oxide nanoparticles: these structures are generally made with oxides of cerium (CeO_2), silicon (SiO_2), titanium (TiO_2), iron (Fe_xO_x) or zinc (ZnO). Their use varies from additives to drugs, cosmetics, food or biosensors.

1.1.2.4 Uniformity and agglomeration state

Based on their chemistry and electromagnetic properties, nanoparticles can exist as suspensions, colloids, as agglomerate or aggregate, or as dispersed aerosols. Thus, magnetic nanoparticles tend to cluster. That is the reason why most engineered magnetic nanoparticles are usually coated with nonmagnetic materials. The properties of these nanomaterials may change depending on the agglomeration state. In fact, nanoparticles tend to behave as larger particles as the size of the agglomerate increases.
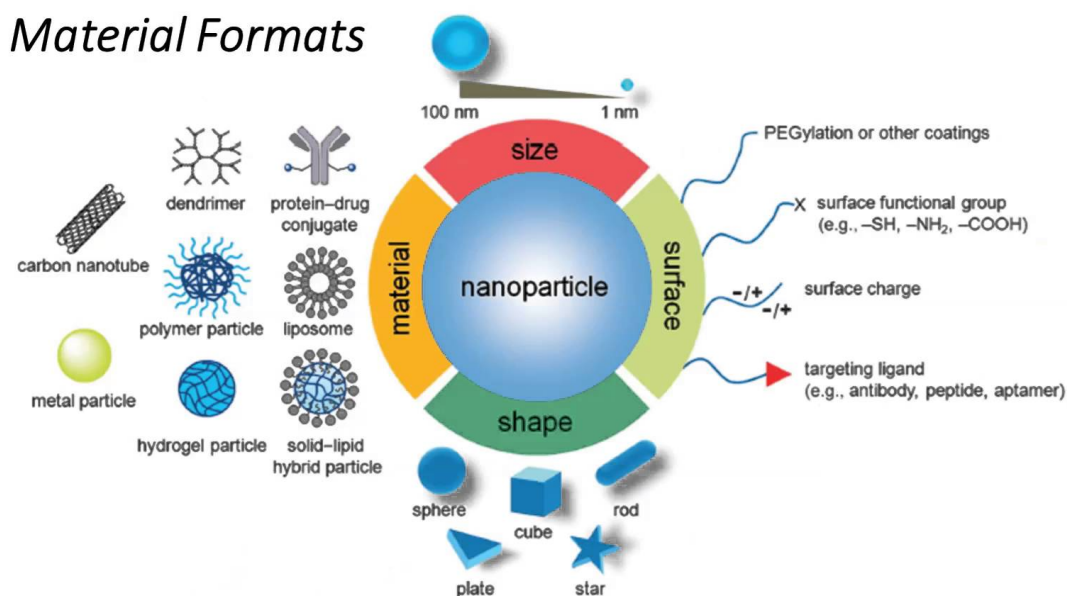
Figure 6. Schematic picture that shows the different features that modify nanomaterials properties

1.1.3 NANOMATERIALS APPLICATIONS

Due to the high number of different nanomaterials and thanks to their unique properties, there are several areas in which nanoscale structures are under active development, ranging from mining to computers, information technology, biotechnology, electronics, aerospace, defense, manufacturing, environment,

agriculture, diesel and fuel additives, automotive components, dental materials, drug delivery systems or pharmaceutics. Here, we will present some examples in order to illustrate how nanoscale materials may help in the development of the industry.

1.1.3.1 Electronics

Nanoelectronics: Recent research has shown some promising applications in this field. For example, cadmium selenide nanocrystals deposited on plastic sheets, have led researchers to form electronic circuits that combine low power requirements, flexibility and a simple fabrication process.[29] Furthermore, iron nanoparticles have also been used as transistors with lower power consumption than transistor-based circuit.[30]

Displays: The use of nanocrystalline materials (mainly quantum dots) to reduce the pixel size is currently available in some gadgets as monitors or phones.[31] These nanostructures can greatly enhance resolution and may significantly reduce cost. Moreover, flat-panel displays constructed with nanomaterials possess much higher brightness and contrast than conventional displays owing to the enhanced electrical and optical properties of the new materials.

Data storage: The use of nanomaterials in devices such as computer hard disks that function based on their ability to magnetize a small area of a spinning disk to record information has enormously increased last years. Disks and tapes containing engineered nanomaterials can store large amounts of information. For example; nanosized magnetic rings have been used in order to make memories with a density of 400 GB per square inch.[32]

High energy density batteries: It has been proved that a prudently combination of carbon nanotubes in conjunction with high-capacity lithium storage compounds can work synergistically to provide higher capacity plus better cycleability than their larger-particle equivalents.[33] Actually, they are bound to play an important role in the enhancement of capacity, energy density and power density of the future generation

lithium-ion batteries. The nanoscience and nanotechnology have presented this opportunity to devise novel architectures in order to achieve the desired performance of batteries with the aim to meet the present and future energy storage requirements.[34]

1.1.3.2 Cosmetics

Some nanoparticles, such as titanium dioxide and zinc oxide are currently used in sunscreens and in the cosmetic industry due to their ability to absorb and reflect UV light together with their apparent innocuousness.[35,36] Gold nanoparticles are under consideration in anti-aging creams because of its brightness, but mainly by acting as antioxidant components.[37] Furthermore, silver nanostructures are claimed to be highly effective in disinfecting the bacteria in the mouth and have also been added to toothpaste.[38]
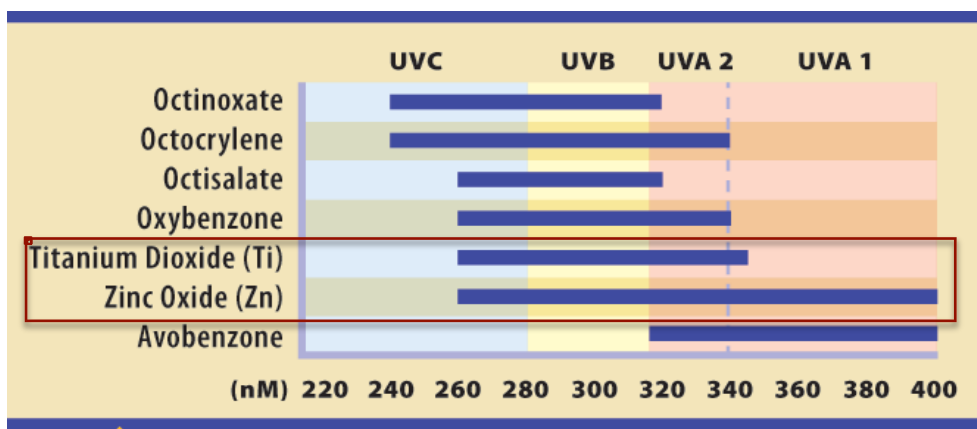
Figure 7. Comparison of different active ingredients of sunscreens regarding their protection against ultraviolet radiation

1.1.3.3 Materials

The application of nanotechnology in materials and construction presents uncountable opportunities and challenges. The use of manufactured nanomaterials in the construction industry should be considered not only for enhancing material properties and functions but also in the context of energy conservation.[39–42]

In fact, carbon nanotubes can remarkably improve mechanical durability by gluing cementitious agents and prevent crack propagation. Incorporation of CNTs as crack bridging agents into nondecorative ceramics can enhance their mechanical strength and reduce their fragility, as well as improve their thermal properties.[43,44]

Furthermore, some metal oxide nanoparticles (like SiO_2 or Fe_2O_3) can be used as filling agents to pack the pores and reinforce concrete; fighting against the weakness originated by the reaction of $CaCl_2$ or $MgCl_2$ with concrete constituents.[41,43] Similarly, the use of silica and TiO_2 nanoparticles has also increased in construction thanks to the supplementary functions that it can provide. For example, silica nanolayers sandwiched between two glass panels can fireproof windows or silica NPs on windows control exterior light as an antireflection coating, contributing to energy conservation.[45] On the other hand, titanium dioxide nanoparticles coated on pavements, walls, and roofs can also work as an antifouling agent to keep the surfaces dirt-free under solar irradiation. In addition to photoassisted bacterial/viral inactivation, the photoinduced superhydrophilic property of TiO_2 prevents hydrophobic dust accumulation on windows.[46,47]

Some metallic nanoparticles have also been tested in construction in order to maximize the mechanical, chemical or even antibiotics properties. For instance, addition of magnetic nickel NPs during concrete formation increases the compressive strength by over 15% as the magnetic interaction enhances the mechanical properties of cement mortars[39] and silver NPs can be embedded in paint to inactivate pathogenic microbes and provide antimicrobial properties to surfaces (e.g., hospital walls).[48]

1.1.3.4 Textiles

Increasing customer demand for durable and functional apparel manufactured in a sustainable manner has created an opportunity for nanomaterials to be integrated into

textile substrates.[49] The market for nanofiber-based products is expected to reach over

$1 billion by 2020.[50] With a demanding market for wearables and a growing trend for

nanofiber-based products, the applications are diverse for nanotextile products

ranging from consumer apparel to medical wearables. In fact, the company Gore-Tex®

has recently incorporated nanostructures into their products for the apparel market.

Some of its examples include a product called Nyagraph 351, which has shown to be

useful for burn protective materials.[51]

Here, we will present some recent examples that reveal how this industry is already

exploring new challenges together with the nanoindustry.

Water and Oil Repellence: Textile industry has tried to produce water-repellence

clothes for several decades. In fact, water repellence can be imparted to textiles by

forming nanowhiskers consisting of hydrocarbons that are 3 orders of magnitude

smaller than a typical cotton fiber. The spaces between individual whiskers are smaller

than a drop of water but larger than water molecules, producing a high surface tension

that allows the water to remain on the surface. The whiskers maintain breathability as

they permeate gases.[52,53]

Another approximation combines water-repellent agents with silica nanoparticles,

which impart hydrophobicity to textiles.[54,55]

On the other hand, textile industry has also focused on the development of oil-

repellent materials. Polyester fabric coated with silicone nanofilaments and treated

with plasma fluorination has been developed to impart superoleophobic properties to

textiles.[56] The produced fabric samples are able to repel alkanes. Furthermore, the

simultaneous combination of hydrophobic and oleophobic properties, given by the

union of different nanomaterials, has already been tested in textiles. In a study carried

out by Hoefnagels et al., cotton fibers were impregnated with SiO_2 particles and

different compounds to obtain a dual-size surface roughness with hydrophobic and

oleophobic characteristics.[57]

Antistatic properties: It has been manifested that ZnO nanoparticles give antistatic

properties when applied to textiles.[58] Thus, ZnO NPs were immobilized on polyester

fabrics through a process with an antistatic finishing agent. As the concentration of ZnO NPs increased in the finishing agent, the antistatic property of the fabric decreased due to reduced dispersion of NPs. In another study, antistatic properties were achieved after utilizing Sb-NP-doped SnO_2 particles in polyacrylonitrile fibers. The particles diffused into the fibers created electrically conductive channels, which produced antistatic properties.[59]

Wrinkle resistance: to impart wrinkle resistance, titanium dioxide and silica NPs have been applied to cotton and silk. TiO_2 was utilized to form cross-links between cellulose molecules.[60–64]

Strength enhancement: the integration of carbon nanotubes in fibres has been widely used to increase the strength and performance and decrease weight. [65–67] Liu et al. proved that the formation of cotton fabrics coated with CNTs improved the tensile strength along the warp and weft directions, showing enhanced in both loading capability and flexibility.[66]

UV blocking: titanium dioxide and zinc oxide nanoparticles have already been cited by their ability to absorb and reflect UV light and their application in cosmetics. ZnO nanorods have been incorporated in cotton to induce scattering at a high UV protective factor rating. [68–70]

Antibacterial properties: multiple nanoparticles have shown antiseptic characteristics.[71–74] For example, Xue et al. designed cotton fibres treated with Ag NPs, which can be applied to socks to prevent the growth of bacteria and fungi.[75] Titanium nanoparticles have also been utilized to impart textiles with antibacterial properties, as they have the ability to form O_2^- and hydroxyl radicals. Through this mechanism, the nanoparticles decompose organic matter including odour molecules, bacteria and viruses.[76,77] Besides, textiles treated with ZnO showed self-cleaning properties in the presence of Gram-negative and positive bacteria.[78–80]

Electrical conductivity: finding the balance between electrical conductivity, flexibility

and comfort of the textile is a new challenge that industry tries to resolve. Last decade, coatings with multiwalled carbon nanotubes and graphene-based woven fabrics have been developed to impart electrical conductivity to cotton. Furthermore, the resulting textile showed dimensional stability in both the warp and the weft directions.[81,82] Power sources: fabrication of multifunctional composite fibres has received attention due to their applications in conductive structures and batteries in the textile industry. For example, carbon nanotubes have been mainly used to design flexible supercapacitor textiles, which were integrated with a photoelectric conversion function to transform solar energy into electrical energy and stored it in a stacked multilayer structure. [83,84] Thus, batteries which can be directly weaved into a textile constitute a promising solution toward seamless integration with functional textiles. Detectors in fabrics: MOFs (metal-organic frameworks, which are compounds consisting of metal ions or clusters coordinated to organic ligands to form one-, two-, or three-dimensional structures),[85,86] built with quantum nanorods have been inserted into cotton fabrics.[87] These materials have shown the potential to be used as colorimetric sensors to detect the presence of toxic gases via the luminescence of the MOFs or the electrical conductivity of the nanorods.[88] These chemical sensors can be incorporated into uniforms or any textile substrate, which may result in a valuable tool in target sectors such as chemical or mining industries.

1.1.4   *BIOMEDICAL APPLICATIONS OF NANOMATERIALS*

Special mention will be made to the possible clinic applications of the nanomaterials, due to the biomedical vision of the present thesis.

The variety of surface chemistries has extended the use of nanostructures to biomedical applications, adding stability, solubility, biocompatibility, biological or therapeutic effects, and optoelectronic properties.[89]

1.1.4.1 Therapy

Many therapeutic applications of nanostructures have been proposed such as photodynamic therapy, drug delivery or alter gene expression.[90] In order to achieve this, lots of nanocompounds with different nature have been assessed in an attempt to improve the therapeutic strategies. Here, we will briefly show some of them in order to give an idea of the current situation of the nanotherapy. For instance, metallic nanostructures have gained interest due to their confinement of electrons, which are able to produce quantum effects like Surface Plasmon Resonance phenomenon as previously described. On the other hand, the optical properties of QDs make them suitable for highly sensitive, long-term, and multi-target bio-imaging applications. The surface properties of the QD crystals are tailored to achieve better solubility, biocompatibility, and target selectivity. Furthermore, graphene and its derivatives are used as starting material for the synthesis of useful nanostructures thanks to their outstanding mechanical, optical, thermal and chemical properties.

Drug delivery: many drugs have limited applications due to poor water solubility, which finally results in poor absorption in the gastrointestinal tract after oral dosing; or rapid degradation (usually by enzymes which degrade the molecule). In this sense, researchers have tried to develop different methodologies that allow increased protection and better biocompatibility. For instance, superparamagnetic iron oxide nanoparticles (SPIONs) can be attached with polymers and capping agents such as cellulose, dextran or PEG that increased bioavailability.[91]

Furthermore, silica nanoparticles differ from other drug delivery carriers because of their unique pore network that facilitates drug dispersion and simultaneously regulates the drug release rate. In addition, their easily functionalized surface enables numerous strategies for achieving sustained drug release via interactions between drug molecules and functional groups that decrease the drug diffusion rate.[92] To name some of the examples, they have been employed as drug delivery systems by covalently grafting rhodamine B,[93] loading cytochrome c to assess the cellular uptake[94] or by attaching antibodies to increase the immune response.[95]

Finally, drug delivery systems using graphene-based nanomaterials have been studied for several years. For example, the anti-inflammatory drug Ibuprofen was released in a controlled way by a chitosan-functionalized graphene oxide nanocarrier;[96] Hu and co-workers developed a graphen nanosheet associated with Dox that was release under certain pH circumstances[97] or graphene oxide and the anticancer drug hypocrellin A were employed to induce the generation of singlet oxygen molecules which killed tumour cells after exposed to light irradiation.[98]

Thermal therapy: therapeutic applications involving nanomaterials are not limited to drug delivery. Actually, killing tumour cells by using heat has also gained interest among researchers working with nanostructures. Thermal therapy can be achieved by applying light (photothermal therapy) or by applying a magnetic field.
Metallic nanoparticles that generate heat from light have been studied for phototherapy cancer treatments for several years.[99,100] Indeed, nanostructures with photothermal therapeutic applications have one property in common: they absorb high near-infrared radiation,[101] mainly by the fact that human tissues strongly absorb in the visible region but not in the near-infrared region.[102] Thus, having high near-infrared absorption ensures that after injecting the plasmonic nanostructures into the body, they are able to exert their photothermal effect, as this radiation can reach the site where the plasmonic nanomaterials are, without losses of radiation due to tissue absorption.[103,104] Gold nanostructures are the main agent used in photothermal therapy, as we will discuss later.
On the other hand, SPIONs have also been extensively studied as "miniaturized heaters", as they can convert the electromagnetic energy supplied by an externally applied alternating magnetic field into heat.[105–107]

Gene delivery: Therapeutic genetic material, including plasmid DNA, siRNA or antisense oligonucleotides, encompasses another important class of biotherapeutic agents that requires careful loading and delivery. However, the delivery of therapeutic genetic material is difficult because intracellular degradation processes after cellular internalization dramatically decrease nuclear access. In this sense, nanotechnology has contributed to better genetic therapy by including nanostructures which are able to

reach the nucleus. For instance, Zhou et al. were able to deliver plasmid DNA (pEGFP) to mammalian cell lines and zebrafish embryos using polyethylenimine with grafted ultra-small graphene oxide[108] or Bao and co-workers developed a graphene oxide nanosystem to deliver a plasmid containing the luciferase gene into HeLa cells.[109] On the other hand, silica nanoparticles have also proved to be promising tools for gene delivery because they provide an insulated space for incorporated genetic material, thereby protecting it from nuclease degradation.[110–112]

Tissue engineering: Tissue engineering is a multidisciplinary field focused on the application of engineering and life sciences for the development of biological substitutes that can repair, maintain or improve tissue's function. Nanoscale design of tissue engineering constructs facilitates generation of biocompatible scaffolds that precisely resemble the native extracellular matrix, provide physiologically relevant biomechanical cues and enable spatiotemporal release of biological factors necessary for functional tissue replacements.

In this sense, carbon derived nanostructures (such as carbon nanotubes or graphene) have been extensively employed as their incorporation into polymers can enhance their physical properties and the performance of the polymer matrix not only by imparting novel properties such as electrical conductivity, but also by playing an important role in reinforcing artificial scaffolds. It has also been demonstrated that dispersing a small fraction of CNTs into a polymer can significantly improve its mechanical strength and also promote osteoinduction, which further stimulates the growth of new bone tissue as well as provides a suitable interface between the native bone and the implant.[113,114]

1.1.4.2 Imaging

The ability of investigation and diagnosis at the molecular or cellular level, through the combination of molecular biology and imaging (*in vivo*) established the basis of molecular imaging.[115] Thus, imaging techniques have driven much improvement in understanding fundamental biological processes facilitating their visualization and

correlating them with their structure, function[116–120] and chemical or biochemical behaviour.[121–123]

In this sense, the availability of high-quality imaging agents is critical in targeting desired molecules and tissues. Hence, the quick development in designing and fabrication of nanoparticles has resulted in an improvement in molecular imaging applications. The unique properties of some nanoparticles (such as paramagnetism, superparamagnetism, surface plasmon resonance or phtoluminescence) have added new dimension in the advancement of contrast agent. For instance, the bi/multifunctional core-shell nanoparticles require shorter imaging time, as only one contrast agent is used while the patients can be scanned by more than one imaging technique.

Magnetic resonance imaging (MRI): MRI is a non-invasive and imaging technique utilized for diagnosis of diseases. This technique is based on the concept that when radio waves are applied, they realign and arrange hydrogen atoms that actually exist inside the body without bringing about any chemical changes in the tissues. As the hydrogen atoms return to their typical arrangement, they discharge or emit energy that fluctuates depending on the body tissue from which they come.

Nanoparticles have shown multiple properties that offer advantages in the fabrication of contrasting agent for MRI. For example, organic fluorophores and super paramagnetic iron oxide are employed in fluorescence and MRI,[124–126] manganese oxide nanoparticles coated with human albumin[127] or with silica[128] or different gadolinium nanoparticles are used as contrast agent in MRI[129]

Computed tomography (CT): CT is a radiography imaging technique that constructs 3D image of a body structure made along an axis from a series of plane cross-sectional images. The amount of radiation absorbed by different tissues is measured by sensors and the differences in X-ray absorption is used by a computer to shape cross-sectional images of tissue known as tomograms.

In this sense, lectin and gold conjugated iron oxide NPs have been utilized as dual modality agents for magnetic resonance and computed tomography imaging,[130] PEG tantalum and bismuth are also used in CT[131,132] or gold nanoparticles coated with gadolinium have been developed as contrasting agents for MRI and X-ray CT.[133]

Positron emission tomography (PET): PET technology is based on the emission of positrons by an imaging agent. Thus, after injecting the radiotracer into the bloodstream of the patient, the positrons react with the electrons presented in the corporal structures. This reaction produces energy in the form of a pair of photons. This energy is received by a scanner, thus creating 3-dimensional images that show the distribution of the imaging agent throughout the body.

Different nanoparticles have been tested as radiotracer in PET modality. For instance, Quinn et al. designed Cu-isotopes-containing liposomes as radiotracer for the detection of parkinsonism.[134] Furthermore, iron oxide nanoparticles coated with different compounds have been studied as multi-modility imaging agent.[135,136] Nanoparticles with radioactive zirconium have also been assessed.[137]

Ultrasound: this method is founded on the sound waves which emerge from an oscillating transducer. After applying high frequency sound waves, the sound echoes off the tissue; with different tissues reflecting varying degrees of sound. These echoes are recorded and displayed as an image.

Bovine serum albumin-stabilised fluorescent gold nanoparticles have been utilized as dual contrast agent for ultrasound/near infrared fluorescent imaging.[138]

Optical imaging: a wide variety of imaging techniques define optical imaging. All of them have in common the basis on illumination light in electromagnetic spectrum, ranging from ultraviolet to visible and infrared regions.

Interestingly, in a study carried out by Nam et al., fluorescent NPs comprise of semiconducting QDs and iron oxide NPs were used for optical and MR imaging; being

able to differentiate malignant tumours from benign tumours.[139] Furthermore, heparin-coated gold nanoparticles[140] and fluor-loaded hyaluronic acid gold nanoparticles[141] have also been employed in optical imaging.

Single photon emission computed tomography (SPECT): this method is quite similar to PET technology. It also requires a gamma-emitting radioisotope, which is injected to the patient. Afterwards, a SPECT gamma camera-equipped scan revolves around the person for detection of the radiotracer. Some nanoparticles have been related to the development of highly enhanced optical imaging tools. For example, silver nanoparticles loaded with radioactive iodine have been employed in order to assess the thyroid function.[142]

1.1.4.3   Sensing

New developments in nanotechnology have advanced the progress of useful and reliable electrochemical sensors and biosensors. Nanomaterial-based electrochemical signal amplifications have great potential of improving both sensitivity and selectivity. Furthermore, functional nanomaterials not only produce a synergic effect among catalytic activity, biocompatibility and conductivity, but also amplify biorecognition events with specifically designed signal tags, leading to highly sensitive biosensing.

Electrochemical enzyme-based biosensors: these sensors combine the high specificity of the enzyme with the sensitivity of electrochemical transducers. Enzyme electrodes are electrochemical probes with a thin layer of immobilized enzyme on the surface of the working electrode. Several examples illustrate the importance of nanoparticles in this area. For instance, graphite nanoparticles and carbon nanofibres have been reported to construct an enzyme biosensor to detect glucose in real samples, which could be extremely useful in the detection of hyperglycaemia in patients with diabetes.[143,144]

Cholesterol detection has also been achieved by the combination of some nanomaterials like copper oxide with the bienzymes cholesterol esterase or cholesterol oxidase.[145,146] This nanosensor will help in the control of chronic diseases such as atherosclerosis or angina.

The detection of several hormones has also been subject of investigation. Thus, Zhao et al. assessed the influence of different silica morphologies on the electrocatalytic activity toward dopamine detection.[147]

Nonenzymatic sensors: The limitations presented in enzymatic sensors such as instability, complicated modification procedures and critical microenvironmental factors, have stimulated the development of nonenzymatic electrochemical sensors with simple modification procedures and good stability. Once again, clinical monitoring of glucose has been studied with different nanomaterials-based nonenzymatic sensors. Hence, Cao et al. designed a nanosensor made by bimetallic PtCu nanochains which showed promising results in the detection of glucose in serum.[148] Furthermore, other groups have been able to synthetize sensors made with different nanostructures such as platinum nanocubes, reduced graphene oxide and copper oxide nanoflowers or titania nanowires, which exhibited highly specificity to glucose in the presence of commonly interfering species like ascorbic acid, dopamine or uric acid.[149,150]

Hydrogen peroxide sensors are under development due to the role of this molecule in disorders such as oxidative stress, diabetes, atherosclerosis or Parkinson disease as well as food safety and environmental protection.[151,152] Carbon nanotubes[153] and Pd-Pt and Pd-Au nanoparticles[154] have exhibited colorimetric and electrochemical detection of H_2O_2. Furthermore, copper sulphide nanoparticles have been able to detect hydrogen peroxide content in human serum and urine samples as well as tumour cells.[155]

Other molecules like copper,[156] nitrite,[157] adenine and guanine,[158] glutathione[159] or dopamine[160] have been measured by detection platforms that were built with different nanostructures.

INTRODUCTION

Genosensors: DNA damage observed by DNA aberrant methylation, represses gene transcription, deregulates gene expression and causes various human diseases. Hence, detecting the DNA aberrant methylation level benefits the early diagnosis of some tumours and the epigenetic therapy for DNA methylation-related diseases. In this sense, a photoelectrochemical immunosensor based on Bi_2S_3 nanorods was developed by Ai's group.[161] This sensor owned excellent photoelectron property and presented high detection specificity, being able to distinguish single-base mismatched sequences.

Gold nanoparticles have also showed highly sensitive detection of DNA methylation when coupled to DNA.[162]

Furthermore, the use of nanostructures in the designing of DNA probes[163,164] enzyme-based amplification[165] or signal amplification[166] has also showed promising results.

Immunosensors: immunoassays based on specific antigen-antibody recognitions have also experienced a great development thanks to the growth of nanomaterials composed-sensors. In this regard, iron and titanium oxides magnetic nanoparticles have been useful in the detection of different compounds such as the biomarker of tumour necrosis factor alpha (TNF-α)[167] or the enzyme OP-butyrylcholinesterase.[166] The main advantage of these nanoparticles is that they can be easily separated from biological matrices by simply exerting an external magnetic field.

Graphene quantum dots,[168] ZnO nanorods[169] or silica nanoparticles[170] have also been tested as photoelectrochemical immunosensor for the detection of monoclonal antibodies and cancer biomarkers.

1.2 GOLD NANOMATERIALS

Gold is a precious metal with a characteristic bright and beautiful tone known as the golden yellow colour. In fact, the historical popularity of Au in the jewellery industry can be attributed to its notable, long-lasting metal lustre and its relative material rarity and value. Indeed, the scarcity of this precious metal makes Au one of the most valuable materials in the world, which contributed to its acceptance as currency dating back to ancient times.

The first international Au currency appeared more than 2500 years ago, when King Croesus improved the refining techniques for Au to mint the first standardized Au coin with a uniform Au content, named "croesid".

In the scientific area, the first report on the production of gold nanomaterials can be attributed to Michael Faraday, who discovered in 1857 that "fine particles" could be formed by treating aqueous $HAuCl_4$ with phosphorus dissolved in CS_2 in a two-phase system.[171] The aqueous suspension of such "fine particles" displayed a beautiful, ruby red colour completely distinct from the golden yellow colour intrinsic to bulk Au.

Indeed, colour is not the only feature that changes when decreasing size. If a one-inch cube of gold is cut into four equal pieces, each of those pieces will retain the physical and chemical properties of the original cube of gold (including melting point, boiling point, etc.). These properties will remain as you continue cutting the gold into smaller and smaller pieces, but once those pieces are so small that they enter the nanoscale, those physical and chemical properties may change.

1.2.1 GOLD NANOMATERIALS PROPERTIES

In addition to the main properties of nanomaterials previously described, Au has a diversity of inherent attributes that makes its nanostructures an attractive platform for several applications, including biomedical applications:

INTRODUCTION

Au is one of the few exceptional metals known for incredible **resistance** against both oxidation and corrosion, and can be stored under atmospheric conditions for millions of years without being tarnished or destroyed. After exposure to air, not even a single atomic layer of gold oxide can be detected on the surface of Au substrate. As a result, Au is the only known elemental metal that is both coloured and can maintain its unique lustre indefinitely.

The **bioinert** nature and apparent lower acute toxicity of gold when compared to other nanomaterials (reported by several *in vitro* and *in vivo* studies which show favourable biocompatibility),[5,7] makes it an excellent candidate for biomedical applications.

As stated before, gold nanomaterials also present **localized surface plasmon resonance** (LSPR). Different parameters such as size, shape, structure, morphology or the environment that surrounds the surface of the nanostructure, determine the LSPR properties of the gold nanomaterial.[5] In general, the LSPR peak of Au nanostructures will be shifted when the dielectric constant of the medium surrounding the nanostructure is altered, which can be employed for optical sensing.

The fact that wavelengths near-infrared region can rapidly penetrate deep into soft tissues because of the low absorption from blood and water as well as the low scattering from soft tissue led biomedical researchers to be more interested in gold nanostructures with LSPR peaks near this region. To this end, different parameters are carefully modified: the shape or aspect ratio of non-spherical nanoparticles, or fine-tuning of the shell thickness in hollow or core-shell nanostructures.[6,7] It is also worth noting that agglomeration of nanoparticles can lead to drastic red shifts for the LSPR peak position as the nanoparticles will electromagnetically interact with each other while approaching.[172]

Furthermore, gold nanostructures with a variety of shapes or morphologies have all been reported with **photoluminescence** properties.[173,174] Luminescence is a process that involves the emission of electromagnetic radiation due to the electronic transition

43

between two different energy levels. It can be classified into many different categories depending on the excitation source, including photo-, chemo-, and electroluminescence, among others. Thus, photoluminescence is a consequence of light absorption, where the emission can be described as either fluorescence or phosphorescence depending on the relaxation mechanism (singlet– singlet versus triplet– singlet) and therefore the emission lifetime (nanoseconds to microseconds versus milliseconds).

The size of the Au nanostructure has a large impact on its photoluminescence properties. In fact, regarding luminescence, the main advantage of gold nanoparticles with respect to bulk gold is that the photoluminescence quantum yield of Au nanoparticles can be enhanced by millions-fold due to the enhancement of the local electromagnetic field on the surface (for instance, Au nanorods with an aspect ratio of 2.0– 5.4 had a photoluminescence quantum yield over 1 million times higher than that of bulk Au).[175–177]

Gold nanoparticles also possess **surface-enhanced Raman scattering** (SERS). This property is based on the transfer of energy between an incident light and the chemical bonds in the molecules involved. Thus the scattered light will show a shift in frequency relative to the incident light.[178]
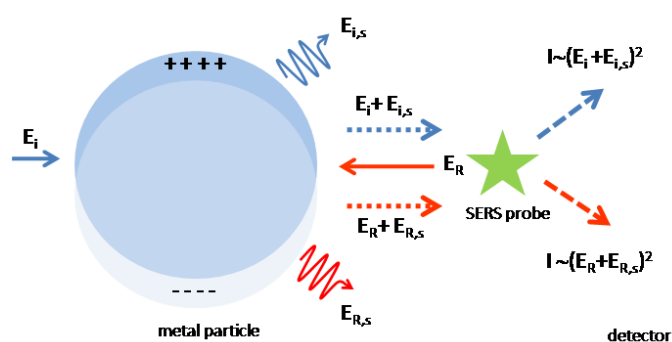
Figure 8. Graphic representation of the surface-enhanced Raman scattering effect that takes place in gold nanoparticles

Thus, gold nanoparticles are able to enhance the Raman scattering by more than 6 orders of magnitude when the probe molecules are deposited on their surface.[179]

INTRODUCTION

Several factors such as the broad and intense LSPR peaks in the visible and NIR regions, the chemical stability, the shape, the size and the gold nanoparticles concentration are involved in the SERS process.

Finally, although Au is widely contemplated as an inert metal, it also has a range of **coordination** chemistry due to its capability to form covalent bonds with various elements.[180,181] For instance, Au is able to establish relative strong covalent bonds with the P, N or S atoms in organic compounds such as phosphines, amines or thiols; which can be used to cap the surface of different Au structures, thus increasing their stability.[182]

1.2.2 GOLD NANOMATERIALS CLASSIFICATION

Regarding the structure of the nanomaterial, nanoscale-gold compounds can be classified into:

1.2.2.1 Gold nanoclusters

It refers to molecular species containing a few to several hundred Au atoms, with their dimensions below a critical size for electronic energy quantization. Taking into account that the critical size for electronic energy quantization is considered to be 2 nm,[183] these structures have gained more attention, since they are considered as a bridge between the Au atom and nanoparticles.[184–186]

1.2.2.2 Gold nanoparticles

This nanostructure is made of nanocrystals characterized by a single-crystal structure with a quasi-spherical projection under TEM imaging.[187] Usually, there is no sharp corner or edge on the entire surface of the particle. To prevent the nuclei from

aggregating together, a stabilizer that can bind to the Au surface must be introduced. In recent years, the synthesis of Au nanoparticles as a pure sample and with a well-controlled size has attracted great interest due to the simplicity in modelling their optical properties.[188]

1.2.2.3   Gold nanorods

Au nanorods have an anisotropic shape, with the positions of their longitudinal LSPR peaks highly sensitive to the aspect ratio.[189,190]

1.2.2.4   Gold nanoplates

Gold nanoplates are formed by plate-like nanostructures enclosed by two relatively large basal planes, together with low aspect ratios. The nanoplates (generally prisms or disks) can form a triangular, hexagonal or circular cross section along the direction parallel to the basal planes. The Au nanoplates typically have edge lengths in the range of 40 nm to 1 μm, with thicknesses varying from 5 to 50 nm.[191]

1.2.2.5   Gold nanoshells

A class of core–shell nanoparticles that are typically prepared by coating colloidal particles made of a dielectric material (such as silica,[192] quantum dots,[193] iron oxide nanoparticles[194] or liposomes[195]) with shells of polycrystalline Au.

1.2.2.6   Gold nanoboxes and nanocages

The main advantage of these gold nanostructures is that they have hollow interiors and/or porous walls, which is extremely useful for applications like encapsulation, controlled release, and drug delivery. Depending on the porosity of the walls, they can be divided into nanoboxes or nanocages.[196–199]

1.2.2.7 Nanostructures with branched arms

The key feature of these gold nanostructures is their structural anisotropy. Their optical properties are similar to those found in Au nanorods. These nanomaterials vary from multipods, to stars, flowers, etc.[200–204]

1.2.3 GOLD NANOMATERIALS APPLICATIONS

Although gold nanoparticles are extensively used in biomedicine, here we will briefly summarize some other applications that have also benefited from the development of gold nanostructures.

1.2.3.1 Catalytic applications

Advanced catalysts usually involve noble metals. Among them, Au has attracted an increasing interest due to its unique physicochemical properties. Thus, the use of Au-based nanomaterials for various catalytic applications has already been reported in scientific journals:

The increased levels of gas methane have led governments to develop strategies to reduce its production. Some approaches were made by employing catalysts based on mixed metal oxides, but they were found to require high temperatures for their activation.[205,206] Contrarily, after controlling some parameters such as the oxidation state, the total composition or the particle size, Dumbre et al. proved that Au nanomaterials show better catalytic activity at reduced temperatures.[207]
Carbon monoxide is another toxic gas that is known to cause harm to the environment and human health. The fact that CO is produced in combustions that take place in vehicles and other industries, results in a great interest to limit its emission to the atmosphere. In this sense, Au nanomaterials have been used in the oxidation of CO to

CO_2 with promising data.[208,209] Among them, it is especially significant the catalytic activity of some gold nanostructures that are able to participate in water-gas shift reactions (a reaction where CO and water react thus resulting in H_2 and CO_2).[210,211] The water-gas shift reaction has been attracting interest as a potential source of pure hydrogen for use in fuel cells and vehicles and to convert the disposable gases produced in automobiles combustion.

On the other hand, when gold nanomaterials are combined with other nanomaterials (like titanium nanoparticles), photocatalysis may occur. As previously described, the SPR absorptions of spherical Au NPs are often in the range of 520-550 nm, which could provide the visible light response for some wide band gap semiconductors. In this sense, several photocatalytic applications of Au/TiO_2 such as aerobic oxidation of alcohol,[212] acetone oxidation,[213] NO oxidation[214] or benzene to phenol oxidation[215] have already been described.

Another approximation that is currently under development is based on the synthesis of gold nanostructures using biomaterials (including organism as bacteria and fungi) as living nanofactories. For instance, Das et al. defined a synthesis protocol of multi-shaped AuNPs by the interaction of Au salts with the cell-free extract of fungal strain *Rhizopus oryzae*.[216] Besides, these bio-integrated nanoparticles acted against contaminants (such as organophosphorus pesticides and dyes) by adsorbing them.

1.2.3.2 Analysis

Remarkable efforts have been made in order to prevent, control and mitigate the environmental contamination caused by pollutants that are known to persist in the environment, resist biodegradation, bioaccumulate in organisms and have deleterious effects on the environment and human health.[217] Gold nanoparticles are the most popular metal NPs in environmental analysis. One of the main reasons is the ease to prepare gold nanostructures in a liquid by reducing chloroauric acid with a reductant. Besides, they can be coated with different compounds such as nucleic acids,

antibodies, polymers or small molecules that have a specific interaction with the analyte.

Electrochemical sensors: Gold nanoparticles with different morphologies have been tested as electrochemical sensors of emerging chemical pollutants due to their high conductivity and activity.[218,219] For example, Xia and co-workers, designed a biosensor by immobilizing estrogen receptors in a supported bilayer lipid membrane modified with gold nanoparticles in order to detect and monitor estrogenic compounds in water samples;[220] while Zhou et al. suggested a method based on the combination of gold an TiO_2 nanoparticles for the detection of mercury in water samples.[221]

Fluorescence detection: Numerous works have manifested the role of gold nanoparticles in detecting chemical pollutants thanks to their quenching properties. In relation to this, a group from China fabricated a biosensor of microcystins based on fluorescence resonance-energy transfer between gold nanoparticles and fluorescent graphene oxide.[222]

Colorimetric detection: The low cost, simple operation and possibility of detection with the naked eye make visual colorimetric detection an attractive tool in on-site monitoring of environmental pollution. AuNPs play a major role in colorimetric detection due to its high extinction coefficient. A general design is based on protecting the AuNPs with a functional group or molecule (like DNA aptamers). After binding the analyte with the protection agent, it will dissociate from the AuNPs, thereby allowing aggregation of AuNPs induced by salt (along with the colloid colour changing from red to blue). Several groups have worked on this mechanism and developed sensors for bisphenol A (BPA),[223] oxytetracycline,[224] mercury,[225] kanamycin[226] or perfluorooctanoic acid[227] in water samples.

Another powerful application is the development of visual lateral flow strip sensors based on gold nanoparticles. Lateral flow strip devices, with the most famous examples of pregnancy testing strip and glucose testing, are particularly suitable for on-site monitoring. In this sense, a lateral flow strip for visual detection of BPA based on BPA antibody-conjugated Au NPs has been object of study.[228]

Surface-enhanced Raman spectroscopy: As formerly described, SERS is a highly sensitive analytical technique that uses nanostructures for obtaining higher intensity spectral fingerprints of molecular analytes. This method is suitable for the detection of trace amounts of pollutants in environmental samples. Regarding this, some compounds have been detected in waters by employing gold nanostructures, such as perchlorate,[229] microcystin[218] or mercury.[230]

Localized surface-plasmon resonance: The change in the colour of gold nanostructures suspensions by the oscillation of the free electrons is also used in the analysis of different compounds in samples. Thus, there have been reported methods for the detection of antibiotics (such as neomycin, kanamycin or streptomycin) in milk[231] or the detection of enrofloxacin residues.[232]

1.2.3.3 Cosmetics

Gold nanoparticles have been studied as a valuable material in cosmeceutical industry for their colorimetric properties. The use of these compounds is extended to deodorants, face packs or antiaging creams.[233] Interestingly, Haveli et al. reported a method to introduce fluorescent gold nanoparticles inside human hair´s central core cortex.[234] Thus, the hairs were able to turn pale yellow and then darkened to a deep brown while the colour remained after repeated washings.

Additionally, gold nanoparticles containing-lipsticks have also been tested. In principle, the incorporation these nanoparticles into lipstick and lip-gloss make it possible to soften or soothe the lips by preventing trans-epidermal water loss. In fact, there exist patents of methods to prepare pigments with gold nanocompounds that provide wide range of colours for a long period of time.[235]

Moreover, several cosmetic companies have developed products that count with the presence of gold nanoparticles. For instance, Chantecaille® developed an antiaging cream formed with infinitely small nanoparticles of pure gold that are said to be bound to silk microfibers to firm and tone skin, while delivering incredible anti-inflammatory, healing, and age defying power.[236] On the other hand, LEXON Nanotech® describe its mask pack as an intensive wrinkle treatment mask sheet that disinfects and immediately hydrates the skin and helps eliminate the fine lines and dryness.[237] The gold nanoparticles are highly effective in penetrating small pores and disinfecting skin. They also help to reduce pore size in order to prevent and treat acne.

1.2.4 BIOMEDICAL APPLICATIONS OF GOLD NANOSTRUCTURES

As mentioned above, Au nanostructures exhibit a variety of optical, physical and chemical properties that make them especially interesting for biomedical applications.
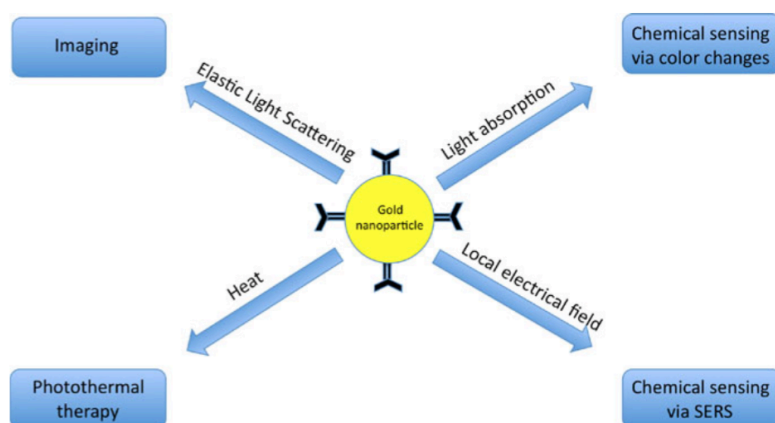
Figure 9. Different applications of gold nanoparticles in function of their physicochemical properties

51

1.2.4.1 Sensing

The LSPR or photoluminescence presented in these nanoparticles have increased their use in the sensing field.

Photoluminescence: Factors like the low toxicity or the high emission efficiency of fluorescent Au nanostructures are the reason why they are considered excellent optical probes for the detection of biological species. Au clusters are superior in terms of photostability and biocompatibility, while their photoluminescence can be readily tuned from the visible to the NIR region.

Thus, two different approximations have been developed in order to employ Au nanostructures as photoluminescence probes: the "turn off" (when the ligand shell on a Au cluster is perturbed by analyte molecules through either covalent bonding or physical adsorption, the photoluminescence from the Au cluster tends to drop significantly) and the "turn on" (it involves an increase in photoluminescence intensity in the presence of analyte molecules, usually caused by the interactions with the protecting ligands or inhibitors adsorbed onto the surface of Au clusters[214]) detection schemes.

As a result, various types of sensors have been developed based on fluorescent Au clusters for the detection of proteins,[238–242] metal ions[243–245] or glucose.[246]

Nevertheless, some disadvantages such as the cost of these sensors and the impossibility to make the sensor portable force to continue investigating for a better gold-based photoluminescence probe.

Sensing Based on Localized Surface Plasmon Resonance: The aggregation or breaking up of Au nanomaterials due to the interactions with the analyte, usually imply a change in the local refractive index, which is accompanied by a shifts for the LSPR peak position. For instance, a suspension of Au nanoparticles would appear red when the interparticle distance is substantially greater than the average particle diameter. As

this distance decreases to a scale less than the average particle diameter, the colour will change from red to blue.

This phenomenon can be used to design and fabricate colorimetric sensors. Indeed, Au nanostructures with different shapes have been utilized as the sensing components for colorimetric detection of various analytes such as DNA,[247] metal ions,[248,249] proteins[250] or small molecules.[251,252]

However, some aspects as the cost derived from the use of gold components and the lower sensitivity of colorimetric compared to those based on photoluminescence still need to be resolved.

Sensing based on Surface-Enhanced Raman Scattering: The sensitivity showed by SERS sensors is higher than those based on photoluminescence. Hence, by attaching Raman active molecules to the surface of Au nanoparticles, SERS tags can be obtained, which have been widely used for Raman reporter assays. It also can be coated with a protective shell and conjugated with a recognition ligand, thus obtaining a SERS tag with good biostability, biocompatibility, and specific binding capability.[218,253]

In spite of the great selectivity and sensitivity, the difficulty to establish quantitative analysis together with the high cost of Au and the requirement of a Raman spectrometer imply a limited scope of use of this technique.

1.2.4.2 Imaging

The use of gold nanomaterials in imaging has also experienced a great increase due to their unique properties, stability and low toxicity. Thus, several techniques have benefited from the development of gold nanostructures:

Imaging based on photoluminescence: Thanks to the quantum confinement effect, numerous gold nanomaterials, like Au clusters, show excellent photoluminescence properties. As previously described, the stable photoluminescence and low toxicity of

the gold clusters make them a better choice as probes than traditional organic dyes or semiconductor quantum dots. Furthermore, the excitation and emission peaks of Au clusters can be readily tuned from the UV to the NIR region, making Au clusters an excellent choice of probes for optical imaging.[249,254]

Imaging Based on Light Scattering: As explained before, the transfer of energy between an incident light and the chemical bonds in the molecules involved generates scattering spectra which can serve as "fingerprints" of the analyte molecule, thus providing specific information for the identification of molecular species by their functional groups.[255]

Consequently, by employing a Raman confocal microscope, Raman spectra can be obtained from different locations of a sample and then organized to generate a Raman image. The use of gold nanoparticles can strongly enhance the intensity of Raman signals, which offers higher signal sensitivity and shorter acquisition times. Indeed, SERS images can be acquired at a high enough speed to enable the real-time tracking of gold nanoparticles.[256]

Imaging Based on Photothermal Conversion: After absorbing the light by a molecule, photons pass the energy to electrons, which will be excited to higher energy levels. Following excitation, two different mechanisms will take place in order to relax down electrons to their ground state: through radiative decay and emit photons, or through non-radiative decay and release heat. Consequently, photoluminescence or photothermal heating will be detected. When the local environment of a constrained size is rapidly heated up and the accumulated heat cannot be quickly dissipated, thermoelastic expansion and explosive vaporization will occur, accompanied by the generation of photoacoustic waves. Generally, fast heat generation and a large gradient in temperature both facilitate the generation of photoacoustic waves.

Therefore, gold nanoparticles are able to convert the energy harvested from light into heat, which allows these nanostructures to be a class of superb contrast agent for photoacoustic imaging.[257]

INTRODUCTION

Taking into account that photoacoustic imaging shares the advantages of both optical and ultrasonic modalities and that the combination with gold nanoparticles offers high sensitivity and high spatial resolution, it has emerged as a versatile imaging modality for various kinds of biomedical applications.[120,257] Besides these imaging methods, Au nanostructures have also been studied as contrast agents for radiological imaging modalities such as X-ray computed tomography, positron emission tomography and Cerenkov luminescence imaging.[258,259]

X-ray computed tomography (X-ray CT): This technique is one of the most used modalities for medical imaging. It can be employed to obtain complementary anatomical information for diagnostics in a cost-effective fashion. On the other hand, the contrast between different types of soft tissues is negligible for conventional X-ray CT, so that a good contrast can only be achieved between hard and soft tissues without contrast agent. As a result, conventional X-ray CT cannot be used alone to differentiate cancerous from normal tissues, rendering it essentially useless for the early stage detection of cancer or cancer metastasis.However, given that the attenuation of X-rays by tissue depends on the electron densities and thus atomic numbers of chemical elements present in the tissue, Au provides a strong contrast relative to most of the naturally occurring elements found in the body.[260]

The presence of Au nanostructures can greatly enhance X-ray attenuation, creating high contrast on the CT image. At the clinically used X-ray energy, Au nanostructures, regardless of their sizes and shapes, have a mass attenuation coefficient 2.7 times greater relative to the conventional iodine-based compounds, together with other advantages such as prolonged presence in the circulation, lower renal toxicity, and well-established surface chemistry for the conjugation of targeting ligands. All these attributes make Au nanostructures promising contrast agents for clinical X-ray CT applications.[261,262]
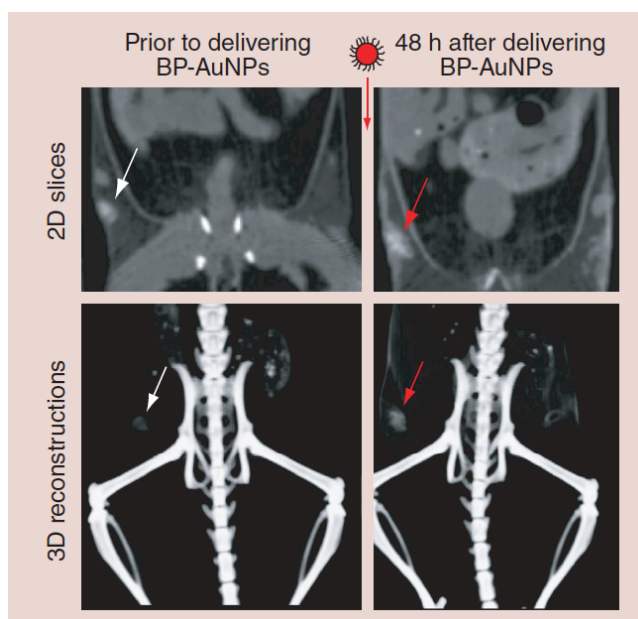
Figure 10. Computed tomography reconstructions showing microcalcifications before and after exposing to bisphosphonate-AuNPs that allow their enhanced detection.

Positron emission tomography (PET): PET is also one of the most frequently used modalities in molecular imaging, and can be employed to collect quantitative information about the expression of molecular species on a biological tissue. In fact, it has been a standard tool for the evaluation of biodistribution and pharmacokinetics of Au nanostructures.

A typical approach is to chelate or covalently attach the radionuclide to the surface of Au nanostructures. Depending on the radionuclide used, the Au nanostructures can be imaged by PET or single photon emission tomography (SPECT). For instance, Xie et al. conjugated gold nanoshells with ^{64}Cu in an attempt to assess the radiolabeling of these Au nanostructures for PET imaging in tumours.[263] In this sense, several studies have been developed to evaluate the biodistribution, tumour targeting and pharmacokinetics of different gold nanostructures.[264–266]

Besides, it is used to obtain valuable information about cellular function and gives insight into the molecular processes of a living organism, enabling diagnosis even before changes at any anatomical are observed. This technique is more sensitive in detecting small lesions than X-ray CT, offering better contrast and serving as a more reliable diagnostic tool.

For all these reasons, X-ray CT and PET scanners are easily accessible in biomedicine. PET is also commonly used for molecular imaging that visualizes cellular functions and biological processes at a molecular level with specially designed contrast agents. They can also be integrated together for multimodality imaging. Thus, it is possible to obtain better results regarding biodistribution, targeted accumulation and clearance of Au nanomaterials by combining the morphological and quantitative data acquired from X-ray CT and a molecular imaging modality such as PET.[117,267]

1.2.4.3 Therapy

Due to their ease of preparation and surface modification, bioinert property and photothermal capability, Au nanostructures are emerging as a new class of platform materials for drug delivery and related applications.

Drug loading: There exist numerous ways to incorporate drug molecules onto the surface or into the interior of the Au nanomaterial. An attractive approach could be to incorporate the –SH or –NH$_2$ group into a drug molecule, due to the strong affinity between Au and S or N, thus loading the drug onto the nanoparticle surface.

Another possibility could be by grafting the drugs to the capping ligands on the surface of the nanomaterial.[268]

Furthermore, electrostatic interaction or van der Waals forces have also showed promising results as means for loading a drug onto the surface,[269,270] as well as hydrogen bonding has also been used as a tool for loading and delivering different drug molecules.[271]

However, other alternatives have also been tested. Au hollow nanostructures such as nanocages or nanoboxes seem to be better choice for drug delivery as the drugs can be loaded in the interiors to increase the loading efficacy and help to prevent the

drugs from being released prior to use. In addition to this, modifications to the surface can be made in order to deliver the drug under certain circumstances (for instance, pH or temperature-sensitive polymer).[272,273]

Controlled release: Releasing the drug in the target tissue, once it has been loaded, supposes a critical step in the pharmaceutical development of a medicine. In this sense, gold nanomaterials have also been studied as smart drug delivery systems, based on their ability to break photosensitive chemical bonds under the irradiation of light.[274] Thus, Au nanomaterials are able to transform light into heat because of their LSPR properties as previously described. The released heat can lead to a local temperature rise in the vicinity of the nanostructure, sufficient to even break the linkage between the drug molecule and Au surface.[275]

Multidrug resistance (MDR): One of the main difficulties of cancer treatment is multidrug resistance. This is a condition under which treatment with drugs becomes useless due to those malignant cancer cells that are not drug-sensitive. Briefly, chemotherapy can only kill the drug-sensitive cells, leaving behind an increased proportion of drug-resistant cells. When the tumour begins to grow again, chemotherapy will fail simply because the remaining tumour cells are no longer responsive to the anticancer drugs.[276,277] Some components of gold nanomaterials have been proved to help against multidrug resistance. For instance, hexadecyltrimethylammonium bromide, a commonly used surfactant in the synthesis of Au nanorods, can serve as an MDR inhibitor. That is the reason why CTAB-stabilized Au nanorods have shown great potential as a multidrug delivery system for overcoming MDR.[278]

Cancer therapy: Besides fighting against multidrug resistance, Au nanostructures can also be directly used as cancer therapeutic agents. In this sense, the therapeutic effects carried out by Au nanostructures can be divided into three categories:

Photothermal therapy (PTT): this treatment relies on the use of hyperthermia to kill tumour cells. This condition is achieved when cells are exposed to temperatures

ranging from 41 to 47 °C for tens of minutes. This situation will denature proteins and destroy cell membranes. The characteristic poor blood supply presented in tumour cells makes them more prone to destruction at an elevated temperature. However, the collateral nonspecific heating which will also destroy healthy tissues implies a major counter indication in photothermal therapy. Nanomaterials can be used to address this issue. The fact that Au nanostructures can absorb electromagnetic energy and convert it into heat through the photothermal effect makes them suitable agents for photothermal therapy. Besides, it is possible to accumulate gold nanomaterials at the tumour zone thanks to passive targeting and/or active targeting enabled by ligands. Thus, the accumulation of Au nanostructures at the desired site will lead to selective heating of target cells after laser irradiation, minimizing potential damage to the surrounding, healthy tissue. This advantage, together with the fact that Au nanostructures can serve as contrast agents for various imaging techniques, would allow physicians to achieve an imaging-guided therapy.

In addition, when pulse laser irradiation is used for PTT with Au nanomaterials, a second cell killing mechanism participates. The high photon density under pulse laser irradiation is usually absorbed by Au nanomaterials by heat dissipation. However, this mechanism may be insufficient, thus leading to an extremely rapid rise in local temperature and provoking a phenomenon termed cavitation effect. This effect is responsible for the perforation of plasma membranes, leading to an influx of extracellular Ca^{2+} and causing cell death.

Furthermore, it is well worth noting that the high photothermal conversion efficiency of Au nanostructures minimizes the required particle dosage for PTT. This makes Au a more attractive choice as a hyperthermia-inducing agent over magnetic nanomaterials, which induce hyperthermia under an alternating magnetic field, but require a relatively high dose for effective treatment. Au nanostructures with strong absorption in the NIR region (including nanorods, nanoshells, nanocages, and nanostars) are particularly well-suited for PTT, owing to the penetration depth of lasers at such wavelengths.

Nevertheless, some safety complications need to be resolved before this therapeutic method can enter clinical applications. To begin with, the laser power used in most cases for Au nanostructure-mediated PTT is far exceed the skin tolerance threshold. Secondly, it is still needed a strategy to attack deep tumours, as the penetration depth of PTT is still low. In this sense, magnetic hyperthermia is a more suitable technique, as there is no limitation on the penetration depth from the alternating magnetic field. Finally, gold nanoparticles are still considered relatively expensive, so that their use is limited nowadays.

Photodynamic Therapy: Photodynamic therapy (PDT) is focused on killing cells through the use of singlet oxygen ($^1O_2$) generated photochemically. After irradiating light at some specific wavelengths, a light-sensitizing agent can convert endogenous O_2 to $^1O_2$ to induce cell death. In this sense, gold nanomaterials have been studied as delivery vehicles for organic photosensitizers (in an attempt to increase the water solubility of these agent)[279,280] and as photosensitizers themselves,[281–284] as the excitation of Au nanomaterials by light, provokes an energy transfer from the electrons at excited states to molecular oxygen, leading to the generation of ROS. Furthermore, gold nanostructures can be excited in the NIR regions (reaching deeper zones in the body) and are far more stable than common organic photosensitizers.

X-ray Radiotherapy: this therapy is based on the death of cancer cells by generating photoelectrons, which provoke the ionization of water and formation of reactive free radicals. Furthermore, these free radicals may attack the hydrogen atoms from ribose sugars, then damaging the DNA content. This technique provides much deeper penetration than the NIR light used in the previous cancer treatments.

Nevertheless, although X-ray radiotherapy is a method that only affects the area under irradiation, the main inconvenience is the lack of selectivity, meaning that both cancerous and normal cells in the path of X-rays will be killed indiscriminately.

In order to avoid it, radiosensitizers made of heavy elements with high atomic numbers can be used to absorb and thus concentrate the X-rays in the area where the

radiosensitizers are located. Thus, Hainfeld et al. showed a notable increase in survival time in mice treated with 1.9 nm Au clusters and exposed to X-rays.[285] Furthermore, the high density, low toxicity and large coefficient of energy absorption make Au nanomaterials a promise tool as radiosensitizers for X-ray radiotherapy.[286,287]

1.2.5 BIODISTRIBUTION AND TOXICITY OF GOLD NANOPARTICLES

In spite of the multiple advancements in Au nanomaterials for *in vivo* imaging and therapy, further toxicity studies are needed in order to clarify whether these nanostructures can be translated into the clinics. These issues can either hamper the efficacy/efficiency or cause adverse effects.

1.2.5.1 In vitro studies

The first aim of *in vitro* applications is to assess the interactions between Au nanostructures and cells, which include the uptake of nanostructures by them and the subsequent delivery to various compartments within the cell. By understanding the *in vitro* delivery, accumulation, degradation, toxicity and elimination of Au nanostructures, we will be able to develop safe nanomaterials that will be incorporated into applications *in vivo*. In other words, only with an adequate understanding of the cellular responses can the properties of Au nanostructures be effectively engineered and optimized for *in vivo* applications in terms of drug delivery, imaging contrast enhancement and therapy.[9]

Intracellular distribution: Regarding the cellular distribution of these nanoparticles, several *in vitro* studies have been performed. Upon administration, AuNPs seem to aggregate in endosomal/lysosomal vesicles but not in organelles, such as the nucleus. Furthermore, endocytosis seems to be the main route of entry.[288–291]

Gold nanoparticles and ROS production: In relation to the possible toxicity of different

nanostructured gold compounds, previous studies have been published. Particularly, the metallic nature of the AuNPs and the presence of the transition metal core encourage the production of reactive oxygen species (ROS) leading to oxidative stress.[292,293] Furthermore, once these nanoparticles enter a biological system, they can strongly associate with a diverse range of molecules present in the intracellular environment. Among them, lipids, nucleotides, low-molecular-weight species and proteins are known to establish strong interactions with these nanoparticles, which could cause an imbalance in the oxidative status and therefore the function of these molecules. Thus, Thakor et al. observed that after treating Hep G2 cells with AuNPs, at the relatively early time points, there were increases in antioxidant enzyme concentrations, which appeared to balance any deleterious effects associated with ROS, thereby protecting the cell.[292] Although the antioxidant enzyme concentrations continued to increase over time, the amount of ROS produced most likely overwhelmed these antioxidant defences since Hep G2 cells demonstrated evidence of oxidative stress-induced damage with increased tissue phospholipid and protein oxidation. Nevertheless, the main hypothesis holds that while AuNPs treatment induces oxidative stress, the cells may be able to avoid cell death through autophagic pathways. It is also likely that the oxidative environment could trigger off the autophagic process, rather than a direct cellular reaction to AuNPs presence in the cell.[293]

Nevertheless, other researchers have observed no sign of oxidative stress after administering AuNPs to cell cultures[290] or even a decrease in oxidative stress markers.[294] In this sense, the effect of gold nanoparticles on the oxidative status remains unclear.

DNA damage: In relation to the DNA damage caused by the exposure of culture cells to Au nanoparticles, Li et al. showed that they were able to inhibit cell proliferation by downregulating cell cycle genes.[289] Moreover, AuNPs not only seem to cause oxidative damage but also affect genes associated with genomic stability and DNA repair.

It has also been observed that the nanoparticles diameter plays a crucial role regarding genotoxicity.[295] Thus, smaller diameters (5 nm) induced a dose-dependent increment

in DNA damage, together with cell cycle arrests in G1 phase. On the contrary, larger nanoparticles showed no signs of obvious DNA toxicity.

1.2.5.2   In vivo studies

Different from *in vitro* applications that usually involve one type of cell, *in vivo* applications have to deal with many different types of cell lines involved in the transportation of nanostructures from the site of administration to the target organ. Upon entering the body, the nanostructures need to reach the target site and be selectively accumulated before any diagnosis or treatment can be conducted.[9]

Gold nanoparticles and tissue distribution: The biodistribution of Au nanostructures refers to their propagation into different types of tissues, organs and systems. Biodistribution and cellular uptake are dramatically dependent on size, morphology and surface chemistry.[296–298] Several factors must be taken into account in order to assess the localization of gold nanoparticles in the organs and tissues of interest, such as degree of aggregation, the presence of targeting ligands and the time of circulation in blood, among other things.[299] For example, De Jong et al. demonstrated that the fate of AuNPs after intravenous administration depends on their size.[300] According to their results, the smallest particle studied (with 10 nm of diameter) revealed the most widespread tissue distribution at 24 h after injection, while bigger AuNPs were found in liver, spleen and blood. In any case, liver seemed to have the highest concentration of AuNPs.

In fact, the physical dimensions of Au nanostructures seem to be extremely important in terms of nanoparticles dissemination.[301] For nanostructures with a size smaller than 6 nm, they will be rapidly filtered out and cleared by the kidneys, while those larger than 200 nm will be rapidly retained by spleen. Interestingly, the reticuloendothelial system (RES), which involves organs such as liver, spleen and bone marrow (rich in macrophages, Kupffer cells and monocytes), plays a critical role due to its ability to engulf and digest particulate materials. Longmire et al. proved that the RES was

responsible for the clearance of most nanostructures larger than 10 nm, regardless of their shape, morphology, and surface chemistry.[302]

When nanoparticles are placed in a biological fluid, they associate with a range of biomolecules via opsonization, forming a surrounding corona.[303] This corona can be schematically divided in two parts: a "soft" corona, in which biomolecules are dynamically exchanged between medium and particles, and a "hard" corona, composed of biomolecules having a strong affinity for the particle surface.[304] This corona creates an envelope that could completely mask the intrinsic functionalities of the nanoparticles.[305] Then, the Au nanostructures will be rapidly uptaken by the phagocytic cells in the RES. The liver seems to be the most important organ in Au clearance from the plasma due to its abundance of Kupffer cells, whose function is to eliminate foreign substances through phagocytosis.

Regarding cancer treatment, it is worth noting that the fact that the walls of blood vessels inside a tumour are leaky, allows nanostructures to pass through, while healthy endothelial cells do not allow nanostructures to go through the tight junctions (with a gap of ~ 0.4 nm).[306] Besides that, the insufficient drainage also facilitates the accumulation of nanostructures inside the tumour due to the largely absent and/or dysfunctional lymphatic system. This phenomenon is known as the enhanced permeability and retention effect and has served as a basis for the passive targeting in cancer therapy.[307] Generally, nanostructures with dimensions in the range of 30 – 200 nm show better retention by the tissue resistance, shifting the equilibrium toward extravasation and leading to enhancement in tumour accumulation.[308] This approach, together with the fact that gold nanoparticles can be bound to different ligands (such as peptides,[309] antibodies[310] or nucleic acids[311]), thus improving their tumour targeting efficiency, have aided to the development of gold nanocompounds as antitumor agents.

In terms of toxicity, the scarce available data indicate that Au nanoparticles are not toxic in the long term and that the hazardous deleterious effects are most likely to show up in the first few days to weeks after administration. Several studies show that

INTRODUCTION

Au nanoparticles are prone to accumulate in the major organs without exerting any adverse impact on the animals during the whole period (ranging from weeks to years).[101,312,313] For instance, Hainfeld et al assessed the effect of 1.9 nm Au clusters as X-ray contrast and radiotherapy enhancement, and found an increased survival rate after a year with no apparent adverse effect observed.[285]

The mechanism of elimination of Au nanoparticles from the body by urine and bile has also been under active research. The complex process of renal clearance implies glomerular filtration, tubular secretion and reabsorption. Thus, when nanoparticles circulate through the glomerular vessels, they can enter the proximal tubule through the porous glomerular capillary wall via physical filtration or electrostatic interaction. They may also be resorbed before ultimately being eliminated from the body. In any case, it is now well established that biological features of the organ limit the particles that can be processed by the kidney. Basically, since the nanoparticles need to pass through multiple layers of cell before the drainage, the functional pore size is typically on the scale of 5 nm for spherical particles.[314] Besides that, hydrodynamic diameter (HD) has a drastic effect on excretion efficiency. For instance, ultra-small core size objects (<6 nm) can soon become coated with serum proteins as they circulate in the blood, increasing their HD and blocking renal excretion.[302] This fact indicates that the filtration of nanoparticles is highly size-dependent; nanoparticles larger than the threshold can only accumulate in the kidney with little chance of being eliminated.

On the other hand, when AuNPs size is larger than renal filtration cut-off, nanoparticles are eliminated from the blood by the RES and thus tend to accumulate in the spleen and liver. However, although Kupffer cells are related to the clearance of nanoparticles from the bloodstream, hepatocytes seem to carry out the capture, catabolism and excretion of gold nanostructures, mainly via the biliary system.[276]

Gold nanoparticles and damage in lipids and proteins: The effect of gold nanoparticles on the structural integrity of lipids and proteins has also been under study. Free radicals are able to "steal" electrons from the lipids in cell membranes, thus resulting in lipids degradation and cell damage. ROS are also able to interact with

amino acids from cell proteins to carbonyl derivatives (like aldehydes and ketones), thus modifying the structure of these components. Thiobarbituric acid reactive substances (TBARS) and protein carbonyl groups are accepted markers of the amount of lipids and proteins that have been oxidized by highly reactive free radicals.

In this sense, increased levels of TBARS in liver, lung, heart and kidney were found after intraperitoneally injecting 10 nm AuNPs to Wistar-Kyoto rats.[315] Similar results were found in a study performed by Ferreira et al.[316] In this case, 10 and 30 nm AuNPs produced a clear rise in lipid peroxidation after both, acute and long-term exposure. On the other hand, it has already been proved that there exists a relation between gold nanoparticles and protein damage. Thus, Thakor et al. observed a significant increase in protein oxidation after exposing human cells to gold nanoparticles.[292] Analogously, Abdelhalim found that gold nanoparticles caused an imbalance in the antioxidant levels that resulted in an overproduction of ROS and, consequently, an increase in protein carbonyl groups.[317]

Gold nanoparticles and inflammation: Several studies have been developed in order to determine whether the treatment with gold nanoparticles could trigger off an inflammatory response. Although some authors indicated that these nanomaterials were able to induce acute inflammation,[318,319] it is widely accepted that gold nanoparticles do not modify the expression of inflammation-related cytokines.[320–322]

Biochemical parameters and gold nanoparticles: Similarly to what is described about the inflammation process, the effect of gold nanoparticles on the levels of various biochemical parameters has also been under consideration. In fact, the obtained results have been debated. Some authors suggest that the contact with gold nanoparticles have led to a rise in the expression of some biochemical parameters, bringing together cell death and promoting the harmful effects of some diseases.[316,323] However, several researchers indicate the absence of alterations in biochemical parameters after administering gold nanoparticles.[324,325] Regarding this controversy, the present thesis will try to clarify whether treatment with gold nanoparticles establishes a biochemical disorder.

2. AIMS

As described in the introduction of this doctoral thesis, the presence of gold nanoparticles in multiple applications and products is continuously growing due to the unique properties that materials show when designed in the nanometer scale. Special mention deserves the clinical applications of gold nanoparticles in biomedicine. However, it is mandatory to assess the potential risks that the exposure to these structures may imply regarding public health.

The main aim will be to address *the study of the metabolic alterations derived from the exposure to gold nanoparticles, as well as their biodistribution and repercussion on the oxidative status.*

This general objective will be accomplished by the achievement of these specific goals:

A. *IN VITRO* EXPERIMENTS: Hepatocellular carcinoma (Hep G2) and colorectal carcinoma (HT-29) cells will be exposed to AuNPs under different conditions in order to assess the effects on cell homeostasis by:

- *Evaluating the production of radical oxygen species and cytotoxicity of hepatocytes exposed to citrate-stabilised gold nanoparticles:* this study will be performed to assess whether the exposure to gold nanoparticles may induce the overproduction of ROS and consequently have a repercussion on the cell viability.

- *Assessing the DNA integrity of Hep G2 cells treated with gold nanoparticles:* DNA may be damaged if an external agent increases ROS. The comet assay will be completed to determine whether there exists any relation between the exposure to three different gold nanoparticles and an increase in the DNA breaks.

- *Evaluating the intracellular localization of gold nanostructures over time:* the final fate of the different nanostructures inside the cell will be studied by TEM.

B. *IN VIVO* EXPERIMENTS: Experimental animals were treated with three different sizes of gold nanoparticles, in an attempt to study the alterations that may be related, in terms of:

- *Protein and lipid damage:* the effect of the exposure to gold nanoparticles on the macromolecules that form the cell structures will be also evaluated by the measurements of the lipid peroxidation and protein carbonyl groups.

- *Gold biodistribution:* this study was performed to determine the concentration of gold in multiple organs, thus allowing us to establish the organs that play an important role in the accumulation and elimination of the gold nanoparticles.

- *Intracellular localization:* similarly to what is proposed in vitro, TEM images will be obtained to evaluate the fate of gold nanoparticles. These results will determine any possible differences with the in vitro studies.

- *Biochemical and inflammatory status:* the influence of the AuNPs exposure on the levels of biochemical and inflammatory parameters will be assessed in an attempt to determine if these nanostructures are able to induce a major damage or an inflammatory response.

- *Haematological markers:* the determination of the haematological parameters in rats treated with AuNPs will provide information about the possible effect that these nanocompounds may have on the integrity of the bone marrow and the formation of red and white blood cells, as well as some key factors related to anaemic states such as haemoglobin concentration or haematocrit.

3. MATERIALS & METHODS

3.1 GOLD NANOPARTICLES

Citrate-stabilized gold nanoparticles (AuNPs) with 10, 30 or 60 nm of diameter size suspended in ultrapure water at 50 mg·L^{-1} were purchased at the National Institute of Standard and Technology (NIST RM 8011, 8012 and 8013, Gaithersburg, USA). These nanoparticles represent commercially available reference materials and are specifically certified for the mean size and their distribution (evaluated by several analytical characterisation techniques) and their total gold concentrations. The reference values obtained by TEM (given by the manufacturer) were 8.9 ± 0.1, 27.6 ± 2.1, and 56.0 ± 0.5 nm respectively. The lowest dose of AuNPs used in the present study is one of the most employed one in toxicity assays.[290,326] The highest dose was chosen in order to evaluate the possible negative effects.

3.2 IN VITRO STUDIES

3.2.1 Cell culture conditions

Hepatocellular carcinoma (Hep G2) and colorectal carcinoma (HT-29) cell lines were obtained from the Cell Culture Resource Centre at the University of Granada, Spain. The cells were precultured in 25cm^2 culture flasks in RPMI-1640 medium (containing 2.0 mg mL^{-1} sodium bicarbonate) supplemented with 10% (v/v) FBS and 2 mmol·L^{-1} glutamine (Sigma, St Louis, MO, USA). The culture flasks were maintained in a cell incubator at 37ºC in a humidified atmosphere of 5% CO_2 and 95% air. Medium was replaced every 2–3 days after rinsing with PBS (Sigma, St Louis, MO, USA). Upon reaching confluence, cells were treated with trypsin–EDTA solution (Sigma, St Louis, MO, USA) and split 1/10 to allow for continuous growth.

3.2.2 Short-term cell viability assay

Hepatocytes were treated for 16 or 32 h with a final concentration of 10 µg·L^{-1} or 10 mg·L^{-1} of 10, 30 or 60 nm size gold nanoparticles. Experiments were carried out to

assess cell viability using lactate dehydrogenase (LDH) assay according to manufacturer´s protocol (Cytotoxicity Detection Kit, Mannheim, Germany). Briefly, lactate dehydrogenase is a stable cytoplasmic enzyme present in all cells. It is rapidly released into the cell culture supernatant upon damage of the plasma membrane. Thus, the culture supernatant is collected cell-free and incubated with the reaction mixture from the kit. The LDH activity is determined in an enzymatic test: In the first step NAD+ is reduced to NADH/H+ by the LDH-catalyzed conversion of lactate to pyruvate. In the second step the catalyst (diaphorase) transfers H/H+ from NADH/H+ to the tetrazolium salt INT which is reduced to formazan.

Consequently, an increase in the amount of dead or plasma membrane-damaged cells results in an increase of the LDH enzyme activity in the culture supernatant. This increase in the amount of enzyme activity in the supernatant directly correlates to the amount of formazan formed during a limited time period. Therefore, the amount of colour formed in assay is proportional to the number of lysed cells. The formazan dye formed is water-soluble and shows a broad absorption maximum at about 500 nm, whereas the tetrazolium salt INT shows no significant absorption at these wavelengths.

3.2.3 ROS production

Hep G2 cells were seeded in a 6-well plate and incubated overnight in order to allow them to grow. The cells were incubated with 10, 30 or 60 nm size gold nanoparticles at 10 $\mu g \cdot L^{-1}$ or 10 $mg \cdot L^{-1}$ for 16 or 32 h. ROS overproduction was assessed by including a non-fluorescent probe (H_2DCFDA). This cell-permeant compound is a chemically reduced form of fluorescein used as an indicator for reactive oxygen species (ROS) in cells. Upon cleavage of the acetate groups by intracellular esterases and oxidation by ROS, the non-fluorescent H_2DCFDA is converted to the highly fluorescent 2',7'-dichlorofluorescein (DCF).

Fluorescence was measured using a microplate reader (Infinitive 200, Tecan, Zürich, Switzerland). The excitation wavelength was set to the absorption maximum (485 nm)

and emission was recorded to 538 nm. These results were normalized by the cell viability.

3.2.4 Comet assay

Hep G2 cells were allowed to grow until 60% confluence was reached. Afterwards, cell cultures were exposed to 10 mg·L^{-1} 10, 30 or 60 nm size gold nanoparticles for 16 h. Positive control cells were treated with 100 mmol·L^{-1} H$_2$O$_2$ for 1 h. Upon treatment, cells were treated with trypsin–EDTA solution (Sigma, St Louis, MO, USA) and centrifuged until getting a pellet. Cells were suspended in 1 mL PBS (Sigma, St Louis, MO, USA).

Three microscope glass slides per sample were pre-coated with 1 % NMP agarose on one side. 30 µL cell suspension were mixed with 65 µL of LMP agarose solution (final LMP agarose concentration 0.5%). Drops of each agarose-cell suspension were added on each pre-coated slide and placed for 1 h at 4ºC in the lysis solution that contained NaCl 2.225 M (Sigma, St Louis, MO, USA), Na$_2$EDTA 88.9 mM (Merck, Darmstadt, Germany), Tris 8.8 mM (Merck, Darmstadt, Germany), NaOH 0.22 M (Sigma, St Louis, MO, USA), 10% DMSO (Sigma, St Louis, MO, USA) and 1% Triton X-100 (Sigma, St Louis, MO, USA). Electrophoresis (1 V/cm) was carried out for 20 min at 4ºC using electrophoresis solution (Na$_2$EDTA 1 mM and NaOH 300 mM, pH>13). Slides were neutralised three times (5 min every time) with Tris 0.4 M. Ethanol was used to fix slides. Finally, samples were stained with DAPI (1 µg·mL^{-1}) and analysed using a fluorescence microscope (Eclipse Ni; Nikon Instruments Europe B.V., Badhoevedorp, The Netherlands). 150 nucleoids per sample (50 nucleoids per slide) stained with DAPI were scored by computerized image analysis (Comet Assay IV, Perceptive Instrument, Suffolk, UK). DNA damage was determined by comparing moment tails among groups.

3.2.5 Image studies

HT-29 cells were treated with 10 mg·L^{-1} AuNPs for 2, 4 or 16 h in order to determine their subcellular location throughout time. Once the exposure time had finished, cells were prepared to be visualised by TEM.

3.3 IN VIVO STUDIES

3.3.1 Animals

In this experiment, male Wistar rats weighing 190-220 g (Charles River Laboratories, L'Arbresle, France) were randomly divided into four groups. Control group: eight rats were injected 0.4 mL ultrapure water·day^{-1}. AuC 10 group: eight rats were injected 0.4 mL·day^{-1} 10 nm size gold nanoparticles solution. AuC 30 group: eight rats were injected 0.4 mL·day^{-1} 30 nm size gold nanoparticles solution. AuC 60 group: eight rats were injected 0.4 mL·day^{-1} 60 nm size gold nanoparticles solution. In all cases, the administration route was intraperitoneal.

All rats were allowed free access to drinking water and diet (the semi-synthetic diet AIN93M[327]) and weight gain and intake of food and water were monitored throughout the experimental period. From day 0 of the experiment, all animals were housed in individual metabolic cages designed for the separate collection of faeces and urine and the animal behaviour was monitored along the experiment. The cages were located in a well-ventilated, temperature-controlled room 21±2ºC with relative humidity ranging from 40 to 60%, and a light:dark period of 12 h. On day 9, the rats were anaesthetised with a solution of ketamine (0.75 mg·kg^{-1} body weight, Fatro Ibérica, Barcelona, Spain) and xylazine (0.10 mg·kg^{-1} body weight, Fatro Ibérica, Barcelona, Spain), and exsanguinated by cannulating the posterior aorta. Blood was collected (with heparin as anticoagulant) and taken for quantification of blood parameters. Afterwards, it was centrifuged (Beckman, Fullerton, CA, USA) at 3,000 rpm for 15 min to separate the serum. The liver, kidney, spleen, brain, lung, testicle, femur, heart, intestine and gastrocnemius muscle were removed, weighed, placed in pre-weighed polyethylene vials, and stored at -80ºC.

The organ to body weight ratios (which represent the number of grams of tissue for every 100 grams of body weight) was calculated by dividing the weight of the organ by the total body weight and multiplying by 100 to get the final percentage.

All experiments were undertaken according to Directional Guides Related to Animal Housing and Care (European Community Council, 2010), and the Animal Experimentation Ethics Committee of the University of Granada approved all procedures.

3.3.2 Liver homogenisation

Liver was homogenised in 0.05 M phosphate buffer (pH 7.8) containing 1 g L^{-1} Triton X-100 and 1.34 mM of EDTA using a Micra D-1 homogeniser (ART moderne Labortechnik; Müllheim-Hügelheim, Germany) at 18,000 rpm during 30 s followed by treatment with Sonoplus HD 2070 ultrasonic homogeniser (Bandelin, Berlin, Germany) at 50% power for 10 s.

3.3.3 Determination of protein carbonylation and lipid peroxidation in liver

The levels of protein carbonyl groups were assessed using the Protein Carbonyl Kit (Cayman Chemical Company, MI, USA) and following manufacturer´s instructions.

Thiobarbituric acid reactive substances (TBARS), as a marker of lipid peroxidation, were measured by an adaptation of the method of Ohkawa et al. in rat liver homogenates[328]. Concisely, 0.5 g dry tissue were homogenised in phosphate buffer (final concentration 10% w/V). 0.2 mL of homogenised livers were mixed with 0.1 mL of 8.1 % sodium dodecyl sulfate, 0.75 mL of 20 % acetic acid and 0.75 mL of 0.8 % thiobarbituric acid. The reaction mixture was finally made up to 2 mL with ultra-pure water. After vortexing, samples were incubated for 60 min in 95 °C and cooling with tap water; 2 mL of butanol–pyridine solution 15:1 (v/v) was added. The mixture was shaken and centrifuged at 3,000 rpm for 7 min. The organic layer was measured spectrophotometrically at 532 nm. Standard solutions of MDA were used for calibration and the values were expressed in nmol MDA·g^{-1} of tissue.

3.3.4 Gold content in tissues

The extracted organs were previously freeze-dried (Cryodos56, Barcelona, Spain). Prior to the determination of the content of trace elements in each tissue, a microwave digestion of each sample is required as sample pre-treatment for the analysis in ICP-MS. Therefore, 50 mg of each tissue were weighed (with a 5 digits weight balance) into a digestion vial of the microwave system (Milestone, Sorisole, Italy), followed by the addition of 10 mL of *aqua regia* (a combination of HCl and HNO_3 in proportion 3:1) for the determination of gold content in organs. When the sample had been digested, the extract was collected and made up to a final volume of 15 mL with ultra-pure water (18.2 Ω) obtained using a Milli Q system (Millipore, Bedford, MA, USA) for subsequent analysis. Besides, all the plastic containers used in the analysis were previously cleaned with super-pure nitric acid and ultra-pure water. Total gold levels in samples were determined by collision cell ICP–MS (He mode) (Agilent 7700, Waldbronn, Germany). Calibration curves were prepared following the Rh addition technique as an internal standard (final Rh concentration 1 ppb), using stock solutions of 1000 mg·L^{-1} (Merck). The method was validated by recovery studies in samples of organs enriched with Au standards. The percentage of CV obtained was 2.9% for Au. The mean of five separate determinations was used. The instrumental settings of the ICP-MS are presented in the next table.

Table 1. Instrumental setting of the ICP-MS for the measurements of gold content in tissues

	INSTRUMENTAL SETTINGS
Instrument	Agilent 7700
RF power	1500 W
Auxiliary gas flow	0.87 L·min^{-1}
Coolant gas flow	15.5 L·min^{-1}
Dwell time	100 ms
Isotope monitored	^{197}Au
Nebulizer	Meinhard-Type

Spray chamber	Peltier-cooled Scott-type spray chamber
Nebulizer gas flow	1.01 L·min^{-1}

3.3.5 Haematological parameters

Different haematological parameters were measured with a blood autoanalyser (KX-21 Automated HematologyAnalyzer, Sysmex Corporation, Kobe, Japan). White blood cells (WBC), red blood cells (RBC), haemoglobin (HGB), haematocrit (HCT), mean corpuscular haemoglobin (MCH), mean corpuscular haemoglobin concentration (MCHC) and red cell distribution width (RDW) data were recorder for further analysis.

3.3.6 Determination of proinflammatory parameters

Interleukin-1ß (IL-1ß), interleukin-6 (IL-6), interleukin-10 (IL-10) and tumour necrosis factor alpha (TNF-α) levels were determined in liver using the kit Milliplex MAP Rat Cytokine/Chemokine Magnetic Bead Panel, RECYTMAG-65K, with the Luminex xMAP detection system (EMD, Millipore Corporation, Billerica, MA, USA). Assays were performed according to the manufacturer's instructions. Briefly, 50 mg liver tissue were homogenised with 500 µL of buffer (Roche, FNN00071). Then, samples were centrifuged at 10,000 rpm for 5 min at 4ºC and supernatants were collected. 25 µL of supernatants were incubated with magnetic microspheres (whose surfaces are coated with the cytokines antibodies) in a 96 well plate. A calibration curve was prepared from a IL-1ß, IL-6, IL-10 and TNF-α solution. The analysis was performed using a MAGPIX system (Millipore, Germany).

3.3.7 Determination of biochemical parameters

Glucose, urea, uric acid, triglycerides, albumin, cholesterol, gamma glutamyl transpeptidase (γ-GT), alkaline phosphatase, glutamic oxaloacetic transaminase (GOT)

and glutamic pyruvic transaminase (GPT) in plasma were measured with enzymatic colorimetric tests in an Olympus AU5800 autoanalyser (Beckman Coulter, California, USA).

3.4 TEM

Intestine cell cultures and liver samples were fixed with fresh primary fixative (1.5% glutaraldehyde, 1.0% formaldehyde in 0.05 M sodium cacodylate buffer, pH 7.4) and post-fixed with secondary fixative (1% osmium tetroxide, 1% potassium ferrocyanide in ultra-pure water) followed by dehydration with ascending series of alcohol before embedding samples in epoxy resin. Ultra-thin sections were cut and doubly stained with uranyl acetate and lead citrate. A transmission electron microscope LIBRA 120 PLUS microscope at 120 kV (Carl Zeiss SMT., Oberkochen, Germany) was used to determine the fate and uptake of AuNPs into cells.

3.5 STATISTICAL ANALYSIS

All variables and indexes were analysed with descriptive statistics, and the results are reported as the mean and standard deviation. Statistical comparisons among the groups were performed by the Mann-Whitney test, a nonparametric testing for unrelated samples. For the bivariate analysis, Spearman's coefficient of correlation was calculated. All analyses were carried out with the version 20.0 of the Statistical Package for Social Sciences (SPSS Inc., Chicago, IL). Differences were considered significant at the 5% probability level.

4. RESULTS

4.1 IN VITRO

4.1.1 Cell viability assay

Cell viability was assessed with the lactate dehydrogenase assay in Hep G2 cells. The AuNPs provoked a decrease in viability at 16 h, compared to the control group. This viability tended to normalise after 32 h. No significant differences were found regarding the size of the nanoparticles.
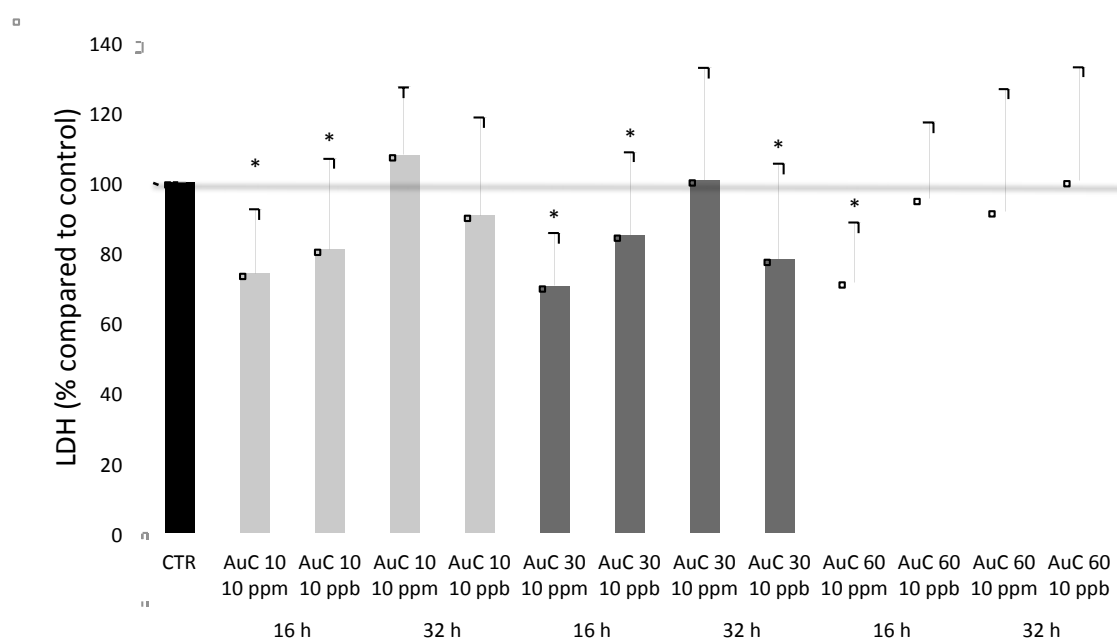
Figure 11. Cell viability assay in hepatic cells. Values shown are means ± SD, CTR (Control cells); AuC 10 (cells treated with 10 nm AuNPs); AuC 30 (cells treated with 30 nm AuNPs); AuC 60 (cells treated with 60 nm AuNPs). [*] Different from control group. P<0.05

4.1.2 ROS production

The effect of AuNPs on the generation of ROS was confirmed after observing an increase in every sample treated with 10 ppm AuNPs at 16 h. This overproduction was normalised after 32 h of treatment. As expected, these results agree with those

related to cell viability; thus revealing a growth in cell mortality as the ROS production increases.
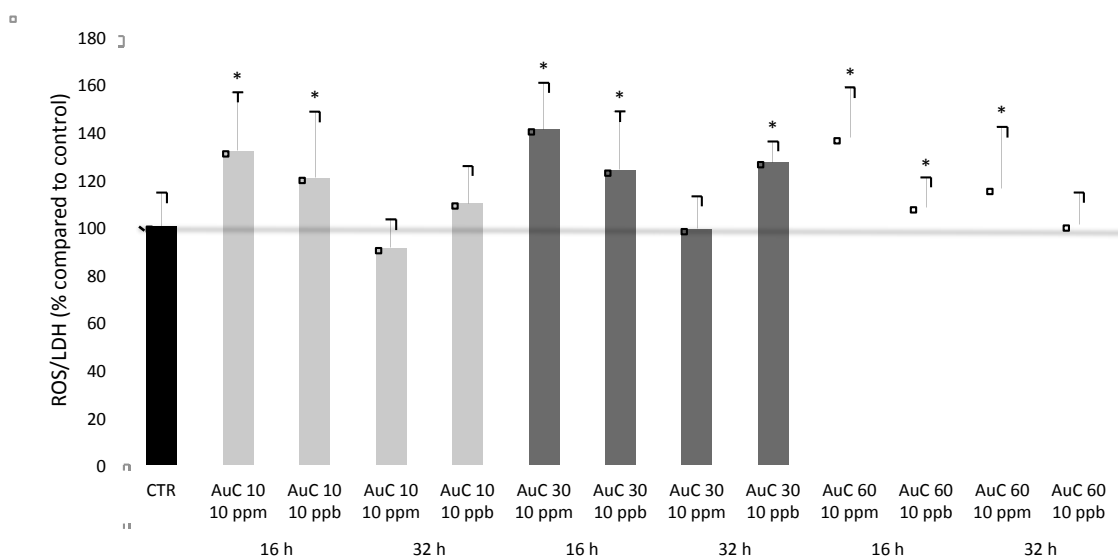
Figure 12. ROS production in hepatic cells. Values shown are means ± SD, CTR (Control cells); AuC 10 (cells treated with 10 nm AuNPs); AuC 30 (cells treated with 30 nm AuNPs); AuC 60 (cells treated with 60 nm AuNPs). * Different from control group. P<0.05

4.1.3 AuNPs-induced oxidative damage to DNA

Moment tail measurements showed that there was a significant increase in the DNA damage of all treated groups compared to the negative control cells. In fact, the smaller the nanoparticle size, the higher the damage observed. No significant differences were found between the positive control cells and the cell culture treated with 10 nm AuNPs. 30 and 60 nm AuNPs caused higher increases of moment tail compared to the negative control cells, although these increases were lower than the positive control group.

Table 2. Moment tails of control and treated hepatocytes.

Positive	AuC 10	AuC 30	AuC 60	Negative

	control				control
Moment tail	12.91±6.46	17.45±7.51	8.06±2.88[a,b]	4.26±6.34[a,b]	1.38±1.05[a,b,c]

Values showed are means ± SD. Positive control (cells treated with H_2O_2); AuC 10 (cells treated with 10 nm AuNPs); AuC 30 (cells treated with 30 nm AuNPs); AuC 60 (cells treated with 60 nm AuNPs); Negative control (cells without treatment). [a] Different from positive control group; [b] Different from AuC 10; [c] Different from AuC 30. $P<0.05$

4.1.4 Image studies

Three different exposure periods were tested in colon cells in order to determine the effect of time on subcellular location and possible degradation of AuNPs. Images revealed that in early stages after the exposure to the nanoparticles, they are easily found throughout cytosol and extracellular spaces. However, AuNPs were relocated along time, being found in nucleus and lipid drops after 16 h of exposure.
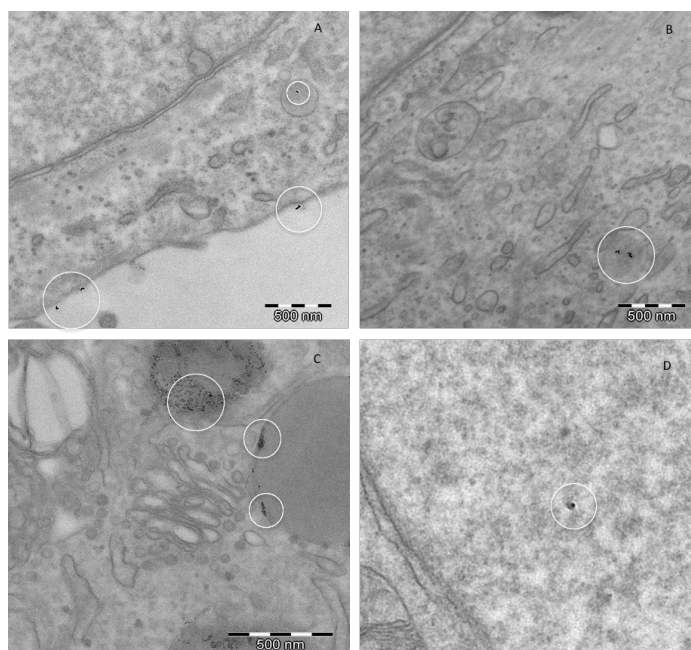
Figure 13. TEM images from colon cells treated with 10 nm AuNPs. A (nanoparticles are found outside the cell after 2 h of administration); B (free AuNPs throughout cytosol after 4 h of treatment); C (metabolised nanoparticles are stored in lipid drops after 16 h of treatment); D (AuNP inside the nucleus of a cell)

82

4.2 IN VIVO

4.2.1 Behavioural toxicity assessment

The intraperitoneal injections were well tolerated, with no clinical signs of toxicity after gold administration and rats did not exhibit social alterations throughout the experiment.

4.2.2 Body weight, food and water intake

Results from the body weight indicate that the increase of weight was slower in those rats treated with gold nanoparticles compared to the control group. This tendency was statistically significant in the AuC 10 group at day 4 (at the middle of the experimental period) and AuC 10 and AuC 30 at day 9 (end of the experimental period). These results agreed with those related to food intake. Thus, the amount of diet ingested was similar at the beginning of the experiment and it decreased throughout the exposure time in all treated groups.

Regarding water consumption, a different effect was found. There was a significant increase in all treated group compared to the control in relation to the water intake. Interestingly, this increase is associated with the body weight gain. Thus, the more water intake the less body weight increase was found.
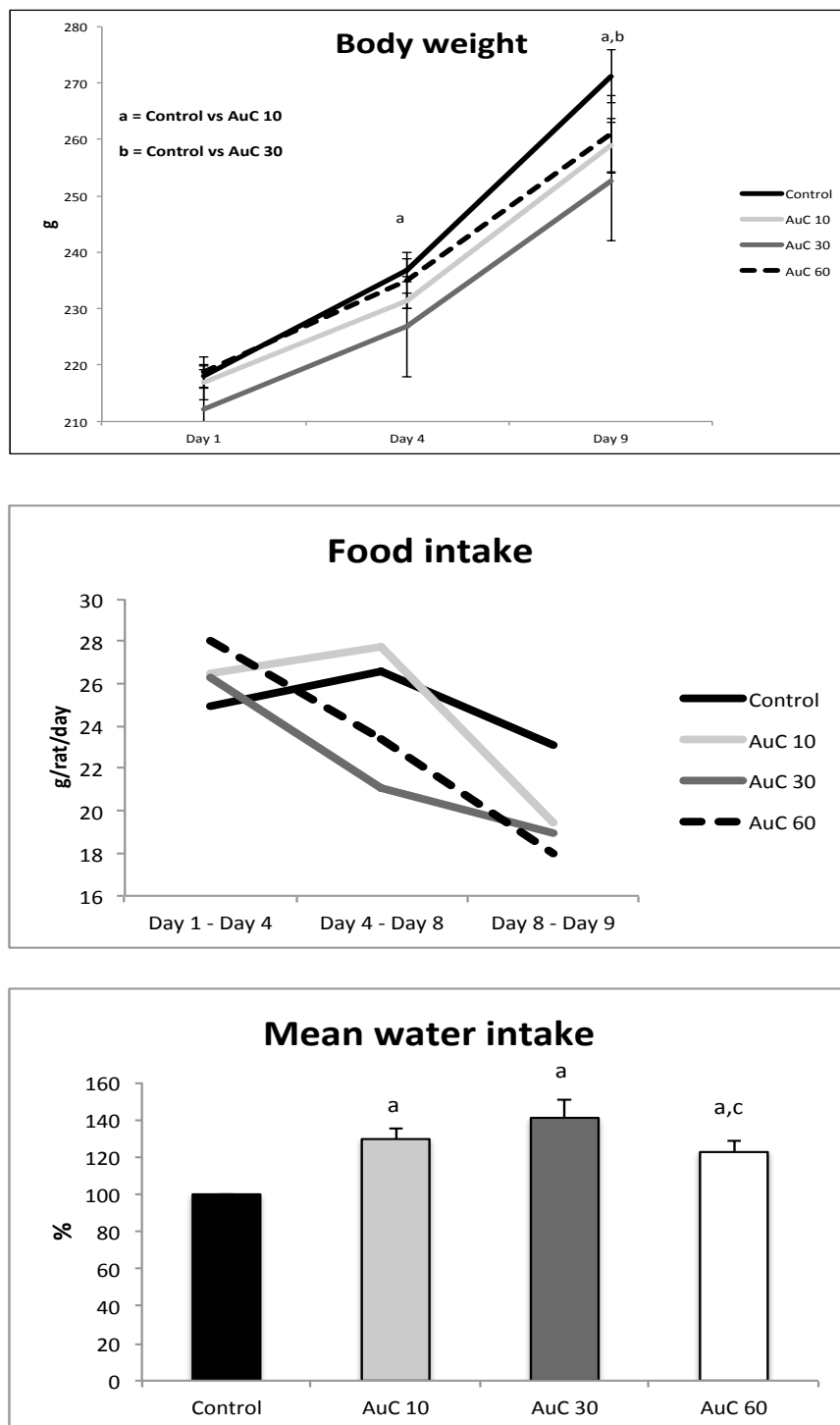
Figure 14. Body weight gains, total food intakes and percentages of water consumption of the different experimental groups. Values shown are means ± SD, Control (Control group); AuC 10 (rats treated with 10 nm AuNPs); AuC 30 (rats treated with 30 nm AuNPs); AuC 60 (rats treated with 60 nm AuNPs). [a] Different from control group, [b] different from AuC 10, [c] different from AuC 30 group. P<0.05

RESULTS

4.2.3 Organ to body weight ratios

Data from organ weights compared to total body weights point out that no significant differences were found in any treated group when comparing to the control rats.

Table 3. Organ to body weight ratios from the experimental groups.

	Organ to body weight ratios			
	Control	**AuC 10**	**AuC 30**	**AuC 60**
Liver/body	2.73±0.14	2.73±0.02	2.78±0.20	2.61±0.09
Kidney/body	0.34±0.02	0.35±0.04	0.35±0.01	0.37±0.01
Spleen/body	0.26±0.03	0.27±0.05	0.22±0.03	0.25±0.03
Heart/body	0.32±0.03	0.31±0.02	0.33±0.04	0.31±0.02
Brain/body	0.70±0.03	0.70±0.05	0.75±0.05	0.72±0.02
Lung/body	0.58±0.08	0.50±0.04	0.43±0.03	0.43±0.04
Testicle/body	0.53±0.09	0.58±0.05	0.58±0.07	0.55±0.04
Muscle/body	0.58±0.02	0.55±0.06	0.59±0.08	0.65±0.04

Values are shown as mean±SD. Control (Control rats); AuC 10 (rats treated with 10 nm AuNPs); AuC 30 (rats treated with 30 nm AuNPs); AuC 60 (rats treated with 60 nm AuNPs).

4.2.4 Evaluation of the lipid peroxidation

TBARS measurements indicate that the treatment with AuNPs caused a significant rise in lipid peroxidation. The increase was slightly higher in those rats treated with 10 nm AuNPs.

TBARS
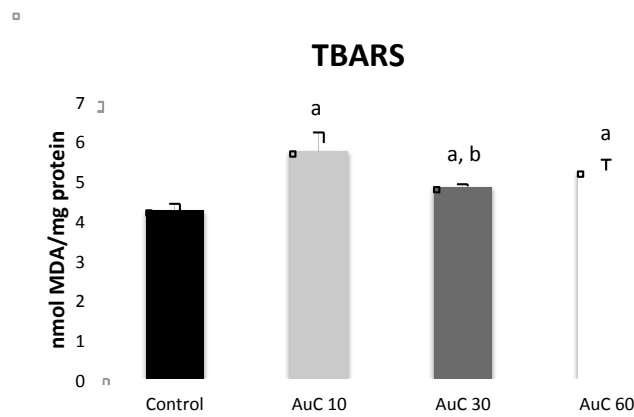
Figure 15. Comparison of the lipid peroxidation in livers of the experimental animals. Values shown are means ± SD, Control (Control group); AuC 10 (rats treated with 10 nm AuNPs); AuC 30 (rats treated with 30 nm AuNPs); AuC 60 (rats treated with 60 nm AuNPs). [a] Different from control group, [b] different from AuC 10 group. P<0.05

These results indicate that the exposure to gold nanoparticles caused a 35%, 14% and 23% increase in lipid damage in the AuC 10, AuC 30 and AuC 60 groups respectively, compared to the control group.

4.2.5 Influence of AuNPs on protein carbonylation

The administration of AuNPs caused a significant rise in the protein carbonyl groups formation, compared to the control groups. No differences were found among the treated groups.

Figure 16. Protein carbonylation in livers of rats treated with AuNPs. Values shown are means ± SD, Control (Control group); AuC 10 (rats treated with 10 nm AuNPs); AuC 30 (rats treated with 30 nm AuNPs); AuC 60 (rats treated with 60 nm AuNPs). [a] Different from control group. P<0.05

RESULTS

The obtained data reveal that there was a 168%, 112% and 174% (±81%) increase in protein damage in the rats treated with 10, 30 and 60 nm gold nanoparticles respectively, compared to the control group.

4.2.6 TEM images

After administering the nanoparticles to the animals, slides of liver samples were observed by transmission electron microscopy. AuNPs were stored in lipid drops; although the size of these nanoparticles was smaller than the original ones (~6-8 nm). Some single, non-aggregated AuNPs were also found dispersed throughout the cytosol.
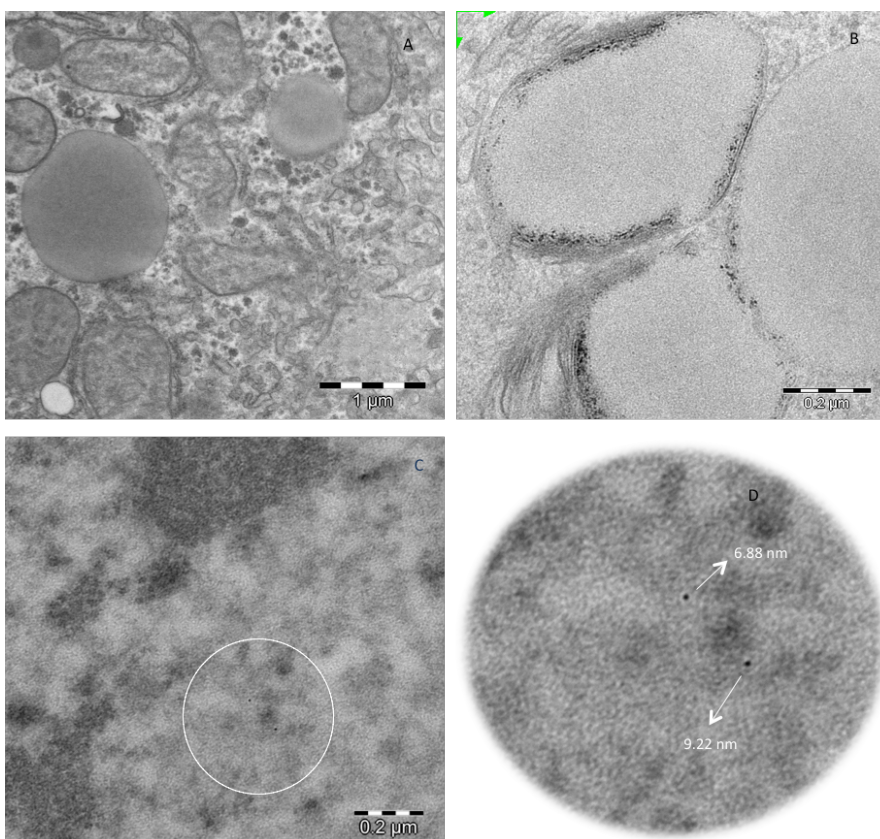
Figure 17. TEM images from hepatocytes of untreated rats (A) versus rats treated with AuC 10 (B, C and D). A (subcellular structures with clean lipid drops among them); B (lipid drops with small nanoparticles); C (nucleus from a cell with two nanoparticles inside it); D (enlargement from image C, with the sizes of two nanoparticles)

In the case of the organs exposed to 10 nm AuNPs, some nanoparticles were able to cross the nucleus membrane and were found inside it.

4.2.7 Gold content in rat organs

ICP-MS measurements in the liver and kidney showed that the rats treated with 10 and 30 nm AuNPs accumulated the highest concentration of gold, showing no significant differences between both groups. Lower content of gold was found in the group treated with 60 nm AuNPs, although it was significantly higher than the control animals.

Figure 18. Gold content in liver and kidney of animals exposed to AuNPs. Values shown are means ± SD, Control (Control group); AuC 10 (rats treated with 10 nm AuNPs); AuC 30 (rats treated with 30 nm AuNPs); AuC 60 (rats treated with 60 nm AuNPs). [a] Different from control group, [b] different from AuC 10, [c] different from AuC 30 group. P<0.05

RESULTS

In accordance with the previous organs, all exposed rats showed significant higher content of gold in the spleen. Especially remarkable was the amount of gold in the rats treated with the 60 nm size AuNPs. In contrast with the rest of analysed organs, the spleen was the unique organ where the deposits of gold in those animals treated with 60 nm AuNPs were significantly higher.
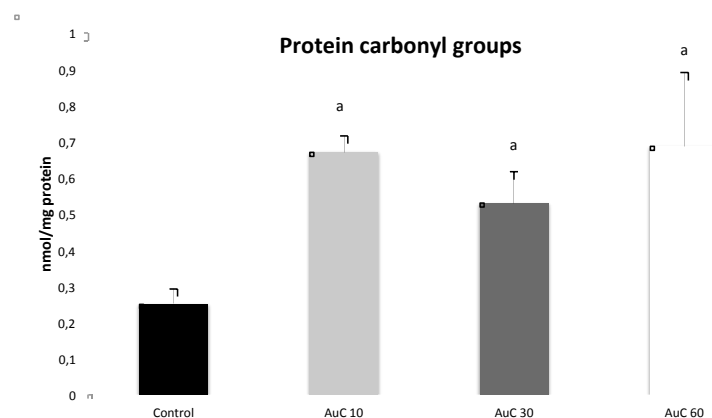

Figure 19. Gold concentration in spleen of rats treated with AuNPs. Values shown are means ± SD, Control (Control group); AuC 10 (rats treated with 10 nm AuNPs); AuC 30 (rats treated with 30 nm AuNPs); AuC 60 (rats treated with 60 nm AuNPs). [a] Different from control group, [b] different from AuC 10. $P<0.05$

In relation to the intestine, a very marked, significant increase was observed in the gold levels after injecting the three studied nanoparticles, even though the administration route was not enteral but intraperitoneal. Especially relevant was the high abundance of 10 nm AuNPs in this tissue.

Figure 20. Gold content in intestine of rats exposed to AuNPs. Values shown are means ± SD, Control (Control group); AuC 10 (rats treated with 10 nm AuNPs); AuC 30 (rats treated with 30 nm AuNPs); AuC 60 (rats treated with 60 nm AuNPs). [a] Different from control group. $P<0.05$

Regarding the excreta, although relevant levels of gold were detected in 24 h urine of exposed rats compared to the untreated group, it resulted not to be the main excretion route in any of the studied AuNPs sizes, as the results showed that the concentration of gold in faeces was much higher, especially when the administrated AuNPs sizes were 10 and 30 nm.

Figure 21. Gold concentration in urine and faeces of animals treated with AuNPs. Values shown are means ± SD, Control (Control group); AuC 10 (rats treated with 10 nm AuNPs); AuC 30 (rats treated with 30 nm AuNPs); AuC 60 (rats treated with 60 nm AuNPs). [a] Different from control group. P<0.05

In relation to the muscle, although no significant differences were observed, an important tendency to accumulate was detected among groups treated with nanoparticles, especially in the case of the rats exposed to 10 nm AuNPs. Similar pattern was perceived in heart and bone; although AuC 10 group did not showed higher accumulation when compared to other treated groups.
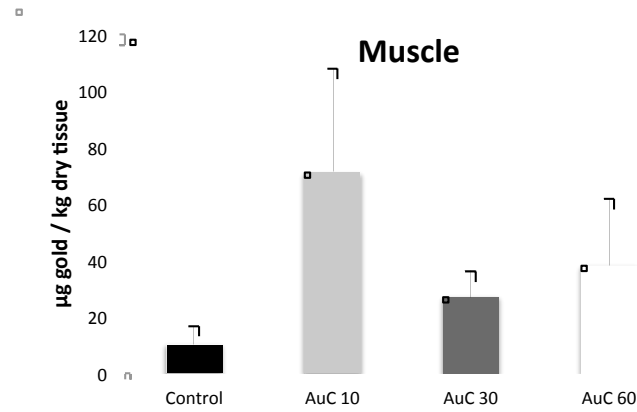
Figure 22. Gold content in gastrocnemius muscle of rats treated with AuNPs. Values shown are means ± SD, Control (Control group); AuC 10 (rats treated with 10 nm AuNPs); AuC 30 (rats treated with 30 nm AuNPs); AuC 60 (rats treated with 60 nm AuNPs).

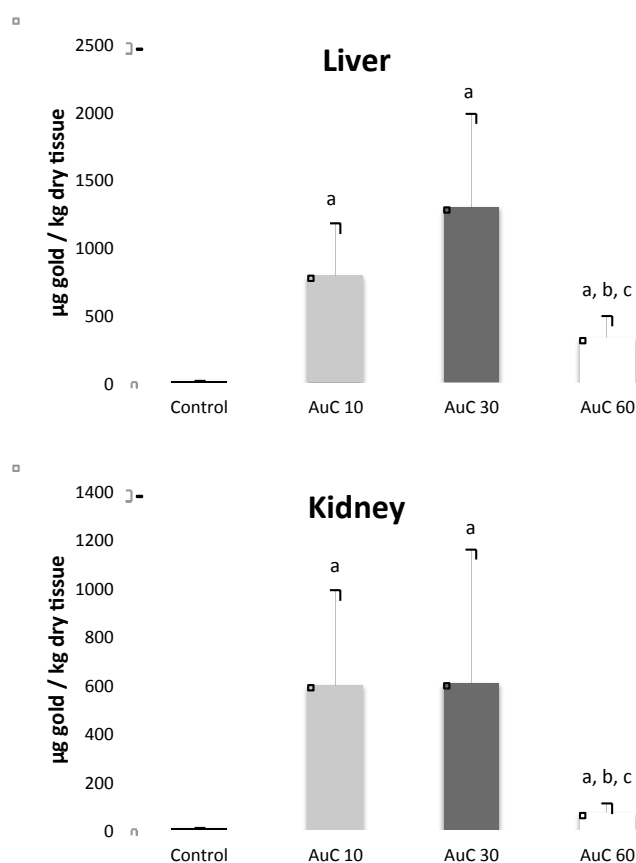**Figure 23. Gold content in heart of rats exposed to AuNPs.** Values shown are means ± SD, Control (Control group); AuC 10 (rats treated with 10 nm AuNPs); AuC 30 (rats treated with 30 nm AuNPs); AuC 60 (rats treated with 60 nm AuNPs).

Figure 24. Gold content in bone of rats treated with AuNPs. Values shown are means ± SD, Control (Control group); AuC 10 (rats treated with 10 nm AuNPs); AuC 30 (rats treated with 30 nm AuNPs); AuC 60 (rats treated with 60 nm AuNPs).

10 and 60 nm AuNPs showed a relevant tendency to accumulate in testicles, even though no significant changes were observed when compared to control and 10 nm AuNPs-exposed rats.
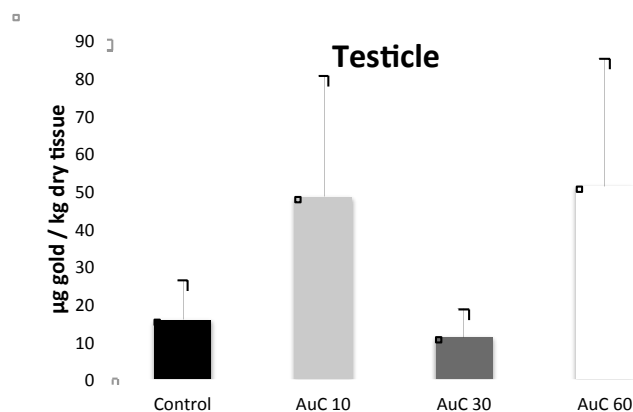
Figure 25. Gold concentration in testicle of rats exposed to AuNPs. Values shown are means ± SD, Control (Control group); AuC 10 (rats treated with 10 nm AuNPs); AuC 30 (rats treated with 30 nm AuNPs); AuC 60 (rats treated with 60 nm AuNPs).

Regarding brain and lungs, no changes were measured among groups, thus indicating that gold did not accumulate in these organs.
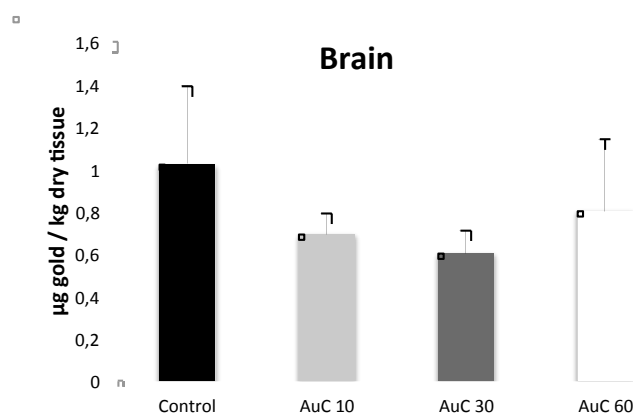
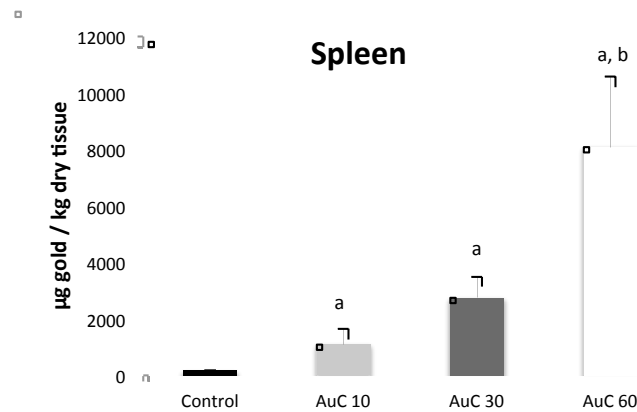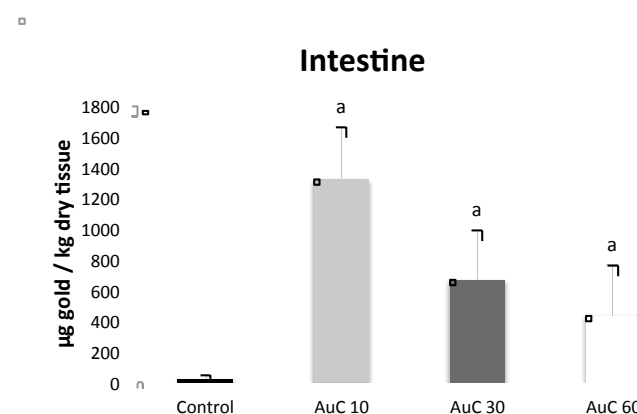**Figure 26. Gold content in brain of rats treated with AuNPs.** Values shown are means ± SD, Control (Control group); AuC 10 (rats treated with 10 nm AuNPs); AuC 30 (rats treated with 30 nm AuNPs); AuC 60 (rats treated with 60 nm AuNPs).
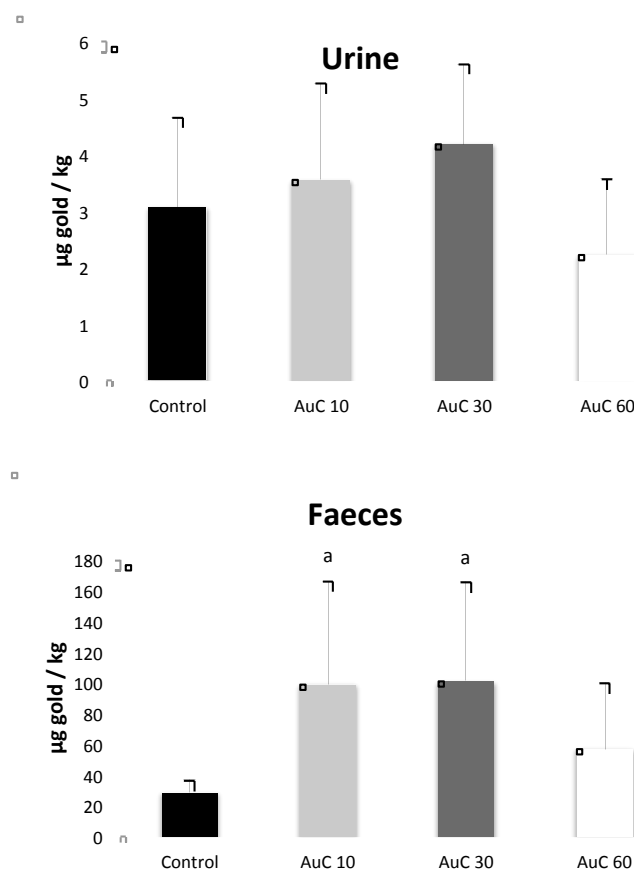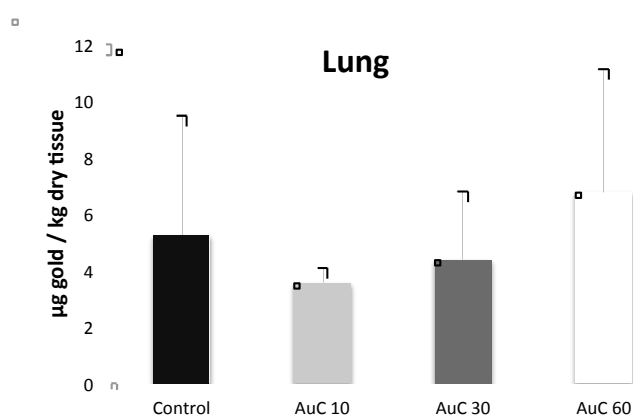
Figure 27. Concentration of gold in lung of animals treated with AuNPs. Values shown are means ± SD, Control (Control group); AuC 10 (rats treated with 10 nm AuNPs); AuC 30 (rats treated with 30 nm AuNPs); AuC 60 (rats treated with 60 nm AuNPs).

Regarding plasma, no detectable amount of gold was found in any group, as the measurements were lower than the limit of detection of the instrument.

Table 4. Gold content in plasma (µg / kg).

	Control	**AuC 10**	**AuC 30**	**AuC 60**
Plasma	< 0.00	< 0.00	< 0.00	< 0.00

Control (Control rats); AuC 10 (rats treated with 10 nm AuNPs); AuC 30 (rats treated with 30 nm AuNPs); AuC 60 (rats treated with 60 nm AuNPs)

4.2.8 Haematological parameters

The study of the effect of gold nanoparticles on several haematological parameters showed interesting results. Although treated groups showed decreased values of RBC and haematocrit compared to the control animals (AuC 10 group showing significantly lower concentrations), the increase of the nanoparticle diameter caused a recovery in these levels (in fact, there were significant differences in the group treated with 60 nm nanoparticles compared to the AuC 10 group). On the other hand, the effect of exposure to the nanomaterials on the content of WBC also exhibited a reduction although this effect was only significant in those rats treated with 10 and 60 nm when

comparing to the control. Finally, all treated group presented significant lower values regarding the MCH and MCHC parameters, compared to the control rats.

Table 5. Haematological parameters from the different groups.

	WBC (10^3/μL)	RBC (10^6/μL)	HGB (g/dL)	HCT (%)	MCH (pg)	MCHC (g/dL)
Control	8.33± 1.94	8.08± 0.42	16.27± 1.15	46.23± 1.62	19.67± 0.49	34.92± 1.16
AuC 10	4.00± 0.85[a]	7.39± 0.10[a]	13.97± 0.23[a]	41.47± 0.42[a]	18.65± 0.66[a]	33.30± 0.76[a]
AuC 30	7.55± 0.64	7.36± 0.20	14.55± 1.05	43.00± 2.85	18.60± 0.52[a]	32.87± 0.39[a]
AuC 60	4.47± 1.10[a]	7.76± 0.10[b]	14.47± 0.26[a]	43.77± 0.70[b]	18.65± 0.24[a]	33.07± 0.74[a]

Values are shown as mean ±SD. WBC (white blood cells); RBC (red blood cells); HGB (haemoglobin); HCT (haematocrit); MCH (mean corpuscular haemoglobin); MCHC (mean corpuscular haemoglobin concentration). Control (Control rats); AuC 10 (rats treated with 10 nm AuNPs); AuC 30 (rats treate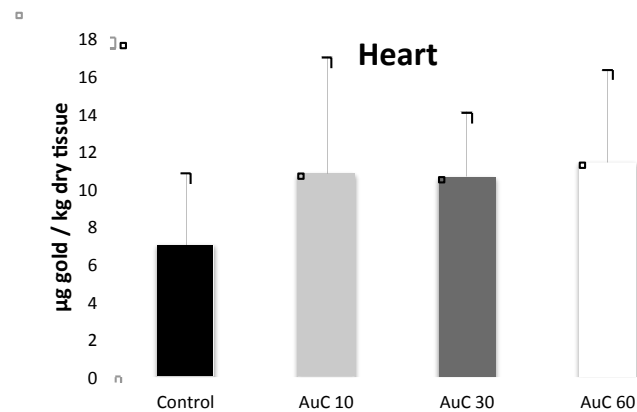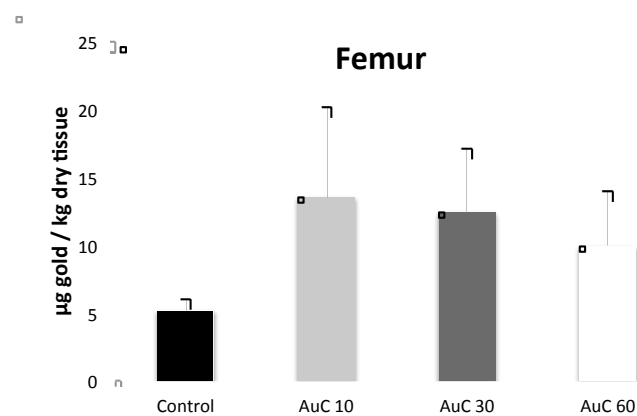d with 30 nm AuNPs); AuC 60 (rats treated with 60 nm AuNPs). [a] Different from control group; [b] Different from AuC 10. $P<0.05$

4.2.9 Inflammatory parameters

Four different markers were measured in liver in order to determine the beginning of an inflammatory syndrome: TNF-α, IL-1ß, IL-6 and IL-10. No significant changes were found in any case regarding these factors.

Table 6. Inflammatory markers measured in liver.

	Control	AuC 10	AuC 30	AuC 60
TNF-α	0.088±0.012	0.091±0.010	0.097±0.096	0.096±0.012
IL-1ß	0.88±0.15	0.77±0.03	0.80±0.07	0.82±0.05
IL-6	11.82±2.57	11.84±2.47	11.54±1.31	11.40±1.06
IL-10	1.48±0.22	1.31±0.08	1.35±0.10	1.34±0.17

Values are shown as mean±SD. Control (Control rats); AuC 10 (rats treated with 10 nm AuNPs); AuC 30 (rats treated with 30 nm AuNPs); AuC 60 (rats treated with 60 nm AuNPs).

4.2.10 Biochemical parameters

Several biochemical factors were measured in this experiment: glucose, urea, uric acid, triglycerides, albumin, cholesterol, γ-GT, alkaline phosphatase, GOT and GPT. Data support that no changes took place in rats treated with AuNPs compared to control group.

Table 7. Biochemical parameters from plasmas of the experimental animals.

	Control	AuC 10	AuC 30	AuC 60
Glucose (mg/dL)	143.75±17.99	207.25±88.80	147.75±16.68	137±22.01
Urea (mg/dL)	30.75±3.30	18.75±6.40	24.50±2.38	27.00±1.41
Uric acid (mg/dL)	0.92±0.27	0.81±0.14	1.03±0.38	0.91±0.33
Triglycerides (mg/dL)	98.5±20.02	113.25±43.96	111.00±16.45	94.75±24.93
Cholesterol (mg/dL)	46.75±2.99	56.75±14.57	60.25±5.56	55.00±8.79
Albumin (g/L)	30.25±1.71	30.25±1.26	28.25±0.96	29.25±2.06

γ - GT (U/L)	< 3	< 3	< 3	< 3
Alkaline phosphatase (U/L)	175.00±54.84	205.75±49.22	169.00±50.21	175.00±51.31
GOT (U/L)	82.25±4.42	77.50±7.42	80.25±5.85	84.25±9.60
GPT (U/L)	17.75±1.71	18.00±3.56	18.00±2.45	17.00±3.65

Values are shown as mean±SD. Control (Control rats); AuC 10 (rats treated with 10 nm AuNPs); AuC 30 (rats treated with 30 nm AuNPs); AuC 60 (rats treated with 60 nm AuNPs).

4.2.11 Correlations

The bivariate study revealed the existence of a significant relation, among which the following are particularly important: AuNPs size correlated positively with gold content in spleen (r = 0.895; p < 0.01); AuNPs size correlated negatively with gold content in kidney (r = - 0.837; p < 0.01); AuNPs size correlated negatively with gold content in intestine (r = - 0.736; p < 0.05).

5. DISCUSSION

Nanotechnology can be defined as the use of nanomaterials for human benefit. Nanoscale refers size dimensions between approximately 1 and 100 nm because at this scale the properties of materials differ with respect to their physical, chemical and biological properties from a larger scale. In this sense, any form of a structure that has one or more dimensions in the nanoscale is known as nanomaterial.[145] In fact, humanity has been in contact with nanoparticles since its beginning, due to natural processes such as volcanic ashes, marine aerosols, fine sand or even viruses. Nevertheless, there has been an enormously increase in the human exposure to nanostructures during last years because of the growing interest that these materials have awaken in multiple areas of technology like cosmetics,[329,330] agriculture,[331] electronics,[34] clothing[332] or catalysis.[333] Particularly, biomedicine has enormously increased its interest in gold nanomaterials due to their special characteristic as nanoparticles (small size, high surface area, etc.) but also as metallic structures (stability, heating, unique optical properties, etc.). As a result, gold nanoparticles have proved to be useful in sensing,[334,335] imaging[336,337] or therapy (*per se*[338,339] or as vehicles to deliver a variety of chemical agents including anticancer drugs, antibiotics, amino acids, peptides, glucose, antioxidants, nucleic acids, and isotopes[268]). In fact, recent studies have been focused on the use of gold nanoparticles as "theranostic" agents, it is, drugs that can act as imaging/sensing agents and therapeutic agents at the same time.[340–342]

Nevertheless, we should not forget that it is also within this size range that most cellular machinery operates. This includes the organelles, motility machinery, and other protein and chromatin complexes within cells, the signalling pathways, the viruses that infect cells, and the secreted molecules that communicate with other cells, or cause their destruction.[343] That is the reason why the increase in their use has raised concerns about the possible interactions *in vivo* and the unexpected responses inside humans and other living organisms. Although the toxicity caused by the exposure to gold nanoparticles is currently under investigation, and multiple studies have been conducted in order to clarify the possible damage in humans,[344–346] the purpose of this thesis is trying to solve some partially unanswered questions as the role of the size, time and dose of gold nanoparticles in the ROS production in cell

cultures and their implications in the damage to macromolecules; their intracellular location; their biodistribution and bioaccumulation *in vivo*, and their impact on the biochemical parameters and inflammatory markers.

Thus, on the one hand, this study was aimed to determine the effect of three sized AuNPs in cell viability and determine whether an increase in cell mortality may be caused by an increase in the ROS production. Furthermore, we wanted to assess if the ROS overproduction may have a repercussion on the DNA stability. Finally, a deep study regarding the subcellular localization and integrity was also developed *in vitro*.

On the other hand, an *in vivo* study was also designed in an attempt to assess the gold biodistribution, and evaluate if gold nanoparticles may exert any effect on the animal behaviour, may interact with other macromolecules such as lipids or proteins; to assess the intracellular localization, and finally to determine whether the exposure to this nanomaterial could trigger an immune response and destabilise the biochemical parameters.

5.1 *IN VITRO*

5.1.1 Cell viability, ROS production and DNA damage *(page 80; figures 11 & 12; table 2)*

In this sense, our first approach was to evaluate if the exposure to gold nanoparticles may affect the cell viability of a cell culture. Several groups have previously studied this goal although there is no agreement. It is well accepted that gold nanoparticles affect cells viability, but many factors may be related. For instance, Coradeghini et al. proved the increased mortality of mouse fibroblasts exposed to 5 nm citrate-stabilised AuNPs at 50 µmol·L^{-1} for 72 h,[347] while Freese and coworkers just observed cytotoxicity at 500 µmol·L^{-1} for 48 h.[348] For their part, Leite et al. did not detect an increase in cell

mortality in mouse myoblastoma cells after exposing them to 5 nm PEG-AuNPs for 24 h up to 254 nmol·L^{-1}.[349]

In order to clarify this, we used hepatocytes (Hep G2 cells) due to the key role of the liver in metabolic processes and detoxification in the organism. After exposing hepatic cells to different AuNPs concentrations and exposure times, a clear time and dose-dependent effect was found. In fact, the cell viability was lower at 16 h and it decreased as the gold nanoparticles concentration increased. Thus, while it is true that hepatocytes are initially affected by the presence of gold nanoparticles and as a consequence their cell viability is compromised; somehow these cells manage to recover and show no signs of cell mortality at 32 h. Interestingly, no differences were found among treated cultures, which indicates that cells responded similarly to the presence of the three gold nanoparticles sizes.

Once cell viability decrease had been observed, our next step was to assess whether this mortality may be related to the presence of ROS. In fact, gold nanoparticles have been related to imbalances in oxidative status *in vitro*.[350,351] It is generally well accepted that several factors such as size, shape, charge and even cell line may influence the ROS production of these nanoparticles.[318] In fact, Mateo et al. proved that the total content of glutathione (GSH) was significantly depleted in HeLa and Hep G2 cells after treatment with AuNPs, which confirmed that GSH interaction with AuNPs is a crucial detoxification mechanism against AuNP-induced cytotoxicity.[351] In this sense, our results are in full agreement with those of cell viability, showing that the exposure of hepatocytes to AuNPs caused a time and dose-dependent increase in ROS production. Only slight impairments on the oxidative status were found 32 h after the exposure, whereas 16 h caused a growth in ROS production in both 10 ppb and 10 ppm. Although there are no significant differences, the highest dose of AuNPs tended to provoke more damage. Thereby, it is clear that AuNPs are able to induce an initial oxidative damage that consequently provokes an increase in cell mortality. Similarly to what previously observed, cells manage to control the ROS overproduction after 32 h of exposure, probably by means of the increase in the antioxidant activity, thus restoring the cell viability index.[293]

DISCUSSION

After confirming that gold nanoparticles were able to cause oxidative damage measured by ROS production at 16 h and 10 ppm, comet assay was used in order to assess whether this ROS overproduction might cause DNA damage under the same conditions, thus provoking the aforementioned increase in cell mortality. In literature, the effect of gold nanostructures on DNA has been investigated for several years. As exposed to ROS production, gold nanoparticles-induced genotoxicity results have been controversial. For instance, several studies reveal that gold nanoparticles show no oxidative DNA damage *in vitro*,[290] meanwhile other groups suggest that false positive results obtained with Comet assay may have been due to the possibility of direct contact between the residual, intracellular AuNPs and DNA during the assay procedure.[352] On the other hand, some authors found that gold nanoparticles were able to induce DNA damage *in vitro* after treatment with AuNPs capped with either sodium citrate or polyamidoamine dendrimers (PAMAM).[353] Furthermore, other authors suggest that these nanomaterials are involved in cell cycle arrest in G1 phase[354] or G2/M phase, depending on the gold concentration.[355] For their part, Cardoso et al. showed DNA damage in the cerebral cortex of adult rats after acute and chronic administration.[356] The fact that gold nanoparticles have been proved to induce genotoxicity *in vivo*, seems to confirm that these nanomaterials are involved in DNA damage despite possible errors in sample handling *in vitro*, as previously suggested. In our case, tail moment measurements were chosen as a more complex parameter which relates the smallest detectable size of migrating DNA (reflected in the comet tail length) and the number of broken pieces (represented by the intensity of DNA in the tail)[357] thus providing more information regarding the extension of the DNA damage. Our results proved that AuNPs induced DNA breaks. Furthermore, the damage increased as the nanoparticle size decreased.[295] Thus, cell culture exposed to 60 nm gold nanoparticles showed no differences compared to the negative control cells, whereas Hep G2 cells treated with 10 nm AuNPs showed moment tails similar to those from the positive control, where cells were exposed to hydrogen peroxide. Taking into account that the effective diameter of the nucleus pore is around 35 nm,[358] it is probable that the 10 and 30 nm nanoparticles were able to cross the nucleus membrane, thus favouring the DNA breaks by the ROS overproduction. As we will discuss later, this fact was confirmed for both, *in vitro* and *in vivo,* by TEM images

(figures 13 and 17), where several nanoparticles were found inside the nucleus after treatment with 10 nm AuNPs. The fact that DNA breaks were only observed in some samples (in those treated with smaller nanoparticles) corroborate that these nanoparticles cause DNA damage independently of the samples manipulation.
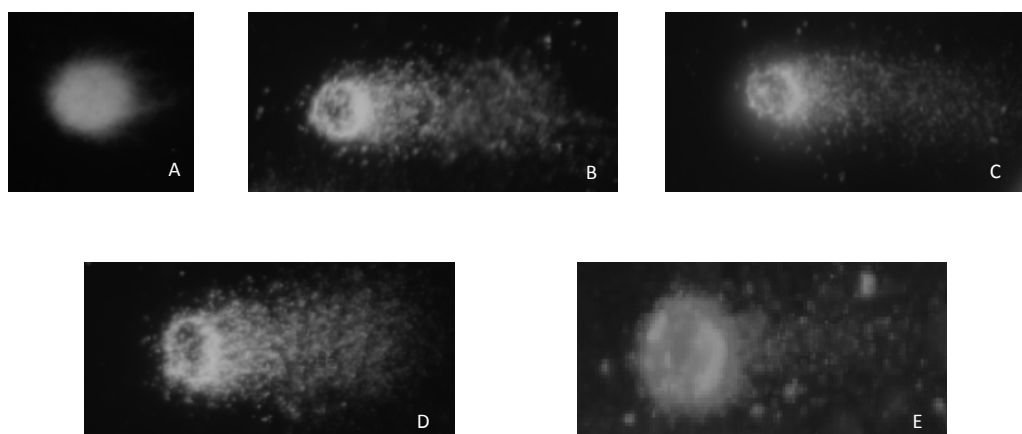
Figure 28. Comets from hepatic cells. A (cell without treatment); B (cell treated with H_2O_2); C (cell treated with 10 nm AuNPs); D (cell treated with 30 nm AuNPs); E (cell treated with 60 nm AuNPs)

5.2 *IN VIVO*

5.2.1 *Food and water consumption and body weight* (page 83; figure 14)

In relation to the experimental animals, no signs were found regarding behavioural disorders after injecting the three sized gold nanoparticles (10, 30 and 60 nm AuNPs), which led us to confirm that gold nanoparticles exert no alterations on the brain structure that may affect the social conduct of these animals. These results agree with those obtained by Naz and coworkers who did not find any changes in behaviour after treating mice with three different gold nanoparticles.[359] Changes in conduct are not mentioned in those papers that describe brain damage due to gold exposure;[356] which may suggest that gold nanoparticles are not involved in conduct disorders.

The effect of gold nanomaterials on the food and water intake has been poorly studied and opposing results are described. Some authors defend that the administration of these nanoparticles induced an increase in food intake and body weight;[360] while some researchers show that no changes were observed after treating rats with gold nanoparticles.[359] However, different approaches were made in every study (different nanoparticle size, duration or route of administration), which may influence the obtained results. Our *in vivo* data show a significant decrease in the body weight and a clear tendency to decrease food intake.

The fact that all rats underwent intraperitoneal injection (even control rats), indicates that no post-traumatic effect can be recorded. However, rats treated with 10 nm AuNPs were able to decrease body weight and increase water intake at day 4. These effects were also observed in the group treated with 30 nm AuNPs at the end of the experimental period. This fact led us to consider that gold nanoparticles induced a reduction of the body weight gain by replacing food by water intake in a time and size dependent way. Furthermore, although 60 nm size AuNPs showed the same tendency, their effect was lower, thus reinforcing the size dependency. These results agree with those from Chen and coworkers, who describe a significant loss of fat tissue related to a decrease in food intake after administering 21 nm gold nanoparticles[361]. Other researchers have also pointed out that high doses of 8, 12, 17 and 37 nm AuNPs intraperitoneally injected to BALB/C mice could cause sever sickness which included fatigue, loss of appetite and weight loss.[362] .

5.2.2 Lipid and protein damage (page 85; figures 15 & 16)

Once it had been shown that gold nanoparticles increased ROS production and consequently DNA breaks *in vitro*, we also wanted to assess if the exposure to AuNPs may affect the lipid and protein components of the animals. The fact that liver is in charge of metabolic processes and detoxification and elimination of xenobiotics,

together with the point that this organ was one of the tissues with more gold concentration, encouraged us to measure the levels of lipid peroxidation. This marker has been widely measured in literature in order to determine the damage in lipids caused by oxidative stress.[9,292,363] In 2010 Li et al. observed that 20 nM 20 nm gold nanoparticles provoked an increase in the hydroperoxide concentration and the MDA modified protein adducts in lung fibroblasts after incubating for 72 h.[293] However, to date, very few studies have been conducted in order to assess the integrity of the lipid components after treating with gold nanomaterials *in vivo*.[316,363] In our case, as exposed in the results section, the rats treated with 10, 30 and 60 nm gold nanoparticles suffered a 35%, 14% and 23% increase, respectively, in the lipid oxidation compared to the controls. These data confirm that the gold nanomaterial provoked a considerable damage in the lipid structures, although no differences were found regarding the size of the nanoparticles.

Protein carbonyl groups are commonly used as biomarker of protein oxidation. In the case of protein structures, scarce publications have been conducted in order to establish a relation between gold nanoparticles exposure and protein damage. In 2008 Tedesco and coworkers determined the effect of gold nanoparticles on the protein carbonylation level in a bivalve aquatic organism *(Mytilus edulis)*. They concluded that the exposure to 750 ppb 13 nm AuNPs for 24 h clearly provoked an increase in the carbonylation of the proteins in one of their key organs (gill).[364] For their part, Ferreira et al. proved that 70 µg·kg^{-1} 10 nm AuNPs increased the carbonyl protein levels in the kidney and heart of rats treated with a single intraperitoneal injection.[316] Furthermore, they also concluded that the long-term exposure (28 days) to 30 nm AuNPs in the same conditions caused an increase in the protein carbonylation in the same organs. We tried to confirm these results by measuring the protein carbonyl groups in the liver of the rats. It was observed an enormous increase in the protein carbonylation levels in the rats injected with 10, 30 and 60 nm AuNPs (168%, 112% and 174% superior, respectively). Interestingly, the percentage of protein damage is substantially higher than that found in the lipid component and may be explained by the ease lipids are oxidized even in normal conditions, so that the increase provoked by the administration of gold nanoparticles was not so representative. Thus, the fact that the

protein oxidation is enormously higher in the treated groups indicates the real damage that the gold nanoparticles can exert over the tissues.

These results indicate the increased production of free radicals in this organ, which became concomitant with the increased production of TBARS and protein carbonyl groups. In our view, the fact that lipid and protein damage showed no significant differences among treated groups may be caused by the higher availabity of lipid and protein components in the cells (among others, they form the cell membranes and are also present in the cytoplasm). Thus, they can be more easily attacked by the ROS. The fact that the DNA is enclosed inside the nucleus mean that gold nanoparticles have to cross a size-restricted membrane, hence hindering the damage.

5.2.3 Intracellular localization *(page 87; figure 17)*

As reported by other groups, AuNPs were observed by TEM under different experimental conditions.[9,290,365,366] In fact, most of them agree with the idea that gold nanoparticles are easily taken up by cells and incorporated into vesicles[345] or dispersed throughout the cytoplasm. Besides, some of these studies indicate that no degradation is observed and gold structures remain intact regardless their size,[367] coating,[368] charge[369] or shape.[370] Interestingly, most of the TEM studies performed in the liver of experimental animals point out that macrophages (especially the Kupffer cells) played an important role in the uptake of gold nanoparticles and their removal from the circulation.[313,362,371]

In our *in vivo* analysis, gold nanoparticles were visualized as single particles throughout the cytoplasm or as smaller aggregates inside lipid drops. These findings together with the fact that high levels of gold were also found in the spleens of the treated rats, led us to consider that the nanostructures could be digested thanks to the phagocytic activity of macrophages, as previously suggested. Thus, the enzymatic compounds from the lysosomes of the macrophages would act by neutralising and storing the nanoparticles in the lipid drops in an attempt to reduce their toxicity.

Furthermore, as published in our article,[372] HPLC-ICP-MS measurements of the organs of treated rats confirmed the presence of gold nanoparticles fraction (a peak was observed at 4 min in the case of rats treated with 30 nm AuNPs) and low-molecular Au species (a high peak was detected at 6 min); which confirmed that these nanomaterials were gradually digested and remained stored in vesicles, as observed by TEM images.

It has also been documented that time plays a key role in the final destination of the gold nanoparticles inside cells. For instance, Coradeghini and coworkers determined that gold nanoparticles were found throughout the cytosol after 2 h, but inside vesicles after 24 h *in vitro*.[347] Similarly, other groups were able to visualize them inside vesicles after 24 h of treatment.[348,349] Hence, a longitudinal *in vitro* study was designed with the purpose to observe the uptake process that occurs after cells are exposed to AuNPs. On this occasion, HT-29 human intestinal cells were chosen due to the importance of this organ in the absorption and uptake of molecules and substances by oral administration, due to the high amount of gold that was detected by ICP-MS and in an attempt to confirm the effects previously observed in liver. The TEM study revealed that after 2 h of exposure most nanoparticles were primarily dispersed throughout the cytoplasm as individual particles or around the external membrane, trying to get into the cells. Similar results were observed after 4 h of exposure, although few particles were found outside the membrane. Instead, a large number of them were localised in the cytoplasm and some of them appeared to be already stored in lipid drops. Finally, after 16 h of treatment, most particles were relocated and observed in the lipid structures. Furthermore, some 10 nm AuNPs were able to cross the nucleus membrane and were detected inside it. To our best knowledge, it is the first time that gold nanoparticles are visualised in this cell compartment (both in cells and hepatocytes). Complementary HPLC-ICP-MS results present in the article published by our group,[372] revealed the absence of low molecular Au species (in cells treated with 10 nm AuNPs a single peak at 5 min was detected, that corresponds to the AuNPs fraction) which confirmed that no gold nanoparticles degradation took place *in vitro* and supported the hypothesis that macrophages and Kupffer cells are responsible for the AuNPs metabolism *in vivo*.

DISCUSSION

5.2.4 Gold biodistribution

5.2.4.1 Liver, kidney and spleen *(pages 88 and 89; figures 18 & 19)*

The gold biodistribution after administering AuNPs *in vivo* has been a subject of study in recent years. In 2008, De Jong et al. performed a kinetic study to determine the influence of particle size on the *in vivo* tissue distribution of spherical-shaped gold nanoparticles, by intravenously injecting 10, 50, 100 and 250 nm gold nanoparticles to WU Wistar-derived rats.[300] After 24 h, animals were sacrificed and samples were measured by ICP-MS. For all gold nanoparticle sizes the majority of the gold was demonstrated to be present in liver and spleen. Similarly, Sun and coworkers studied the effect of different shapes of gold nanostructures on their accumulation and toxicity.[373] They concluded that Au sphere-shaped nanomaterials displayed the best biocompatibility and that all gold nanostructures were preferentially accumulated in liver and spleen. On their part, Yang et al. went a step further and stated that AuNPs were primarily deposited in the mononuclear phagocyte system such as liver and spleen of mice injected 12 mg NPs·kg^{-1} body weight (6 nm size).[374] The possible role of the mononuclear phagocyte system in the Au nanomaterials biodistribution had been previously studied by other authors.[315,367,375] Our results showed a similar pattern, but with a clear size-dependency. Thus, 10 and 30 nm sized AuNPs seem to accumulate more in the liver; whereas 60 nm AuNPs demonstrate a clear inclination to store in the spleen.

The fact that these macrophages are able to capture the gold nanostructures and metabolise them *in vivo* reinforce the results obtained by the TEM study and HPLC-ICP-MS measurements (published by our group[372]), where degradation was only found *in vivo*.

Furthermore, the kidney seems to be a critical organ in terms of AuNPs biodistribution. Many studies indicate that small nanoparticles are accumulated in kidney in an attempt to excrete them by the urine. Balasubramanian et al. observed that 20 nm gold nanoparticles tended to accumulate in kidney two months after intravenous

administration.[376] They also pointed out that this accumulation was related to an increase in the blood levels, thus indicating that gold was being removed from the storage organs in an attempt to eliminate the nanomaterial from the body. In another study of 2016, the charge of the nanoparticles determined the final destination.[369] Hence, positively charged gold nanoparticles accumulated extensively in the glomeruli of the nephrons, suggesting that these nanoparticles were filtered by this organ at a different rate than the neutral or negatively charged nanoparticles. In our case, kidney showed higher concentration of gold in those rats treated with 10 and 30 nm. On their part, rats treated with 60 nm also showed significant differences when compared to the control group, although to a lesser extent. This clear size-dependence is confirmed by the correlations study, which shows a negative relation beteween AuNPs size and gold content in kidney (r = - 0.837; p < 0.01). Definitely, gold content increases as the AuNPs size decreases. In our view, the fact that smaller nanoparticles presented higher gold concentration in kidney indicates an attempt to eliminate them by urine. Nevertheless, higher nanoparticles are unable to be filtered by the nephrons and consequently their concentrations are lower. These results match with the hypothesis established by Abdelhalim, who suggested that when AuNPs size is larger than renal filtration cut-off, nanoparticles are not excreted in urine. They are instead eliminated from the blood by the reticuloendothelial system and tend to accumulate in the spleen and liver.[377,378] Hence, the spleen would be a key organ in the AuNPs metabolism. As indicated above, our results also showed that the gold accumulation increased in the spleen as the size of the administered nanoparticles augmented. This fact was also supported by the correlation index, which reveals a strong positive relation between gold content in spleen and AuNPs size (r = 0.895; p < 0.01)

5.2.4.2 Intestine and faeces *(pages 89 and 90; figures 20 & 21)*

Regarding the intestine, few studies have measured the impact of the exposure of gold nanoparticles on the gold intestinal content. Some authors, like Keene et al., do not mention the presence of gold in intestine in Balb/C mice intravenously treated with 10 nm AuNPs, even though intestines were harvested.[379] On the other hand, Koyama and

coworkers determined the biodistribution of 15 nm AuNPs in C57BL/6 mice who received the nanoparticles by intravenous injection or intratracheal instillation.[380] Their results indicated that over 95% of nanoparticles were observed in the liver and 3% in the spleen in mice intravenously injected. Nonetheless, following intratracheal instillation, more than 25% of the administered nanoparticles were observed in the intestine after 6 h. Zhu and coworkers also observed that intestine was the main site of accumulation in fish (*Oryzias latipes*) after exposing to 20 nmol·L^{-1} 14 nm AuNPs for 24, 72 and 120 h.[381] On their part, Morais et al. described the existence of gold in small intestine of Wistar rats, which were intravenously injected 0.8 mg AuNPs·kg^{-1} body weight.[368] Gold content was assessed at the selected times 0.5, 2, 6 and 24 h. Thus, the highest concentration of gold was found 2 h after injection. Their conclusions agree with our findings showing that the accumulation in intestines of treated rats was higher as the nanoparticle size decreased. These data were subsequently reinforced by the correlation index, which describes a negative relation between gold concentration in intestine and AuNPs size (r = - 0.736; p < 0.05). These results together with the fact that the increase in gold concentration measured in faeces, and taking into account that the administration route of the nanoparticles was intraperitoneal (and not enteral), probes that faecal is the main endogenous route of elimination of the nanoparticles.

In relation to this, faeces were also collected in order to determine the gold content. The excretion route of nanoparticles may be decisive to assess the kinetics of the nanoparticles as well as the possible toxicity that may derive. In this sense, scientific community usually agree that some factors such as the charge, the coatings and especially the route of administration play a central role in the removal of the nanoparticles. For instance, in an article from 2014 it was shown that functional groups conjugated on the surface of AuNPs produce differences in blood kinetics, organ distribution and elimination pattern.[382] The researchers intravenously administered three types of gold nanoparticles (polyethylene glycol-AuNPs, carboxyl AuNPs and amine AuNPS) to Balb/C mice. As a conclusion, nanoparticles coated with PEG and NH$_2$ showed lower levels in bile than the carboxyl nanoparticles. On the contrary, the excretion of nanoparticles via urine or bile is determined primarily by the core

composition and not by size.[367] Takeuchi et al. also studied the biodistribution and excretion of 20, 50 and 100 nm gold nanoparticles.[383] For that purpose, ddY mice were intravenously injected and subsequently sacrificed at different end points (from 5 minutes to 24 h). Interestingly, the three differently sized gold nanoparticles showed much higher gold concentrations in faeces than in urine at every time points, and no significant differences regarding the size were found after 24 h. Our results show a similar pattern, where faecal excretion appears to be the main elimination route from the body and size seems not to be a differentiating factor. Moreover, as exposed above, these data complete those found in intestine where higher concentrations of gold were observed in comparison to the kidney.

5.2.4.3 Urine *(page 90; figure 21)*

The role of urine in the excretion of gold nanoparticles also focused our attention. In this regard, Zagainova and coworkers explained that PEG- gold nanoparticles were found in urine just 4 h after the intravenous injection to CD-1 mice.[384] A day later, no indication of nanomaterials was detected. Similarly, they state that the nanoparticles are rapidly eliminated from the blood and simultaneously accumulate in the reticuloendothelial system and renal tissues. It is possible that their accumulation in the liver may indicate the hepatobilliary path of excretion with faeces in later stages. This completely matches our results and may explain the high concentrations found in liver, spleen and kidney.

Analogous results were described by Simpson et al., who observed that for glutathione-coated gold nanoparticles, a large percentage of particles (30%) were voided through the renal system within 1 h and 60% were excreted within 8 h, in BALBc/cAnNHsd mice subcutaneously injected several AuNPs concentrations, ranging from 0 to 60 μmol·L^{-1}.[385]

In a study developed by the Kreyling´s group, three different nanoparticles (Au-Phos nanoparticles and two PEG-AuNPs) and two administration routes (intravenous injection and intratracheal instillation) were tested in Wistar-Kyoto rats.[386] According to their results, the Au-Phos NPs increased 100 times the first 24 h after intravenous

injection. On the contrary, no increase of the AuNPs in the urine was detected for either of the PEGylated NP types. In their view, it may be caused by the augmented blood circulation found in the PEGylated nanoparticles and their higher hepato-biliary clearance. No data regarding AuNPs elimination after intratracheal administration are described.

The results obtained from our study in 24 h urine clearly show much lower Au levels among treated rats, thus excluding the urine as a main via of excretion for citrate-stabilised gold nanoparticles. In our opinion, although AuNPs are accumulated in kidneys, the renal cut-off blocks the filtration of these nanostructures. Other studies have reported that nanostructures of hydrodynamic diameter (H_D) > 5.5 nm accumulate in the kidney without undergoing renal clearance.[387,388] Thus, the biliary clearance plays a critical role trying to decrease the concentration of gold from the tissues.

5.2.4.4 Muscle *(page 91; figure 22)*

The present study also assesses the influence of AuNPs exposure on the gold content in the muscle (*gastrocnemius*). In 2014, You et al. described the presence of gold in the skeletal muscles of mice intravenously treated with 43 nm sized PEG-gold nanospheres.[389] Animals were injected at a dose of 12.5 mg·kg^{-1}, for a total of 10 injections, administered daily for 5 injections per week over a 2-week period. According to their study, the gold content in this tissue was statistically higher in animals treated with these nanostructures than the control group, although no quantitative data are presented in the publication. They also assessed the long-term elimination of this element from the organ. Hence, the results showed that the levels of Au decreased 45.2% from day 14 to 90, being the organ with the lowest gold concentration among all organs studied.

A different gold nanostructure (nanocluster) was used by You and coworkers to determine whether the administration of these nanocompounds might induce their accumulation in different tissues.[390] According to them, the storage of gold in different organs follows a biphasic pattern. Most of the Au nanoclusters are cleared at the first

phase, with a major accumulation in liver and kidney. However, these nanostructures are also steadily accumulating in the muscle, and the stored Au nanoclusters gradually release into the blood in the second phase, that induces a re-distribution and re-accumulation of the nanocompounds in all blood-rich organs; which may explain the long-term elimination of gold in the muscle.

On their part, Morais et al. collected the *quadricepts femoris* as a sample of skeletal muscle.[368] After a slight initial increase of the gold content in the tissue (which corresponded to 0.04% of the injected dose in its highest point), concentrations returned to basal levels after 24 h post injection.

Finally, the results published by Sun et al. revealed that no gold content was found in muscle within the whole time post injection (seven days), which led them to consider that muscle is not a storage organ of these nanoparticles.[373]

Our data show an important tendency to accumulate in muscle. Even though there are no significant differences among groups (probably due to the standard deviations derived from the limit of detection of the instrument or the sample size), it is specially relevant the high concentration of gold in those rats treated with 10 nm AuNPs (their gold content is 700% higher than the control group), which also reinforces the fact that these nanoparticles show the widest biodistribution and therefore they are the most toxic nanostructures. The fact that the same tendency was found in heart (a special skeletal muscle), we consider that these tissues may play an important role in terms of gold storage organ.

5.2.4.5 Heart *(page 91; figure 23)*

In relation to the heart, there is no a consensus regarding the role that it may play in the bioaccumulation of AuNPs. In a study published in 2011, Wistar rats were intraperitoneally injected with three differently sized AuNPs for 3 or 7 days. Although the existence of these gold nanostructures in heart was not quantitatively assessed, 10 and 20 nm citrate-stabilised AuNPs demonstrated to cause congested heart muscle with prominent dilated blood vessels, extravasations of red blood cells and the

presence of inflammatory cells infiltrates, while 50 nm AuNPs did not affect the heart structure.[317] It remained unclear whether these controversial results may be related to the coating (in general, citrate is known to be more toxic than PEG[391]), size or administration route.

In an attempt to answer these questions, several groups studied the size effect on gold bioaccumulation in the heart. Thus, Sonavane and coworkers observed that 200 and 100 nm AuNPs showed high concentrations of gold in heart, while groups treated with 15 and 50 nm AuNPs presented a low amount of Au in this tissue.[392] The same pattern was described in a recent publication from Takeuchi et al., where the accumulation of gold in heart after administering 20 and 60 nm citrate-stabilised AuNPs was less than 0.2% of the injected dose, whilst rats exposed to 100 nm AuNPs exhibited high accumulation after 6 h.[383] Sun and coworkers also described that no gold signal was found in heart of KM mice treated with 50 nm citrate-stabilised AuNPs, thus supporting the hypothesis that smaller nanoparticles tend to accumulate in other organs and avoid heart.[373]

On the contrary, there are some studies in literature that reveal a significant concentration of gold in heart after administering small nanoparticles to experimental animals. For instance, Yang and coworkers detected a moderate accumulation in the hearts of mice intravenously treated with 13 nm PEG-AuNPs.[321] Moreover, they concluded that the accumulation of AuNPs in this organ did not affect cardiac function or induced cardiac hypertrophy, cardiac fibrosis or cardiac inflammation under these conditions.

Our data follow a similar pattern. Although no significant changes were observed in those groups exposed to AuNPs, a strong tendency to accumulate gold was detected in all treated groups. In fact, the gold content in the hearts of these animals was approximately 160% higher than the controls. Furthermore, the fact that no differences in the heart to body weight ratios were found among groups (table 3) also points out a normal function of the tissue and that no heart damage was caused by the exposure to these gold nanoparticles.

5.2.4.6 Bone *(page 91; figure 24)*

In relation to the accumulation of gold in bone, very few studies have been published. In 2010, Wang et al. evaluated the bioaccumulation and morphological development of different tissues after injecting AuNPs into zebrafish embryos.[393] Their results showed that no differences in the development of the pharyngeal skeleton between injected and uninjected control embryos were observed. These findings led them to conclude that the gold nanoparticles used in this study did not have any detectable toxic effects on embryo development. However, no signs of gold accumulation in the bone were disclosed. On their part, Morais et al. observed traceable amounts of Au in the bone (shaft of femur) of rats treated with citrate-stabilised gold nanoparticles, even though the concentration rapidly decreased after 24 h.[368]

Although the femur bone is less vascularised than those organs where the concentration of gold is significant, a clear tendency to accumulate was found. Thus, the content of gold in the treated groups was 250% higher on average in comparison to the control animals. Furthermore, the smallest nanoparticles showed the highest accumulation, which once again reinforces the hypothesis that these nanostructures exhibit the most deleterious effects in terms of gold biodistribution. In any case, the consequence of gold nanoparticles exposure in the bone structure and their accumulation might be an object of study in future research.

5.2.4.7 Testicles *(page 92; figure 25)*

Scarce data are available regarding the accumulation of gold in testicles. Most studies are focused on crucial organs (highly vascularised) such as liver, kidney or spleen; but few results are presented concerning the implication of AuNPs exposure in the homeostasis of reproductive organs; and those which are published do not reach to a complete agreement. For example, Wang and coworkers used three different surface-charged gold nanoclusters (3 nm) to examine the biodistribution over a period of 90 days in C57 mice.[394] The animals received a single intraperitoneal injection. Their

results showed that gold nanoclusters were accumulated in testicles (especially the negative Au nanoclusters) after 1, 7, 30, 60 and 90 days. Han et al. stated comparable conclusions, after treating Sprague-Dawley rats with 13 and 105 nm size gold nanoparticles by inhalation.[395] In this study, gold concentration in the organs was measured after 1, 3 and 28 days after exposure. Interestingly, only the smallest nanoparticles were able to reach the testicles (as show our data, their biodistribution was also wider). Furthermore, significant differences between control rats and group treated with 13 nm AuNPs were only found on day 1; which may indicate not only a clear size-dependence, but also that gold nanoparticles were rapidly removed from this tissue. On their part, De Jong et al., showed that a small amount of gold was measured in the testicles of rats treated with 10 nm AuNPs, but no concentration of this element was found in the animals injected with 50, 100 and 250 nm sized gold nanoparticles,[300] thus reinforcing the idea of size-preference for smaller nanostructures. These results were later completed by a study performed by Balasubramanian et al.[396] In this occasion, they observed a slight accumulation of gold nanoparticles in testicles of rats that underwent 15-day inhalation exposure to airborne of 20 nm AuNPs. No signs of accumulation were found in the reproductive organs of rats treated with 7 nm AuNPs under the same conditions.

In view of the different results reached by researchers last years, it is hard to obtain a clear conclusion about size or time-preference of AuNPs in the testicles. Our results show a clear size-dependent accumulation. Although no significant changes were observed among groups, the concentration of gold in the rats exposed to 10 and 60 nm AuNPs was approximately 300% higher that the one found in the control animals. These data may agree with the previous ones that described the absence of gold content in testicular tissue of rats 7 days after a single intravenous injection of 20 nm AuNPs.[376] However, a surprisingly gradual accumulation of AuNPs in testis (among other organs) was found in the groups that were kept for one and two months after injection, along with reduction of AuNPs in urine and faeces; which may indicate that AuNPs were inefficiently cleared from the body through the urine and faeces and AuNPs could undergo redistribution in the body after one month. Taking into account that our results show a clear attempt by the gold nanoparticles to be eliminated from

the body by faeces, together with the fact that low levels of gold was measured in urine but high concentrations of this element were present in the kidney (as stated by the Balasubramian´s group), may indicate that an inefficient elimination could result in a later biodistribution, which also reinforces the fact that the concentration of gold in the groups treated with 10 and 30 nm AuNPs was noteworthy higher.

5.2.4.8 Brain *(page 96; figure 26)*

Among all organs studied by ICP-MS, the most controversial is the brain. It is unclear whether gold nanoparticles are able to cross the blood-brain barrier (BBB). Most researchers who support the idea of nanomaterials ability to get into the brain agree that the nanoparticles size supposes the main limiting factor for their entrance. Betzer et al. assessed three different gold nanoparticles systems that may overcome the restrictive mechanism of the BBB.[397] Their results indicated that the smallest gold nanostructure (20 nm size) showed the highest accumulation within the brain. However, although there are significant differences among groups, it still remains unclear whether the ability to cross the BBB was due to the nanomaterial size or to the special coating used in this study (insulin molecules). Similarly, Zagainova et al. observed some single nanoparticles in the brain of mice intravenously injected 40 nm sized AuNPs.[384] Other groups show analogous results.[300,374,386,398]

Nonetheless, many authors state the fact that BBB fully restrict the entrance and consequently gold nanoparticles are completely unable to access the brain. In a study previously mentioned, Balasubramanian et al. recorded the biodistribution of 20 nm AuNPs in more than 25 organs for 1 day, 1 week, 1 and 2 months after an intravenous injection in rats.[376] Their results were clear: No Au was found in any of the brain areas measured (olfactory bulb, frontal cortex, hippocampus, striatum, thalamus/hypothalamus, brainstem and cerebellum) at any time point. Similar results were described by Sadauskas and coworkers, who intravenously or intraperitoneally injected 40 nm AuNPs to adult mice.[399] No gold was found in brain after 1, 4 or 24 h, thus dismissing the hypothesis that the route of administration may be a factor that influences in the brain accumulation.

DISCUSSION

The effect of the size on the accumulation in the brain has also been subject of discussion. In 2017, Talamini and coworkers compared the brain accumulation of two different gold nanostructures.[344] For this purpose, spherical (two different sizes), rod-like and star-like AuNPs were intravenously injected to male CD-1 mice. Although their results showed an unequal biodistribution of the nanomaterials in several organs, no differences were found in brain, which indicates that shape is a minor factor regarding brain accumulation. Furthermore, they also observed that the levels of gold in brain were lower than the threshold of detectability for both groups treated with spherical nanoparticles at any time-points. This also suggests that the size does not play any role in influencing the passage through the blood-brain barrier.

Our data agree with these results, as no significant were found among groups treated with gold nanoparticles and the control group. In our view, the blood-brain barrier avoids the entrance of these nanostructures and protects the central nervous system from their effects.

5.2.4.9 Lungs *(page 93; figure 27)*

The accumulation of gold in the lungs has been extensively studied for several years. Contrary to what was formerly discussed with other organs, the route of administration has an enormous impact on the concentration of gold nanostructures in this tissue. It is totally accepted that the inhalation or instillation routes cause a significant increase in the lungs concentration compared to other organs. Furthermore, this higher accumulation is independent of size, shape or coating when administered by inhalation, although at different scales. It has also been confirmed that gold nanoparticles are able to translocate from lungs and accumulate in secondary organs.[386,396] Nevertheless, lungs have also been able to store gold when exposed by different routes of administration. For instance, Sonavane et al. found high amounts of gold in lungs after a single intravenous injection to mice.[392] Moreover, although all AuNPs sizes studied were accumulated in lungs, they observed a size-dependent pattern, where the smallest gold nanoparticles (15 nm) tended to

accumulate more than bigger nanostructures. Similar results were previously described by De Jong et al., although they confirmed that larger nanoparticles (100 and 250 nm) were hardly detected.[300]

Interestingly, AuNPs have also been found in lungs after oral administration. As described by Hillyer and coworkers, gold was found in lung after feeding BALB/c mice with colloidal AuNPs. A clear size-dependency was detected. Thus, 4 nm AuNPs tended to accumulate in high proportion in lungs, while 58 nm were not found in this organ.[400] Schleh et al. described analogous results in 2012, further suggesting that negatively charged nanoparticles were more prone to accumulate in lungs that positively charged ones.[401]

In relation to the concentration of gold in lungs of animals treated with AuNPs by intraperitoneal administration, very few studies have been published. In 2013, Abdelhalim was able to measure fluorescence emission peak intensities in lungs of Wistar rats intraperitoneally injected with 10, 20 and 50 nm AuNPs after 3 and 7 days[315] proving that AuNPs were accumulated in this organ. According to this work, the accumulation was size- and time-dependent, showing a higher increase with the smallest size and the shortest time parameters.

In our case, no significant differences were found among groups, which indicate that citrate-stabilised AuNPs were unable to reach the lungs, independently of size. In any case, further studies are needed in order to determine the role of lungs as storage organs of gold nanoparticles after intraperitoneal administration.

5.2.4.10 Plasma *(page 93; table 4)*

In relation to the gold content in plasma, several hypotheses have been described in literature. Numerous parameters seem to be fundamental. Among others, researchers have focused on the nanoparticles coating. Some studies reveal that polyethylene glycol (PEG)-stabilized gold nanoparticles show a longer half-life when compared to other gold nanoparticles.[367,385,402] On the contrary, it is well established that citrate-stabilised gold nanoparticles are rapidly removed from plasma, probably by the action

of the protein corona, which favours the uptake by tissues and cells from the immune system.[373] To verify this, Morais et al. studied the biodistribution of gold nanoparticles with different surface coatings.[368] Among them, citrate-AuNPs exhibited the fastest removal from plasma.

The levels of gold in plasma have also been proved to be dependent on the nanoparticle size. As described by several authors, the stability and duration of the gold nanostructures in blood generally increase as the diameter decreases.[359,367,392,403] Surprisingly, the role of the route of administration in the AuNPs blood circulation has not been profoundly studied. Some studies have proved that gold nanostructures are highly present in plasma just after intravenous administration.[318,404] Other groups also point out the presence of gold nanoparticles in blood after subcutaneus administration.[405] Similarly, gold nanoparticles have observed to be translocated from the respiratory tract to plasma.[387] In 2015, Bednarski et al. published a study where the importance of the influence of the route of administration was assessed (by comparing the intravenous and oral administrations).[378] Their results established that the administration route did not have any effect on the blood concentration of these nanoparticles. In any case, further studies should be addressed in an attempt to confirm this hypothesis.

In our case, gold nanoparticles were not found in plasma after 9 days of treatment. These results confirm the idea that citrate-stabilised AuNPs are rapidly removed from plasma and further accumulated in other organs, which ratifies the fact that these type of gold nanoparticles have a short half-life in blood.

5.2.5 Haematological parameters (page 94; table 5)

The role that the exposure to gold nanoparticles may play in the haematological markers have been subject of several studies; although results are difficult to fully understand. For instance, Lasagna-Reeves et al. performed an *in vivo* study where male C57/BL6 mice were intraperitoneally injected with 12.5 nm citrate-stabilised AuNPs for 8 days, with doses ranging from 40 to 400 µg·kg^{-1} body weight.[406] According

to their results, no changes were observed in the RBC, WBC, haemoglobin, haematocrit, MCV, MCH, MCHC and RBW in any treated group; thus concluding that gold nanoparticles are not related to alterations in the haematopoietic factors.

Nevertheless, most researchers agree that these nanostructures modify the values of these parameters, even though the way they affect is quite unclear. For example, in 2013 Sengupta and coworkers determined the effects that the acute and chronic administration of gold nanoparticles may produce in the haematological parameters of mice.[407] For that purpose, animals designated for the acute study received a dose of 1, 2 or 10 mg·kg^{-1} body weight of 50 nm citrate-stabilised AuNPs by intravenous injection; while mice selected for the chronic study were treated for 90 days with 1 or 2 mg·kg^{-1} body weight AuNPs by intraperitoneal injection. Their data revealed that WBC values and haemoglobin concentrations increased in both experiments, while RBC ascended with the highest dose of gold nanoparticles in the acute experiment. Analogous results were published by Chen and coworkers, who studied the differences between male and female mice treated with gold nanoparticles.[408] An increase in WBC, RBC, PLT and HCT of male mice treated with 22.5 nm AuNPs; while female mice showed elevated values of MCH and MCHC. These data led them to conclude that male mice may suffer more serious toxicity than female mice when treated with gold nanoparticles, as WBC and RBC are directly related to infection and inflammation.

On the other side, many studies defend the idea that gold nanoparticles induce a decrease in the haematological parameters. For example, Zhang et al. assessed the possible toxicological effects of gold nanoparticles exposed by different administration routes (intravenous, intraperitoneal and oral administrations).[409] To do this, male mice were treated with 220 µg of 13.5 nm citrate-stabilised AuNPs for 28 days. A decrease in the number of red blood cells was found in mice intraperitoneal and orally treated. They finally stated that the intraperitoneal and oral administrations of gold nanoparticles provoked damage to the haematopoietic system and consequently induced the highest toxicity. Two years later, the same group performed a similar study where GSH and BSA-protected gold nanoclusters were intraperitoneally injected to female mice at the concentration of 7550 µg·kg^{-1} body weight for 24 h and 28

days.[410] Their results indicate that both gold nanoclusters were able to cause a decrease in the levels of WBC, RBC, MCH and MCHC at 24 h. However, these parameters showed no significant differences after exposing for 28 days; which might suggest that gold nanoclusters trigger an initial damage to the haematopoietic process that was finally normalised.

Our results show a clear decrease in the values of WBC, RBC, HGB and HCT in the groups treated with 10 and 60 nm AuNPs (especially significant in the case of the smallest nanoparticles). Moreover, the MCH and MCHC parameters were decreased in all treated group compared to the control rats. In view of these data, several conclusions can be obtained. The decrease in the MCH usually indicates the formation of erythrocytes with smaller diameter. This idea is corroborated by the fact that the HCT is also lower. Furthermore, the diminution of both parameters together with the decrease in the MCHC may point out a reduction in the haemoglobin production and the existence of an anaemic state, derived from the exposure to gold nanoparticles. Definitively, the administration of AuNPs affected the function of the bone marrow. Analogous data were published by Saleh et al., who observed a clear decrease in the MCHC of hamsters daily treated with 30 ppb of 18 nm citrate-stabilised AuNPs by intraperitoneal injection.[411] They finally concluded that the obtained results might be attributed to the ability of the AuNPs to cross the fenestrated endothelial membrane of the bone marrow, thus interfering with the normal erythropoiesis, resulting in immature red blood cells.

5.2.6 Inflammatory status (page 95; table 6)

The effect of gold nanoparticles on the inflammatory status has also been controversial. However, in this respect, inflammation is certainly not unique to AuNPs and seems to be one of the major toxic effects of nanoparticles exposure. Thus, Khan and co-workers have published several studies where reveal a transient increase of some cytokines as IL-1ß, IL-6 and TNF-α in liver and kidney after the intraperitoneal administration of naked gold nanoparticles.[319,412] Similar results were described by

Durocher and colleagues, who highlighted the increase of IL-8 cytokine levels after *in vitro* and *in vivo* exposure with both positively and negatively-charged nanoparticles.[413]

On the contrary, Chen et al. reported a reduction in TNF-α and IL-6 mRNA levels in the fat together with a significant fat loss, whereas no detectable toxicity was detected in liver or kidney.[361]

In our case, the treatment with AuNPs did not modify the levels of inflammatory parameters, compared to the control group. The lack of inflammatory response has also been described.[320] In our view, although AuNPs caused an increase in ROS production and, as a result, it increased the damage in proteins and lipids, the experimental conditions (dose and time) used in this study were insufficient to trigger an inflammatory response and, therefore, tissue damage.

To our view, the disparity in exposure time and dose found in bibliography may explain the different results. In fact, most of the studies where an inflammatory increase was observed were performed under acute conditions, with higher AuNPs doses used to assess the possible toxicity derived from the exposure to these nanomaterials.[319,413]

5.2.7 Biochemical assessment *(page 95; table 7)*

Some groups have also tackled the study of the effects that the exposure to gold nanoparticles may induce *in vivo* on the biochemical markers. They are generally accepted as indicators of certain organs injury; such as liver, kidney or heart; and an increase in their plasma levels usually indicates that some factor (drug, illness, extreme exercise, etc.) is causing an aggression. In the case of the exposure to gold nanostructures, PEG-AuNPs seem to be the most toxic in terms of biochemical disorders, as reflect the studies published by the scientific community. For example, Bednarski et al. proved that livers from Wistar rats treated with a single intravenous injection of 25 nm PEG-AuNPs were affected, after detecting an increase in the alanine aminotransferase (ALT) and aspartate aminotransferase (AST) levels.[378] Interestingly, no changes were found when comparing the levels of total cholesterol and triglycerides among control and treated groups, which might reveal that the damage in

this organ was not extremely severe. On their part, Zhang and coworkers tried to assess the toxic effect of different PEG-AuNPs sizes.[414] Consequently, C57 mice were intraperitoneally treated with 5, 10, 30 or 60 nm PEG-AuNPs for 28 days. In this case, a high dose (4 mg·kg^{-1} body weight) was tested. Their results determined that 10 nm gold nanoparticles caused renal damage (with a decrease in the globulin and total protein levels), while 60 nm PEG-AuNPs produced renal and liver toxicity (by increasing the level of ALT and the concentration of creatinine). Two years later, the same group evaluated the possible differences existing between sexes when exposed to gold nanoparticles.[408] In this case, 4, 22, 29 and 36 nm PEG-AuNPs were tested; although the same dose and duration were used. The obtained data led them to conclude that the smallest nanoparticles caused liver damage in male mice to a larger extent (as showed the increases in ALT, AST levels); while the biggest gold nanoparticles tended to provoke a higher renal toxicity in the same group, as proved by the increase in the creatinine levels.

The study of the renal and liver functions after the treatment with gold nanoparticles was also performed by other group in 2013.[377] In this case, 10 and 50 nm citrate-stabilised gold nanoparticles were intraperitoneally injected to Wistar-Kyoto rats for 3 days, although the exact dose administered is not published. They observed an increase in the AST and gamma glutamyl transferase (γ - GT) in both treated groups compared to the control animals. However, contrarily to previously described, a decrease in the ALT concentrations were measured when treated with 10 and 50 nm AuNPs. Furthermore, no significant changes were observed in the urea and creatinine levels.

Our results showed that no alterations occurred in any of the biochemical parameters studied in any of the treated group, compared to the controls. These data coincide with those published by Lasagna-Reeves and coworkers, who did not observe any change in the total bilirubin, alkaline phosphatase, uric acid, urea or creatinine levels after intraperitoneally injecting different doses (40, 200 or 400 µg·kg^{-1} body weight) of 12.5 nm citrate-stabilised gold nanoparticles for 8 days.[406]

As exposed in relation to the inflammatory markers, in our opinion, the dose and duration used in this experiment was high enough to induce an increase in the ROS production that consequently provoked damage in the protein, lipid and DNA

components. However, it was not sufficient to alter the biochemical parameters, thus indicating that the damage was relatively low. The fact that the three gold nanoparticles sizes did not exhibit significant changes also confirms that there are no differences regarding size at the dose and time studied. Furthermore, these data also reinforce the idea that citrate-stabilised AuNPs may be less toxic in terms of biochemical alterations than other gold nanostructures.

6. CONCLUSIONS

The work accomplished in this doctoral thesis leads us to the conclusions that are summarized in the following points:

1. The exposure of cell lines to 10, 30 and 60 nm citrate-stabilised gold nanoparticles increases the reactive oxygen species production in the cell, in a time and dose dependent manner. This increase is finally normalised to control values after 32 h of treatment.

2. The ROS increase is directly related to the decrease in cell viability, this is to say, those cells where the ROS overproduction was higher also showed an increase in cell mortality. Likewise, cell viability was normalised after 32 h of treatment.

3. One of the main mechanisms responsible for the increase in cell mortality that takes place after the ROS overproduction are the breaks in the DNA chain; as it is confirmed by the comet assays carried out. Furthermore, clear size dependence was observed, where 10 nm AuNPs showed damage similar to the control cells. The nucleus membrane acts as a filter, thus avoiding the entrance of particles bigger than 35 nm.

4. The study of the TEM images revealed the progress of the intracellular distribution over time of the three gold nanoparticles sizes used in this project; thus being disperse throughout the cytoplasm in the first phases while they are accumulated inside lipid drops after 24 h of treatment. Especially significant is the case of the 10 nm AuNPs. These nanoparticles could be visualised inside the nucleus for the first time.

5. The exposure of animals to gold nanoparticles also confirmed the damage occurred in the protein and lipid components of the liver, as it is verified by the increases in lipid peroxidation and protein carbonylation of the treated rats.

6. The gold biodistribution study by ICP-MS proved an unequal accumulation of gold regarding the tissue and the gold nanoparticle size. Hence, the reticuloendothelial system plays a crucial role in the metabolism, storage and elimination of the biggest nanoparticles, while the intestinal endogenous via is responsible for the elimination of the smallest AuNPs. Furthermore, 10 nm size gold nanoparticles showed the widest biodistribution and therefore the most deleterious effects.

7. The gold nanoparticles cell distribution by TEM images of hepatocytes of the Wistar rats showed the presence of some single nanoparticles dispersed throughout the cytoplasm as well as accumulated in lipid drops. Once more, 10 nm AuNPs were visualised inside the nucleus.

8. In spite of the oxidative induced deleterious structural effects, the analysis of the biochemical and inflammatory parameters revealed that the exposure to gold nanoparticles under the tested experimental conditions did not cause important tissue damage, as it is verified by the obtained results of the treated groups.

9. The haematological markers showed the presence of smaller erythrocytes as well as lower values of haemoglobin and haematocrit. Moreover the MCH and MCHC parameters were lower in the treated rats compared to the control animals; which may indicate an initial anaemic state by the alteration of the red blood cells formation in the bone marrow.

El trabajo acometido en la presente tesis doctoral nos lleva a las conclusiones que resumiremos en los siguientes puntos:

1. La exposición de líneas celulares a nanopartículas de oro estabilizadas con citrato y de diámetro de 10, 30 o 60 nm aumentan la producción de especies reactivas de oxígeno en el interior celular, de una manera tiempo y dosis dependiente. Dicho aumento se ve estabilizado tras el paso de las horas, retornando a los valores normales tras 32 horas de exposición.

2. El aumento de ROS está directamente relacionado con un descenso en la viabilidad celular; esto es, aquellas células donde la producción de ROS fue superior, también mostró un aumento de la mortalidad celular. Asimismo, la viabilidad celular se vio normalizada tras 32 horas de exposición.

3. Uno de los mecanismos responsables del aumento de la mortalidad celular desencadenado por el aumento de las especies reactivas de oxígeno, es la rotura de la cadena de ADN, tal y como acredita el estudio del cometa realizado. Además, se observó una clara dependencia del tamaño, mostrando las nanopartículas de 10 nm de diámetro un daño equivalente al grupo control positivo. La membrana nuclear actúa como filtro impidiendo la entrada de partículas superiores a 35 nm.

4. El estudio mediante imágenes de microscopía electrónica en cultivos celulares demostró la evolución de la distribución intracelular de las tres nanopartículas ensayadas a lo largo del tiempo; mostrándose dispersas por el citoplasma en los primeros estadíos, mientras que son almacenadas en gotas lipídicas tras 24 horas de exposición. Especial importancia reside en las nanopartículas de 10 nm, que fueron visualizadas por primera vez en el interior del núcleo.

5. La exposición de los animales de experimentación a las nanopartículas de oro confirmó el daño en los componentes lipídicos y proteicos del tejido hepático,

tal y como acreditan los resultados de peroxidación lipídica y carbonilación proteica.

6. La determinación de la biodistribución de oro en los distintos tejidos mediante ICP-MS demostró un acúmulo desigual en relación al órgano y la nanopartícula estudiada. Así, el sistema reticuloendotelial juega un papel crucial en el metabolismo, almacenamiento y eliminación de las nanopartículas de mayor tamaño; mientras que las nanopartículas más pequeñas son principalmente eliminadas por la vía endógena intestinal. Además, las nanopartículas de oro de 10 nm mostraron una biodistribución más amplia y, por consiguiente, mayores daños.

7. El estudio de la distribución intracelular de las nanopartículas de oro en hepatocitos de ratas Wistar mediante microscopía electrónica de transmisión demostró la presencia de algunas nanopartículas dispersas por el citoplasma, así como acumuladas en gotas lipídicas. Nuevamente las nanopartículas de 10 nm fueron visualizadas en el interior nuclear.

8. A pesar del daño oxidativo ocasionado en los componentes celulares, el estudio de los parámetros bioquímicos e inflamatorios reveló que la exposición a nanopartículas en las condiciones experimentales ensayadas no fue suficiente para desencadenar un daño tisular importante, como así lo acreditan los valores obtenidos para los distintos grupos.

9. Los indicadores hematológicos mostraron la presencia de eritrocitos de menor tamaño así como valores de hemoglobina y hematocritos inferiores. Además los parámetros de hemoglobina corpuscular media y concentración de hemoglobina corpuscular media fueron más bajos en los animales tratados que en el grupo control; lo que puede indicar una anemia incipiente por alteración en la formación de glóbulos rojos en la médula ósea.

7. BIBLIOGRAPHY

1.   EUR-Lex - 32011H0696 - EN - EUR-Lex. Available at: http://eur-lex.europa.eu/eli/reco/2011/696/oj. (Accessed: 2nd November 2017)

2.   Aucouturier, M., Mathis, F., Robcis, D., Castaing, J., Salomon, J., Pichon, L. *et al.* Intentional patina of metal archaeological artefacts: Non-destructive investigation of Egyptian and Roman museum treasures. *Corros. Eng. Sci. Technol.* **45,** 314–321 (2010).

3.   Daw, R. Nanotechnology is ancient history. *The Guardian* (2012).

4.   The Project on Emerging Nanotechnologies. Available at: http://www.nanotechproject.org.

5.   Cobley, C. M., Chen, J., Cho, E. C., Wang, L. V. & Xia, Y. Gold nanostructures: a class of multifunctional materials for biomedical applications. *Chem. Soc. Rev.* **40,** 44–56 (2010).

6.   Huang, X., Neretina, S. & El-Sayed, M. A. Gold Nanorods: From Synthesis and Properties to Biological and Biomedical Applications. *Adv. Mater.* **21,** 4880–4910 (2009).

7.   Dreaden, E. C., Alkilany, A. M., Huang, X., Murphy, C. J. & El-Sayed, M. A. The golden age: gold nanoparticles for biomedicine. *Chem. Soc. Rev.* **41,** 2740–2779 (2012).

8.   Willets, K. A. & Duyne, R. P. V. Localized Surface Plasmon Resonance Spectroscopy and Sensing. *Annu. Rev. Phys. Chem.* **58,** 267–297 (2007).

9.   Yang, X., Yang, M., Pang, B., Vara, M. & Xia, Y. Gold Nanomaterials at Work in Biomedicine. *Chem. Rev.* **115,** 10410–10488 (2015).

10.   Wu, Z., Lee, D., Rubner, M. F. & Cohen, R. E. Structural Color in Porous, Superhydrophilic, and Self-Cleaning SiO2/TiO2 Bragg Stacks. *Small* **3,** 1445–1451 (2007).

11.   Vance, M. E., Kuiken, T., Vejerano, E. P., McGinnis, S.P., Hochella, M. F., Rejeski, D. *et al.* Nanotechnology in the real world: Redeveloping the nanomaterial consumer products inventory. *Beilstein J. Nanotechnol.* **6,** 1769–1780 (2015).

12.   Ávalos, A., Haza, A. I., Mateo, D. & Morales, P. Effects of silver and gold nanoparticles of different sizes in human pulmonary fibroblasts. *Toxicol. Mech. Methods* **25,** 287–295 (2015).

13.   Oberdörster, G., Ferin, J. & Lehnert, B. E. Correlation between particle size, in vivo particle persistence, and lung injury. *Environ. Health Perspect.* **102 Suppl 5,** 173–179 (1994).

14.   Grabinski, C., Hussain, S., Lafdi, K., Braydich-Stolle, L. & Schlager, J. Effect of particle dimension on biocompatibility of carbon nanomaterials. *Carbon* **45,** 2828–2835 (2007).

15.   Zhang, Y., Ali, S. F., Dervishi, E., Xu, Y., Li, Z., Casciano, D. *et al.* Cytotoxicity effects of graphene and single-wall carbon nanotubes in neural phaeochromocytoma-derived PC12 cells. *ACS Nano* **4,** 3181–3186 (2010).

16.   Haes, A. J., Haynes, C. L., McFarland, A. D., Schatz, G. C., Duyne, R. P. & Zou, S. Plasmonic Materials for Surface-Enhanced Sensing and Spectroscopy. *MRS Bull.* **30,** 368–375 (2005).

17.   Goodman, C. M., McCusker, C. D., Yilmaz, T. & Rotello, V. M. Toxicity of Gold Nanoparticles Functionalized with Cationic and Anionic Side Chains. *Bioconjug. Chem.* **15,** 897–900 (2004).

18.   Asati, A., Santra, S., Kaittanis, C. & Perez, J. M. Surface-Charge-Dependent Cell Localization and Cytotoxicity of Cerium Oxide Nanoparticles. *ACS Nano* **4,** 5321–5331 (2010).

19.   Hühn, D., Kantner, K., Geidel, C., Brandholt, S., De Cock, I., Soenen, S. J. *et al.* Polymer-Coated Nanoparticles Interacting with Proteins and Cells: Focusing on the Sign of the Net Charge. *ACS Nano* **7,** 3253–3263 (2013).

20.   Shahbazi, M. A., Hamidi, M., Mäkilä, E. M., Zhang, H., Almeida, P. V., Kaasalainen, M. *et al.* The mechanisms of surface chemistry effects of mesoporous silicon nanoparticles on immunotoxicity and biocompatibility. *Biomaterials* **34,** 7776–7789 (2013).

21.   Calatayud, M. P., Sanz, B., Raffa, V., Riggio, C., Ibarra, M. R. & Goya, G. F. The effect of surface charge of functionalized Fe3O4 nanoparticles on protein adsorption and cell uptake. *Biomaterials* **35,** 6389–6399 (2014).

22.   Pal, A. N., Ghatak, S., Kochat, V., Sneha, E. S., Sampathkumar, A., Raghavan, S. *et al.* Microscopic mechanism of 1/f noise in graphene: Role of energy band dispersion. *ACS Nano* **5,** 2075–2081 (2011).

23.   Xiao, L., Takada, H., Gan, X. & Miwa, N. The water-soluble fullerene derivative 'Radical Sponge®' exerts cytoprotective action against UVA irradiation but not visible-light-catalyzed cytotoxicity in human skin keratinocytes. *Bioorg. Med. Chem. Lett.* **16,** 1590–1595 (2006).

24.   Howard, I. A., Mauer, R., Meister, M. & Laquai, F. Effect of Morphology on Ultrafast Free Carrier Generation in Polythiophene:Fullerene Organic Solar Cells. *J. Am. Chem. Soc.* **132,** 14866–14876 (2010).

25.   Yang, K., Feng, L., Hong, H., Cai, W. & Liu, Z. Preparation and functionalization of graphene nanocomposites for biomedical applications. *Nat. Protoc.* **8** (2013).

26.   Jain, S., Patel, N., Shah, M. K., Khatri, P. & Vora, N. Recent Advances in Lipid-Based Vesicles and Particulate Carriers for Topical and Transdermal Application. *J. Pharm. Sci.* doi:10.1016/j.xphs.2016.10.001 (2016)

27.   Felnerova, D., Viret, J.-F., Glück, R. & Moser, C. Liposomes and virosomes as delivery systems for antigens, nucleic acids and drugs. *Curr. Opin. Biotechnol.* **15,** 518–529 (2004).

28.   Kraft, J. C., Freeling, J. P., Wang, Z. & Ho, R. J. Y. Emerging research and clinical development trends of liposome and lipid nanoparticle drug delivery systems. *J. Pharm. Sci.* **103,** 29–52 (2014).

29.   Kim, D. K., Lai, Y., Diroll, B. T., Murray, C. B. & Kagan, C. R. Flexible and low-voltage integrated circuits constructed from high-performance nanocrystal transistors. *Nat. Commun.* **3,** 1216 (2012).

30.   Bhowmik, D., You, L. & Salahuddin, S. Spin Hall effect clocking of nanomagnetic logic without a magnetic field. *Nat. Nanotechnol.* **9,** 59–63 (2014).

31.   Televisores SUHD - Imagen Quantum Dot y HDR | SAMSUNG. Available at: http://www.samsung.com/es/suhdtv/quantum-dot-display/. (Accessed: 1st December 2016)

32.   Subramani, A., Geerpuram, D., Domanowski, A., Baskaran, V. & Metlushko, V. Vortex state in magnetic rings. *Phys. C Supercond.* **404,** 241–245 (2004).

33.   Landi, B., Ganter, M., Cress, C., DiLeo, R. & Raffaelle, R. Carbon nanotubes for lithium ion batteries. *Energy Environ. Sci.* **2,** 638–654 (2009).

34.   Sehrawat, P., Julien, C. & Islam, S. S. Carbon nanotubes in Li-ion batteries: A review. *Mater. Sci. Eng. B* **213,** 12–40 (2016).

35.   Tyagi, N., Srivastana, S. K., Arora, S., Omar, Y., Ijaz, Z. M., Al-Ghadhban, A. *et al.* Comparative analysis of the relative potential of silver, Zinc-oxide and titanium-dioxide nanoparticles against UVB-induced DNA damage for the prevention of skin

carcinogenesis. *Cancer Lett.* **383,** 53–61 (2016).

36.   Osmond-McLeod, M. J., Oytam, Y., Rowe, A., Sobhanmanesh, F., Greenoak, G., Kirby, J. *et al.* Long-term exposure to commercially available sunscreens containing nanoparticles of TiO2 and ZnO revealed no biological impact in a hairless mouse model. *Part. Fibre Toxicol.* doi:10.1186/s12989-016-0154-4 (2016)

37.   Guix, M., Carbonell, C., Comenge, J., García-Fernández, L., Alarcón, A. & Casals, E. Nanoparticles for cosmetics : how safe is safe? *Contrib. Sci.* **0,** 213–217 (2010).

38.   Raj, S., Jose, S., Sumod, U. S. & Sabitha, M. Nanotechnology in cosmetics: Opportunities and challenges. *J. Pharm. Bioallied Sci.* **4,** 186–193 (2012).

39.   Lee, J., Lee, S., Chung, E., Reyes, V. C. & Mahendra, S. Nanomaterials in Civil Engineering. *Springer Handbook of Nanomaterials.* doi:10.1007/978-3-642-20595-8_29 (2013)

40.   Zhang, W., Suhr, J. & Koratkar, N. Carbon nanotube/polycarbonate composites as multifunctional strain sensors. *J. Nanosci. Nanotechnol.* **6,** 960–964 (2006).

41.   Luo, T. Y., Liang, T. X. & Li, C. S. Addition of carbon nanotubes during the preparation of zirconia nanoparticles: influence on structure and phase composition. *Powder Technol.* **139,** 118–122 (2004).

42.   Becher, P. F. Microstructural Design of Toughened Ceramics. *J. Am. Ceram. Soc.* **74,** 255–269 (1991).

43.   Sobolev, K. & Ferrada, M. How Nanotechnology Can Change the Concrete World. *Progress in Nanotechnology*. doi: 10.1002/9780470588260.ch16 (2009)

44.   Sáez de Ibarra, Y., Gaitero, J. J., Erkizia, E. & Campillo, I. Atomic force microscopy and nanoindentation of cement pastes with nanotube dispersions. *Phys. Status Solidi A* **203,** 1076–1081 (2006).

45.   A. K. Rana V. Kiran, S. B. Rana & A. Kumari. Significance of nanotechnology in construction engineering. *Int. J. Recent Trends Eng.* **1,** 46–48 (2009).

46.   Iavicoli, I., Leso, V., Ricciardi, W., Hodson, L. L. & Hoover, M. D. Opportunities and challenges of nanotechnology in the green economy. *Environ. Health* **13** (2014).

47.   Zhu, W., Bartos, P. J. M. & Porro, A. Application of nanotechnology in construction. *Mater. Struct.* **37,** 649–658 (2004).

48.   Kumar, A., Vemula, P. K., Ajayan, P. M. & John, G. Silver-nanoparticle-embedded antimicrobial paints based on vegetable oil. *Nat. Mater.* **7,** 236–241 (2008).

49.   Yetisen, A. K., Qu, H., Manbachi, A., Butt, H., Dokmeci, M. R., Hinestroza, J. P. *et al.* Nanotechnology in Textiles. *ACS Nano* **10,** 3042–3068 (2016).

50.   Markets and Markets. Smart Textiles Market Worth 4,722.81 Million USD by 2020. Available at: http://www.prnewswire.com/news-releases/smart-textiles-market-worth-472281-million-usd-by-2020-519343471.html. (Accessed: 12th December 2016)

51.   Marmot Nano AS Jacket. Available at: http://www.gore-tex.com/product/marmot-nano-as-jacket/1415318110420/. (Accessed: 12th December 2016)

52.   Marmur, A. The Lotus effect: superhydrophobicity and metastability. *Langmuir ACS J. Surf. Colloids* **20,** 3517–3519 (2004).

53.   Gao, L. & McCarthy, T. J. The 'Lotus Effect' Explained: Two Reasons Why Two Length Scales of Topography Are Important. *Langmuir* **22,** 2966–2967

(2006).

54.   Bae, G. Y., Min, B. G., Jeong, Y. G., Lee, S. C., Jang, J. H. & Koo, G. H. Superhydrophobicity of cotton fabrics treated with silica nanoparticles and water-repellent agent. *J. Colloid Interface Sci.* **337,** 170–175 (2009).

55.   Yu, M., Gu, G., Meng, W. D. & Qing, F. L. Superhydrophobic cotton fabric coating based on a complex layer of silica nanoparticles and perfluorooctylated quaternary ammonium silane coupling agent. *Appl. Surf. Sci.* **253,** 3669–3673 (2007).

56.   Artus, G. R., Zimmermann, J., Reifler, F. A., Brewer, S. A. & Seeger, S. A superoleophobic textile repellent towards impacting drops of alkanes. *Appl. Surf. Sci.* **258,** 3835–3840 (2012).

57.   Hoefnagels, H. F., Wu, D., de With, G. & Ming, W. Biomimetic Superhydrophobic and Highly Oleophobic Cotton Textiles. *Langmuir* **23,** 13158–13163 (2007).

58.   Zhang, F. & Yang, J. Application of Nano-ZnO on Antistatic Finishing to the Polyester Fabric. *Mod. Appl. Sci.* **3,** (2008).

59.   Wang, D., Lin, Y., Zhao, Y. & Gu, L. Polyacrylonitrile Fibers Modified by Nano-Antimony-Doped Tin Oxide Particles. *Text. Res. J.* **74,** 1060–1065 (2004).

60.   Wang, C. C. & Chen, C. C. Physical properties of crosslinked cellulose catalyzed with nano titanium dioxide. *J. Appl. Polym. Sci.* **97,** 2450–2456 (2005).

61.   Yuen, C. W., Ku, S. K., Kan, C. W., Cheng, Y. F., Choi, P. S. & Lam, Y. L. Using nano-TiO2 as co-catalyst for improving wrinkle-resistance of cotton fabric. *Surf. Rev. Lett.* **14,** 571–575 (2007).

62.   Lam, Y. L., Kan, C. W. & Yuen, C. W. Wrinkle-resistant finishing of cotton fabric with BTCA - the effect of co-catalyst. *Text. Res. J.* **81,** 482–493 (2011).

63.   Yuen, C. W., Ku, S. K., Li, Y., Cheng, Y. F., Kan, C. W. & Choi, P. S. Improvement of wrinkle-resistant treatment by nanotechnology. *J. Text. Inst.* **100,** 173–180 (2009).

64.   Lu, Y. H., Lin, H., Chen, Y. Y., Wang, C. & Hua, Y. R. Structure and performance ofBombyx mori silk modified with nano-TiO2 and chitosan. *Fibers Polym.* **8,** 1–6 (2007).

65.   Kumar, S., Doshi, H., Srinivasarao, M., Park, J. O. & Schiraldi, D. A. Fibers from polypropylene/nano carbon fiber composites. *Polymer* **43,** 1701–1703 (2002).

66.   Liu, Y., Wang, X., Qi, K. & Xin, J. Functionalization of cotton with carbon nanotubes. *J. Mater. Chem.* **18,** 3454–3460 (2008).

67.   Jiang, K., Li, Q. & Fan, S. Nanotechnology: Spinning continuous carbon nanotube yarns. *Nature* **419,** 801–801 (2002).

68.   Wang, R., Xin, J. H., Tao, X. M. & Daoud, W. A. ZnO Nanorods grown on cotton fabrics at low temperature. *Chem. Phys. Lett.* **398,** 250–255 (2004).

69.   Kathirvelu, S., D'Souza, L. & Dhurai, B. UV protection finishing of textiles using ZnO nanoparticles. *Ind. J. Fibre Text. Res.* **34,** 267-273 (2009).

70.   Moroni, M., Borrini, D., Calamai, L. & Dei, L. Ceramic nanomaterials from aqueous and 1,2-ethanediol supersaturated solutions at high temperature. *J. Colloid Interface Sci.* **286,** 543–550 (2005).

71.   Saito, M. Antibacterial, Deodorizing, and UV Absorbing Materials Obtained with Zinc Oxide (ZnO) Coated Fabrics. *J. Ind. Text.* **23,** 150–164 (1993).

72.   Yeo, S. Y., Lee, H. J. & Jeong, S. H. Preparation of nanocomposite fibers for permanent antibacterial effect. *J. Mater. Sci.* **38,** 2143–2147 (2003).

73.   Lee, H. J., Yeo, S. Y. & Jeong, S. H. Antibacterial effect of nanosized silver

colloidal solution on textile fabrics. *J. Mater. Sci.* **38,** 2199–2204 (2003).

74.	Yeo, S. Y. & Jeong, S. H. Preparation and characterization of polypropylene/silver nanocomposite fibers. *Polym. Int.* **52,** 1053–1057 (2003).

75.	Xue, C. H., Chen, J., Yin, W., Jia, S. T. & Ma, J. Z. Superhydrophobic conductive textiles with antibacterial property by coating fibers with silver nanoparticles. *Appl. Surf. Sci.* **258,** 2468–2472 (2012).

76.	Daoud, W. A. & Xin, J. H. Low Temperature Sol-Gel Processed Photocatalytic Titania Coating. *J. Sol-Gel Sci. Technol.* **29,** 25–29 (2004).

77.	Bozzi, A., Yuranova, T. & Kiwi, J. Self-cleaning of wool-polyamide and polyester textiles by TiO2-rutile modification under daylight irradiation at ambient temperature. *J. Photochem. Photobiol. Chem.* **172,** 27–34 (2005).

78.	Song, J., Wang, C. & Hinestroza, J. P. Electrostatic assembly of core-corona silica nanoparticles onto cotton fibers. *Cellulose* **20,** 1727–1736 (2013).

79.	Simoncic, B. & Tomsic, B. Structures of Novel Antimicrobial Agents for Textiles - A Review. *Text. Res. J.* **80,** 1721–1737 (2010).

80.	Tung, W. S. & Daoud, W. A. Self-cleaning fibers via nanotechnology: a virtual reality. *J. Mater. Chem.* **21,** 7858–7869 (2011).

81.	Shim, B. S., Chen, W., Doty, C., Xu, C. & Kotov, N. A. Smart Electronic Yarns and Wearable Fabrics for Human Biomonitoring made by Carbon Nanotube Coating with Polyelectrolytes. *Nano Lett.* **8,** 4151–4157 (2008).

82.	Li, X., Sun, P., Fan, L., Zhu, M., Wang, K., Zhong, M. *et al.* Multifunctional graphene woven fabrics. *Sci. Rep.* **2,** 395 (2012).

83.	Pan, S., Lin, H., Deng, J., Chen, P., Chen, X., Yang, Z. *et al.* Novel Wearable Energy Devices Based on Aligned Carbon Nanotube Fiber Textiles. *Adv. Energy Mater.* **5** (2015).

84.	Zhang, D., Miao, M., Niu, H. & Wei, Z. Core-Spun Carbon Nanotube Yarn Supercapacitors for Wearable Electronic Textiles. *ACS Nano* **8,** 4571–4579 (2014).

85.	Horcajada, P. *et al.* Metal–Organic Frameworks in Biomedicine. *Chem. Rev.* **112,** 1232–1268 (2012).

86.	Cai, W., Chu, C. C., Liu, G. & Wáng, Y. X. Metal–Organic Framework-Based Nanomedicine Platforms for Drug Delivery and Molecular Imaging. *Small* **11,** 4806–4822 (2015).

87.	Ozer, R. & Hinestroza, J. One-step growth of isoreticular luminescent metal–organic frameworks on cotton fibers. *RSC Adv.* **5,** 15198–15204 (2015).

88.	Zhukovskyi, M., Sanchez-Botero, L., McDonald, M. P., Hinestroza, J. & Kuno, M. Nanowire-functionalized cotton textiles. *ACS Appl. Mater. Interfaces* **6,** 2262–2269 (2014).

89.	Biju, V. Chemical modifications and bioconjugate reactions of nanomaterials for sensing, imaging, drug delivery and therapy. *Chem. Soc. Rev.* **43,** 744–764 (2014).

90.	Lim, W. Q. & Gao, Z. Plasmonic nanoparticles in biomedicine. *Nano Today* **11,** 168–188 (2016).

91.	Kievit, F. M. & Zhang, M. Surface engineering of iron oxide nanoparticles for targeted cancer therapy. *Acc. Chem. Res.* **44,** 853–862 (2011).

92.	Wang, Y., Zhao, Q., Han, N., Bai, L., Li, J., Liu, J. *et al.* Mesoporous silica nanoparticles in drug delivery and biomedical applications. *Nanomedicine Nanotechnol. Biol. Med.* **11,** 313–327 (2015).

93.	He, Q., Zhang, J., Chen, F., Guo, L., Zhu, Z. & Shi, J. An anti-ROS/hepatic fibrosis drug delivery system based on salvianolic acid B loaded mesoporous silica

nanoparticles. *Biomaterials* **31,** 7785–7796 (2010).

94.   Slowing, I. I., Trewyn, B. G. & Lin, V. S. Mesoporous silica nanoparticles for intracellular delivery of membrane-impermeable proteins. *J. Am. Chem. Soc.* **129,** 8845–8849 (2007).

95.   Carvalho, L. V. *et al.* Immunological parameters related to the adjuvant effect of the ordered mesoporous silica SBA-15. *Vaccine* **28,** 7829–7836 (2010).

96.   Rana, V. K., Choi, M., Kong, J., Kim, G. Y., Kim, M. J., Kim, S. *et al.* Synthesis and Drug-Delivery Behavior of Chitosan-Functionalized Graphene Oxide Hybrid Nanosheets. *Macromol. Mater. Eng.* **296,** 131–140 (2011).

97.   Hu, H., Yu, J., Li, Y., Zhao, J. & Dong, H. Engineering of a novel pluronic F127/graphene nanohybrid for pH responsive drug delivery. *J. Biomed. Mater. Res. A* **100,** 141–148 (2012).

98.   Zhou, L., Wang, W., Tang, J., Zhou, J., Jiang, H. & Shen, J. Graphene oxide noncovalent photosensitizer and its anticancer activity in vitro. *Chem. Weinh. Bergstr. Ger.* **17,** 12084–12091 (2011).

99.   Lee, N., Yoo, D., Ling, D., Cho, M. H., Hyeon, T. & Cheon, J. Iron Oxide Based Nanoparticles for Multimodal Imaging and Magnetoresponsive Therapy. *Chem. Rev.* **115,** 10637–10689 (2015).

100.   Cheng, L., Wang, C., Feng, L., Yang, K. & Liu, Z. Functional Nanomaterials for Phototherapies of Cancer. *Chem. Rev.* **114,** 10869–10939 (2014).

101.   Huang, X. L., Zhang, B., Ren, L., Ye, S., Sun, L., Zhang, Q. *et al.* In vivo toxic studies and biodistribution of near infrared sensitive Au-Au(2)S nanoparticles as potential drug delivery carriers. *J. Mater. Sci. Mater. Med.* **19,** 2581–2588 (2008).

102.   Smith, A. M., Mancini, M. C. & Nie, S. Bioimaging: Second window for in vivo imaging. *Nat. Nanotechnol.* **4,** 710–711 (2009).

103.   Ye, E., Win, K. Y., Tan, H. R., Lin, M., Teng, C. H., Mlayah, A. *et al.* Plasmonic Gold Nanocrosses with Multidirectional Excitation and Strong Photothermal Effect. *J. Am. Chem. Soc.* **133,** 8506–8509 (2011).

104.   Huang, P., Rong, P., Lin, J., Li, W., Yan, X., Zhang, M. G. *et al.* Triphase Interface Synthesis of Plasmonic Gold Bellflowers as Near-Infrared Light Mediated Acoustic and Thermal Theranostics. *J. Am. Chem. Soc.* **136,** 8307–8313 (2014).

105.   Johannsen, M., Gneveckow, U., Taymoorian, K., Thiesen, B., Waldöfner, N., Scholz, R. *et al.* Morbidity and quality of life during thermotherapy using magnetic nanoparticles in locally recurrent prostate cancer: results of a prospective phase I trial. *Int. J. Hyperth. Off. J. Eur. Soc. Hyperthermic Oncol. North Am. Hyperth. Group* **23,** 315–323 (2007).

106.   Banerjee, R., Katsenovich, Y., Lagos, L., Mclintosh, M., Zhang, X. & Li, C. Nanomedicine: magnetic nanoparticles and their biomedical applications. *Curr. Med. Chem.* **17,** 3120–3141 (2010).

107.   Amstad, E., Textor, M. & Reimhult, E. Stabilization and functionalization of iron oxide nanoparticles for biomedical applications. *Nanoscale* **3,** 2819–2843 (2011).

108.   Zhou, X., Laroche, F., Lamers, G. E., Torraca, V., Voskamp, P., Lu, Tao. *et al.* Ultra-small graphene oxide functionalized with polyethylenimine (PEI) for very efficient gene delivery in cell and zebrafish embryos. *Nano Res.* **5,** 703–709 (2012).

109.   Bao, H., Pan, Y., Ping, Y., Sahoo, N. G., Wu, T., Li, J. *et al.* Chitosan-functionalized graphene oxide as a nanocarrier for drug and gene delivery. *Small Weinh. Bergstr. Ger.* **7,** 1569–1578 (2011).

110.   Li, X., Xie, Q. R., Zhang, J., Xia, W. & Gu, H. The packaging of siRNA within the

mesoporous structure of silica nanoparticles. *Biomaterials* **32,** 9546–9556 (2011).

111.   Torney, F., Trewyn, B. G., Lin, V. S.-Y. & Wang, K. Mesoporous silica nanoparticles deliver DNA and chemicals into plants. *Nat. Nanotechnol.* **2,** 295–300 (2007).

112.   Radu, D. R., Lai, C., Jeftinija, K., Rowe, E. W., Jeftinija, S. & Lin, V. Polyamidoamine Dendrimer-Capped Mesoporous Silica Nanosphere-Based Gene Transfection Reagent. *J. Am. Chem. Soc.* **126,** 13216–13217 (2004).

113.   Qiu, L., Liu, J. Z., Chang, S. L. Y., Wu, Y. & Li, D. Biomimetic superelastic graphene-based cellular monoliths. *Nat. Commun.* **3,** 1241 (2012).

114.   Wang, L., Lu, C., Zhang, B., Zhao, B., Wu, F. & Guan, S. Fabrication and characterization of flexible silk fibroin films reinforced with graphene oxide for biomedical applications. *RSC Adv.* **4,** 40312–40320 (2014).

115.   Padmanabhan, P., Kumar, A., Kumar, S., Chaudhary, R. K. & Gulyás, B. Nanoparticles in practice for molecular-imaging applications: An overview. *Acta Biomater.* **41,** 1–16 (2016).

116.   Lin, C. H. & Chiang, M. C. Applying Magnetic Resonance Imaging to Structural and Functional Brain Research. *J. Neurosci. Neuroengineering* **2,** 29–37 (2013).

117.   Debbage, P. & Jaschke, W. Molecular imaging with nanoparticles: giant roles for dwarf actors. *Histochem. Cell Biol.* **130,** 845–875 (2008).

118.   Weissleder, R. A clearer vision for in vivo imaging. *Nat. Biotechnol.* **19,** 316–317 (2001).

119.   Weissleder, R. *Molecular Imaging: Principles and Practice*. PMPH-USA (2010).

120.   Wang, L. V. & Hu, S. Photoacoustic Tomography: In Vivo Imaging from Organelles to Organs. *Science* **335,** 1458–1462 (2012).

121.   Frangioni, J. V. New Technologies for Human Cancer Imaging. *J. Clin. Oncol.* **26,** 4012–4021 (2008).

122.   Jaffer, F. A., Libby, P. & Weissleder, R. Molecular Imaging of Cardiovascular Disease. *Circulation* **116,** 1052–1061 (2007).

123.   Asbury, Carolyn. *Brain imaging technologies and their applications in neuroscience.* The Dana Foundation (2011).

124.   Yang, Y. & Yuan, Y. The Control Strategy of a Hybrid Excitation Synchronous Generator in Wind Power Generation Systems. *Adv. Sci. Lett.* **4,** 1381–1386 (2011).

125.   Tomitaka, A., Jo, J., Aoki, I. & Tabata, Y. Preparation of biodegradable iron oxide nanoparticles with gelatin for magnetic resonance imaging. *Inflamm. Regen.* **34,** 045–055 (2014).

126.   Ma, H. L., Xu, Y. F., Qi, X. R., Maitani, Y. & Nagai, T. Superparamagnetic iron oxide nanoparticles stabilized by alginate: Pharmacokinetics, tissue distribution, and applications in detecting liver cancers. *Int. J. Pharm.* **354,** 217–226 (2008).

127.   Huang, J., Xie, J., Chen, K., Bu, L., Lee, S., Cheng, Z. *et al.* HSA coated MnO nanoparticles with prominent MRI contrast for tumor imaging. *Chem. Commun.* **46,** 6684–6686 (2010).

128.   Kim, S. M., Im, G. H., Lee, D., Lee, J. H., Lee, W. J. & Lee, I. S. Mn2+-doped silica nanoparticles for hepatocyte-targeted detection of liver cancer in T1-weighted MRI. *Biomaterials* **34,** 8941–8948 (2013).

129.   Aime, S., Frullano, L. & Geninatti, S. Compartmentalization of a Gadolinium Complex in the Apoferritin Cavity: A Route To Obtain High Relaxivity Contrast Agents for Magnetic Resonance Imaging. *Angew. Chem. Int. Ed.* **41,** 1017–1019

(2002).

130.   He, X., Liu, F., Liu, L, Duan, T., Zhang, H. & Wang, Z. Lectin-Conjugated Fe2O3@Au Core@Shell Nanoparticles as Dual Mode Contrast Agents for in Vivo Detection of Tumor. *Mol. Pharm.* **11,** 738–745 (2014).

131.   Rabin, O., Perez, J. M., Grimm, J., Wojtkiewicz, G. & Weissleder, R. An X-ray computed tomography imaging agent based on long-circulating bismuth sulphide nanoparticles. *Nat. Mater.* **5,** 118–122 (2006).

132.   Oh, M. H., Lee, N., Kim, H., Park, S. P., Piao, Y., Lee, J. *et al.* Large-Scale Synthesis of Bioinert Tantalum Oxide Nanoparticles for X-ray Computed Tomography Imaging and Bimodal Image-Guided Sentinel Lymph Node Mapping. *J. Am. Chem. Soc.* **133,** 5508–5515 (2011).

133.   Alric, C., Taleb, J., Duc, G. L., Mandon, C., Billotey, C., Meur-Herland, A. L. *et al.* Gadolinium Chelate Coated Gold Nanoparticles As Contrast Agents for Both X-ray Computed Tomography and Magnetic Resonance Imaging. *J. Am. Chem. Soc.* **130,** 5908–5915 (2008).

134.   Quinn, N., Critchley, P. & Marsden, C. D. Young onset Parkinson's disease. *Mov. Disord.* **2,** 73–91 (1987).

135.   Jaffer, F. A., Libby, P. & Weissleder, R. Optical and Multimodality Molecular Imaging. *Arterioscler. Thromb. Vasc. Biol.* **29,** 1017–1024 (2009).

136.   Devaraj, N. K., Keliher, E. J., Thurber, G. M., Nahrendorf, M. & Weissleder, R. 18F Labeled Nanoparticles for in Vivo PET-CT Imaging. *Bioconjug. Chem.* **20,** 397–401 (2009).

137.   Keliher, E. J., Yoo, J., Nahrendorf, M., Lewis, J. S., Marinelli, B., Newton, A. *et al.* 89Zr-Labeled Dextran Nanoparticles Allow in Vivo Macrophage Imaging. *Bioconjug. Chem.* **22,** 2383–2389 (2011).

138.   Lin, C. A., Chuang, W., Huang, Z., Kang, S., Chang, C., Chen, C. *et al.* Rapid Transformation of Protein-Caged Nanomaterials into Microbubbles As Bimodal Imaging Agents. *ACS Nano* **6,** 5111–5121 (2012).

139.   Nam, T., Park, S., Lee, S., Park, K., Choi, K., Song, I. C. *et al.* Tumor Targeting Chitosan Nanoparticles for Dual-Modality Optical/MR Cancer Imaging. *Bioconjug. Chem.* **21,** 578–582 (2010).

140.   Sun, I. C., Eun, D., Na, J. H., Lee, S., Kim, I., Youn, I. *et al.* Heparin-Coated Gold Nanoparticles for Liver-Specific CT Imaging. *Chem. Eur. J.* **15,** 13341–13347 (2009).

141.   Alivisatos, P. The use of nanocrystals in biological detection. *Nat. Biotechnol.* **22,** 47–52 (2004).

142.   Chrastina, A. & Schnitzer, J. E. Iodine-125 radiolabeling of silver nanoparticles for in vivo SPECT imaging. *Int. J. Nanomedicine* **5,** 653–659 (2010).

143.   Piao, Y., Han, D. J. & Seo, T. S. Highly conductive graphite nanoparticle based enzyme biosensor for electrochemical glucose detection. *Sens. Actuators B Chem.* **194,** 454–459 (2014).

144.   Jia, X., Hu, G., Nitze, F., Barzegar, H. R., Sharifi, T., Tai, C. *et al.* Synthesis of Palladium/Helical Carbon Nanofiber Hybrid Nanostructures and Their Application for Hydrogen Peroxide and Glucose Detection. *ACS Appl. Mater. Interfaces* **5,** 12017–12022 (2013).

145.   Singh, J., Srivastava, M., Roychoudhury, A., Lee, D. W., Lee, S. H. & Malhotra, B. D. Bienzyme-Functionalized Monodispersed Biocompatible Cuprous Oxide/Chitosan Nanocomposite Platform for Biomedical Application. *J. Phys. Chem. B* **117,** 141–152 (2013).

146.   Cai, X., Gao, X., Wang, L., Wu, Q. & Lin, X. A layer-by-layer assembled and carbon nanotubes/gold nanoparticles-based bienzyme biosensor for cholesterol detection. *Sens. Actuators B Chem.* **181,** 575–583 (2013).

147.   Zhao, W., Wang, K., Wei, Y., Ma, Y., Liu, L. & Huang, X. Laccase Biosensor Based on Phytic Acid Modification of Nanostructured SiO2 Surface for Sensitive Detection of Dopamine. *Langmuir* **30,** 11131–11137 (2014).

148.   Cao, X., Wang, N., Jia, S. & Shao, Y. Detection of Glucose Based on Bimetallic PtCu Nanochains Modified Electrodes. *Anal. Chem.* **85,** 5040–5046 (2013).

149.   Dhara, K., Stanley, J, T, R., Nair, B. G. & T, S. B. Pt-CuO nanoparticles decorated reduced graphene oxide for the fabrication of highly sensitive non-enzymatic disposable glucose sensor. *Sens. Actuators B Chem.* **195,** 197–205 (2014).

150.   Guo, C., Huo, H., Han, X., Xu, C. & Li, H. Ni/CdS Bifunctional Ti@TiO2 Core–Shell Nanowire Electrode for High-Performance Nonenzymatic Glucose Sensing. *Anal. Chem.* **86,** 876–883 (2014).

151.   Wang, T., Zhu, H., Zhuo, J., Zhu, Z., Papakonstantinou, P., Lubarsky, G. *et al.* Biosensor Based on Ultrasmall MoS2 Nanoparticles for Electrochemical Detection of H2O2 Released by Cells at the Nanomolar Level. *Anal. Chem.* **85,** 10289–10295 (2013).

152.   Li, W., Kuai, L., Qin, Q. & Geng, B. Ag–Au bimetallic nanostructures: co-reduction synthesis and their component-dependent performance for enzyme-free H2O2 sensing. *J. Mater. Chem. A* **1,** 7111–7117 (2013).

153.   Wang, H., Li, S., Si, Y., Zhang, N., Sun, Z., Wu, H. *et al.* Platinum nanocatalysts loaded on graphene oxide-dispersed carbon nanotubes with greatly enhanced peroxidase-like catalysis and electrocatalysis activities. *Nanoscale* **6,** 8107–8116 (2014).

154.   Nagaiah, T. C., Schäfer, D., Schuhmann, W. & Dimcheva, N. Electrochemically Deposited Pd–Pt and Pd–Au Codeposits on Graphite Electrodes for Electrocatalytic H2O2 Reduction. *Anal. Chem.* **85,** 7897–7903 (2013).

155.   Bai, J. & Jiang, X. A Facile One-Pot Synthesis of Copper Sulfide-Decorated Reduced Graphene Oxide Composites for Enhanced Detecting of H2O2 in Biological Environments. *Anal. Chem.* **85,** 8095–8101 (2013).

156.   Cui, L., Wu, J., Li, J., Ge, Y. & Ju, H. Electrochemical detection of Cu2+ through Ag nanoparticle assembly regulated by copper-catalyzed oxidation of cysteamine. *Biosens. Bioelectron.* **55,** 272–277 (2014).

157.   Madhu, R., Veeramani, V. & Chen, S.-M. Heteroatom-enriched and renewable banana-stem-derived porous carbon for the electrochemical determination of nitrite in various water samples. *Sci. Rep.* **4,** 4679 (2014).

158.   Gao, Y. S., Xu, J., Lu, L., Wu, L., Zhang, K., Nie, T. *et al.* Overoxidized polypyrrole/graphene nanocomposite with good electrochemical performance as novel electrode material for the detection of adenine and guanine. *Biosens. Bioelectron.* **62,** 261–267 (2014).

159.   Lee, P. T., Ward, K. R., Tschulik, K., Chapman, G. & Compton, R. G. Electrochemical Detection of Glutathione Using a Poly(caffeic acid) Nanocarbon Composite Modified Electrode. *Electroanalysis* **26,** 366–373 (2014).

160.   Metters, J. P., Gomez-Mingot, M., Iniesta, J., Kadara, R. O. & Banks, C. E. The fabrication of novel screen printed single-walled carbon nanotube electrodes: Electroanalytical applications. *Sens. Actuators B Chem.* **177,** 1043–1052 (2013).

161.   Yin, H., Sun, B., Zhou, Y., Wang, M., Xu, Z., Fu, Z. *et al.* A new strategy for

methylated DNA detection based on photoelectrochemical immunosensor using Bi2S3 nanorods, methyl bonding domain protein and anti-his tag antibody. *Biosens. Bioelectron.* **51,** 103–108 (2014).

162.   Jing, X., Cao, X., Wang, L., Lan, T., Li, Y. & Xie, G. DNA-AuNPs based signal amplification for highly sensitive detection of DNA methylation, methyltransferase activity and inhibitor screening. *Biosens. Bioelectron.* **58,** 40–47 (2014).

163.   Cai, B., Wang, S., Huang, L., Ning, Y., Zhang, Z. & Zhang, G. Ultrasensitive Label-Free Detection of PNA–DNA Hybridization by Reduced Graphene Oxide Field-Effect Transistor Biosensor. *ACS Nano* **8,** 2632–2638 (2014).

164.   Lin, M., Wen, Y., Li, L., Pei, H., Liu, G., Song, H. *et al.* Target-Responsive, DNA Nanostructure-Based E-DNA Sensor for microRNA Analysis. *Anal. Chem.* **86,** 2285–2288 (2014).

165.   Wang, Q., Lei, J., Deng, S., Zhang, L. & Ju, H. Graphene-supported ferric porphyrin as a peroxidase mimic for electrochemical DNA biosensing. *Chem. Commun.* **49,** 916–918 (2013).

166.   Zhang, X., Wang, H., Yang, C., Du, D. & Lin, Y. Preparation, characterization of Fe3O4 at TiO2 magnetic nanoparticles and their application for immunoassay of biomarker of exposure to organophosphorus pesticides. *Biosens. Bioelectron.* **41,** 669–674 (2013).

167.   Eletxigerra, U., Martinez-Perdiguero, J., Merino, S., Villalonga, R., Pingarrón, J. M. & Campuzano, S. Amperometric magnetoimmunoassay for the direct detection of tumor necrosis factor alpha biomarker in human serum. *Anal. Chim. Acta* **838,** 37–44 (2014).

168.   Tian, J., Zhao, H., Quan, X., Zhang, Y., Yu, H. & Chen, S. Fabrication of graphene quantum dots/silicon nanowires nanohybrids for photoelectrochemical detection of microcystin-LR. *Sens. Actuators B Chem.* **196,** 532–538 (2014).

169.   Zhang, Y., Ge, L., Li, M., Yan, M., Ge, S., Yu, J. *et al.* Flexible paper-based ZnO nanorod light-emitting diodes induced multiplexed photoelectrochemical immunoassay. *Chem. Commun. Camb. Engl.* **50,** 1417–1419 (2014).

170.   Wu, Y., Xue, P., Kang, Y. & Hui, K. M. Paper-based microfluidic electrochemical immunodevice integrated with nanobioprobes onto graphene film for ultrasensitive multiplexed detection of cancer biomarkers. *Anal. Chem.* **85,** 8661–8668 (2013).

171.   Faraday, M. The Bakerian Lecture: Experimental Relations of Gold (and Other Metals) to Light. *Philos. Trans. R. Soc. Lond.* **147,** 145–181 (1857).

172.   Daniel, M. C. & Astruc, D. Gold Nanoparticles: Assembly, Supramolecular Chemistry, Quantum-Size-Related Properties, and Applications toward Biology, Catalysis, and Nanotechnology. *Chem. Rev.* **104,** 293–346 (2004).

173.   Imura, K., Nagahara, T. & Okamoto, H. Photoluminescence from gold nanoplates induced by near-field two-photon absorption. *Appl. Phys. Lett.* **88,** 23104 (2006).

174.   Tong, L., Cobley, C. M., Chen, J., Xia, Y. & Cheng, J.-X. Bright three-photon luminescence from gold/silver alloyed nanostructures for bioimaging with negligible photothermal toxicity. *Angew. Chem. Int. Ed Engl.* **49,** 3485–3488 (2010).

175.   Mohamed, M. B., Volkov, V., Link, S. & El-Sayed, M. A. The `lightning' gold nanorods: fluorescence enhancement of over a million compared to the gold metal. *Chem. Phys. Lett.* **317,** 517–523 (2000).

176.   Brolo, A. G., Kwok, S. C., Moffitt, M. G., Gordon, R., Riordon, J. & Kavanagh, K. L. Enhanced fluorescence from arrays of nanoholes in a gold film. *J. Am. Chem. Soc.*

127, 14936–14941 (2005).

177.   Ueno, K., Juodkazis, S., Mizeikis, V., Sasaki, K. & Misawa, H. Clusters of Closely Spaced Gold Nanoparticles as a Source of Two-Photon Photoluminescence at Visible Wavelengths. *Adv. Mater.* **20,** 26–30 (2008).

178.   Raman, C. V. & Krishnan, K. S. A New Type of Secondary Radiation. *Nature* **121,** 501–502 (1928).

179.   Tian, Z. Q., Ren, B. & Wu, D. Y. Surface-Enhanced Raman Scattering: From Noble to Transition Metals and from Rough Surfaces to Ordered Nanostructures. *J. Phys. Chem. B* **106,** 9463–9483 (2002).

180.   Häkkinen, H. The gold-sulfur interface at the nanoscale. *Nat. Chem.* **4,** 443–455 (2012).

181.   Freeman, R. G., Grabar, K. C., Allison, K. J., Bright, R. M., Davis, J. A., Guthrie, A. P. *et al.* Self-Assembled Metal Colloid Monolayers: An Approach to SERS Substrates. *Science* **267,** 1629–1632 (1995).

182.   Maity, P., Xie, S., Yamauchi, M. & Tsukuda, T. Stabilized gold clusters: from isolation toward controlled synthesis. *Nanoscale* **4,** 4027–4037 (2012).

183.   Jin, R. Quantum sized, thiolate-protected gold nanoclusters. *Nanoscale* **2,** 343–362 (2010).

184.   Negishi, Y., Nobusada, K. & Tsukuda, T. Glutathione-protected gold clusters revisited: bridging the gap between gold(I)-thiolate complexes and thiolate-protected gold nanocrystals. *J. Am. Chem. Soc.* **127,** 5261–5270 (2005).

185.   Jin, R., Egusa, S. & Scherer, N. F. Thermally-induced formation of atomic Au clusters and conversion into nanocubes. *J. Am. Chem. Soc.* **126,** 9900–9901 (2004).

186.   Wu, Z., Chen, J. & Jin, R. One-Pot Synthesis of Au25(SG)18 2- and 4-nm Gold Nanoparticles and Comparison of Their Size-Dependent Properties. *Adv. Funct. Mater.* **21,** 177–183 (2011).

187.   Sivaraman, S. K., Kumar, S. & Santhanam, V. Monodisperse sub-10 nm gold nanoparticles by reversing the order of addition in Turkevich method--the role of chloroauric acid. *J. Colloid Interface Sci.* **361,** 543–547 (2011).

188.   Njoki, P. N., Lim, I., Mott, D., Park, H., Khan, B., Mishra, S. *et al.* Size Correlation of Optical and Spectroscopic Properties for Gold Nanoparticles. *J. Phys. Chem. C* **111,** 14664–14669 (2007).

189.   Kim, K., Xu, X., Guo, J. & Fan, D. L. Ultrahigh-speed rotating nanoelectromechanical system devices assembled from nanoscale building blocks. *Nat. Commun.* **5,** 3632 (2014).

190.   Hu, M., Chen, J., Li, Z., Au, L., Hartland, G. V., Li, X. *et al.* Gold nanostructures: engineering their plasmonic properties for biomedical applications. *Chem. Soc. Rev.* **35,** 1084–1094 (2006).

191.   Black, K. C., Wang, Y., Luehmann, H. P., Cai, X., Xing, W., Pang, B. *et al.* Radioactive 198Au-Doped Nanostructures with Different Shapes for In Vivo Analyses of Their Biodistribution, Tumor Uptake, and Intratumoral Distribution. *ACS Nano* **8,** 4385–4394 (2014).

192.   Liu, H., Chen, D., Li, L., Liu, T., Tan, L., Wu, X. *et al.* Multifunctional gold nanoshells on silica nanorattles: a platform for the combination of photothermal therapy and chemotherapy with low systemic toxicity. *Angew. Chem. Int. Ed Engl.* **50,** 891–895 (2011).

193.   Jin, Y. & Gao, X. Plasmonic fluorescent quantum dots. *Nat. Nanotechnol.* **4,** 571–576 (2009).

194.   Ji, X., Shao, R., Elliott, A. M., Stafford, R. J., Esparza-Coss, E., Bankson, J. A. *et*

al. Bifunctional Gold Nanoshells with a Superparamagnetic Iron Oxide-Silica Core Suitable for Both MR Imaging and Photothermal Therapy. *J. Phys. Chem. C Nanomater. Interfaces* **111,** 6245–6251 (2007).

195.   Jin, Y. & Gao, X. Spectrally tunable leakage-free gold nanocontainers. *J. Am. Chem. Soc.* **131,** 17774–17776 (2009).

196.   Skrabalak, S. E., Chen, J., Sun, Y., Lu, X., Au, L., Cobley, C. M. *et al.* Gold Nanocages: Synthesis, Properties, and Applications. *Acc. Chem. Res.* **41,** 1587–1595 (2008).

197.   Sun, Y. & Xia, Y. Shape-controlled synthesis of gold and silver nanoparticles. *Science* **298,** 2176–2179 (2002).

198.   Wan, D., Xia, X., Wang, Y. & Xia, Y. Robust synthesis of gold cubic nanoframes through a combination of galvanic replacement, gold deposition, and silver dealloying. *Small Weinh. Bergstr. Ger.* **9,** 3111–3117 (2013).

199.   Au, L., Chen, Y., Zhou, F., Camargo, P. H., Lim, B., Li, Z. *et al.* Synthesis and optical properties of cubic gold nanoframes. *Nano Res.* **1,** 441–449 (2008).

200.   Hao, F., Nehl, C. L., Hafner, J. H. & Nordlander, P. Plasmon resonances of a gold nanostar. *Nano Lett.* **7,** 729–732 (2007).

201.   Cheng, K., Kothapalli, S., Liu, H., Koh, A. L., Jokerst, J. V., Jiang, H. *et al.* Construction and Validation of Nano Gold Tripods for Molecular Imaging of Living Subjects. *J. Am. Chem. Soc.* **136,** 3560–3571 (2014).

202.   Dam, D. H., Culver, K. S. & Odom, T. W. Grafting Aptamers onto Gold Nanostars Increases in Vitro Efficacy in a Wide Range of Cancer Cell Types. *Mol. Pharm.* **11,** 580–587 (2014).

203.   Dam, D. H., Lee, R. C. & Odom, T. W. Improved in Vitro Efficacy of Gold Nanoconstructs by Increased Loading of G-quadruplex Aptamer. *Nano Lett.* **14,** 2843–2848 (2014).

204.   Chen, S., Wang, Z. L., Ballato, J., Foulger, S. H. & Carroll, D. L. Monopod, bipod, tripod, and tetrapod gold nanocrystals. *J. Am. Chem. Soc.* **125,** 16186–16187 (2003).

205.   Choudhary, V. R. & Mondal, K. C. CO2 reforming of methane combined with steam reforming or partial oxidation of methane to syngas over NdCoO3 perovskite-type mixed metal-oxide catalyst. *Appl. Energy* **83,** 1024–1032 (2006).

206.   Solsona, B., López J. M., Concepción, P., Dejoz, A., Ivars, F. & Vázquez, M. I. Oxidative dehydrogenation of ethane over Ni–W–O mixed metal oxide catalysts. *J. Catal.* **280,** 28–39 (2011).

207.   Dumbre, D. K., Choudhary, V. R., Patil, N. S., Uphade, B. S. & Bhargava, S. K. Calcium oxide supported gold nanoparticles as catalysts for the selective epoxidation of styrene by t-butyl hydroperoxide. *J. Colloid Interface Sci.* **415,** 111–116 (2014).

208.   Ribeiro, N. F., Mendes, F. M., Perez, C. A., Souza, M. M. & Schmal, M. Selective CO oxidation with nano gold particles-based catalysts over Al2O3 and ZrO2. *Appl. Catal. Gen.* **347,** 62–71 (2008).

209.   Xu, H., Li, W., Shang, S. & Yan, C. Influence of MgO contents on silica supported nano-size gold catalyst for carbon monoxide total oxidation. *J. Nat. Gas Chem.* **20,** 498–502 (2011).

210.   Idakiev, V., Tabakova, T., Naydenov, A., Yuan, Z. Y. & Su, B. L. Gold catalysts supported on mesoporous zirconia for low-temperature water–gas shift reaction. *Appl. Catal. B Environ.* **63,** 178–186 (2006).

211.   Idakiev, V., Yuan, Z. Y., Tabakova, T. & Su, B. L. Titanium oxide nanotubes as

supports of nano-sized gold catalysts for low temperature water-gas shift reaction. *Appl. Catal. Gen.* **281,** 149–155 (2005).

212. Tsukamoto, D., Shiraishi, Y., Sugano, Y., Ichikawa, S., Tanaka, S. & Hirai, T. Gold nanoparticles located at the interface of anatase/rutile TiO2 particles as active plasmonic photocatalysts for aerobic oxidation. *J. Am. Chem. Soc.* **134,** 6309–6315 (2012).

213. Liu, L., Ouyang, S. & Ye, J. Gold-nanorod-photosensitized titanium dioxide with wide-range visible-light harvesting based on localized surface plasmon resonance. *Angew. Chem. Int. Ed Engl.* **52,** 6689–6693 (2013).

214. Zhang, Y., Chu, W., Foroushani, A. D., Wang, H., Li, D., Liu, J. *et al.* New Gold Nanostructures for Sensor Applications: A Review. *Materials* **7,** 5169–5201 (2014).

215. Zheng, Z., Huang, B., Qin, X., Zhang, X., Dai, Y. & Whangbo, M. Facile in situ synthesis of visible-light plasmonic photocatalysts M@TiO2 (M = Au, Pt, Ag) and evaluation of their photocatalytic oxidation of benzene to phenol. *J. Mater. Chem.* **21,** 9079–9087 (2011).

216. Das, S. K., Das, A. R. & Guha, A. K. Gold nanoparticles: microbial synthesis and application in water hygiene management. *Langmuir ACS J. Surf. Colloids* **25,** 8192–8199 (2009).

217. Liu, Q., Zhou, Q. & Jiang, G. Nanomaterials for analysis and monitoring of emerging chemical pollutants. *TrAC Trends Anal. Chem.* **58,** 10–22 (2014).

218. Zhu, Y., Kuang, H., Xu, L., Ma, W., Peng, C., Hua, Y. *et al.* Gold nanorod assembly based approach to toxin detection by SERS. *J. Mater. Chem.* **22,** 2387–2391 (2012).

219. Huang, J., Zhang, X., Liu, S., Lin, Q., He, X., Xing, X. *et al.* Electrochemical sensor for bisphenol A detection based on molecularly imprinted polymers and gold nanoparticles. *J. Appl. Electrochem.* **41,** 1323 (2011).

220. Xia, W., Li, Y., Wan, Y., Chen, T., Wei, J., Lin, Y. *et al.* Electrochemical biosensor for estrogenic substance using lipid bilayers modified by Au nanoparticles. *Biosens. Bioelectron.* **25,** 2253–2258 (2010).

221. Zhou, L., Xiong, W. & Liu, S. Preparation of a gold electrode modified with Au–TiO2 nanoparticles as an electrochemical sensor for the detection of mercury(II) ions. *J. Mater. Sci.* **50,** 769–776 (2015).

222. Shi, Y., Wu, J., Sun, Y., Zhang, Y., Wen, Z., Dai, H. *et al.* A graphene oxide based biosensor for microcystins detection by fluorescence resonance energy transfer. *Biosens. Bioelectron.* **38,** 31–36 (2012).

223. Mei, Z., Chu, H., Chen, W., Xue, F., Liu, J., Xu, H. *et al.* Ultrasensitive one-step rapid visual detection of bisphenol A in water samples by label-free aptasensor. *Biosens. Bioelectron.* **39,** 26–30 (2013).

224. Kim, Y. S., Kim, J. H., Kim, I. A., Lee, S. J., Jurng, J. & Gu, M. B. A novel colorimetric aptasensor using gold nanoparticle for a highly sensitive and specific detection of oxytetracycline. *Biosens. Bioelectron.* **26,** 1644–1649 (2010).

225. Ma, Y., Jiang, L., Mei, Y., Song, R., Tian, D. & Huang, H. Colorimetric sensing strategy for mercury(II) and melamine utilizing cysteamine-modified gold nanoparticles. *Analyst* **138,** 5338–5343 (2013).

226. Song, K. M., Cho, M., Jo, H., Min, K., Jeon, S. H., Kim, T. *et al.* Gold nanoparticle-based colorimetric detection of kanamycin using a DNA aptamer. *Anal. Biochem.* **415,** 175–181 (2011).

227. Takayose, M., Akamatsu, K., Nawafune, H., Murashima, T. & Matsui, J. Colorimetric Detection of Perfluorooctanoic Acid (PFOA) Utilizing Polystyrene-

Modified Gold Nanoparticles. *Anal. Lett.* **45,** 2856–2864 (2012).

228.   Mei, Z., Deng, Y., Chu, H., Xue, F., Zhong, Y., Wu, J. *et al.* Immunochromatographic lateral flow strip for on-site detection of bisphenol A. *Microchim. Acta* **180,** 279–285 (2013).

229.   Ruan, C., Wang, W. & Gu, B. Surface-enhanced Raman scattering for perchlorate detection using cystamine-modified gold nanoparticles. *Anal. Chim. Acta* **567,** 114–120 (2006).

230.   Du, Y., Liu, R., Liu, B., Wang, S., Han, M. & Zhang, Z. Surface-Enhanced Raman Scattering Chip for Femtomolar Detection of Mercuric Ion (II) by Ligand Exchange. *Anal. Chem.* **85,** 3160–3165 (2013).

231.   Frasconi, M., Tel-Vered, R., Riskin, M. & Willner, I. Surface plasmon resonance analysis of antibiotics using imprinted boronic acid-functionalized au nanoparticle composites. *Anal. Chem.* **82,** 2512–2519 (2010).

232.   Fernández, F., Sánchez-Baeza, F. & Marco, M. P. Nanogold probe enhanced Surface Plasmon Resonance immunosensor for improved detection of antibiotic residues. *Biosens. Bioelectron.* **34,** 151–158 (2012).

233.   Lohani, A., Verma, A., Joshi, H., Yadav, N. & Karki, N. Nanotechnology-Based Cosmeceuticals. *Int. Sch. Res. Not.* **2014,** e843687 (2014).

234.   Haveli, S. D., Walter, P., Patriarche, G., Ayache, J., Castaing, J., Van, E. *et al.* Hair Fiber as a Nanoreactor in Controlled Synthesis of Fluorescent Gold Nanoparticles. *Nano Lett.* **12,** 6212–6217 (2012).

235.   http://www.google.com/patents/EP1909745A1.

236.   https://www.chantecaille.com/nano-gold-energizing-face-cream.html.

237.   http://www.nanotechproject.org/cpi/products/nano-gold-beauty-masks/.

238.   Wang, Y., Wang, Y., Zhou, F., Kim, P. & Xia, Y. Protein-protected Au clusters as a new class of nanoscale biosensor for label-free fluorescence detection of proteases. *Small Weinh. Bergstr. Ger.* **8,** 3769–3773 (2012).

239.   Huang, C. C., Chiang, C. K., Lin, Z. H., Lee, K. H. & Chang, H. T. Bioconjugated gold nanodots and nanoparticles for protein assays based on photoluminescence quenching. *Anal. Chem.* **80,** 1497–1504 (2008).

240.   Chen, C. T., Chen, W. J., Liu, C. Z., Chang, L. Y. & Chen, Y. C. Glutathione-bound gold nanoclusters for selective-binding and detection of glutathione S-transferase-fusion proteins from cell lysates. *Chem. Commun. Camb. Engl* **48,** 7515–7517 (2009).

241.   Triulzi, R. C., Micic, M., Giordani, S., Serry, M., Chiou, W. & Leblanc, R. M. Immunoasssay based on the antibody-conjugated PAMAM-dendrimer-gold quantum dot complex. *Chem. Commun. Camb. Engl.* **48,** 5068–5070 (2006).

242.   Shiang, Y. C., Lin, C. A., Huang, C. C. & Chang, H. T. Protein A-conjugated luminescent gold nanodots as a label-free assay for immunoglobulin G in plasma. *The Analyst* **136,** 1177–1182 (2011).

243.   Durgadas, C. V., Sharma, C. P. & Sreenivasan, K. Fluorescent gold clusters as nanosensors for copper ions in live cells. *The Analyst* **136,** 933–940 (2011).

244.   Chen, Y., Wang, Y., Wang, C., Li, W., Zhou, H., Jiao, H. *et al.* Papain-directed synthesis of luminescent gold nanoclusters and the sensitive detection of Cu2+. *J. Colloid Interface Sci.* **396,** 63–68 (2013).

245.   Huang, C. C., Yang, Z., Lee, K. H. & Chang, H. T. Synthesis of highly fluorescent gold nanoparticles for sensing mercury(II). *Angew. Chem. Int. Ed Engl.* **46,** 6824–6828 (2007).

246.   Jin, L., Shang, L., Guo, S., Fang, Y., Wen, D., Wang, L. *et al.* Biomolecule-

stabilized Au nanoclusters as a fluorescence probe for sensitive detection of glucose. *Biosens. Bioelectron.* **26,** 1965–1969 (2011).

247. Storhoff, J. J., Elghanian, R., Mucic, R. C., Mirkin, C. A. & Letsinger, R. L. One-Pot Colorimetric Differentiation of Polynucleotides with Single Base Imperfections Using Gold Nanoparticle Probes. *J. Am. Chem. Soc.* **120,** 1959–1964 (1998).

248. Xu, X., Daniel, W. L., Wei, W. & Mirkin, C. A. Colorimetric Cu2+ Detection Using DNA Modified Gold Nanoparticle Aggregates as Probes and Click Chemistry. *Small Weinh. Bergstr. Ger.* **6,** 623–626 (2010).

249. Yang, B., Zhang, X., Liu, W., Hu, R., Tan, W., Shen, G. *et al.* Fluorosurfactant-capped gold nanoparticles-based label-free colorimetric assay for Au^{3+} with tunable dynamic range via a redox strategy. *Biosens. Bioelectron.* **48,** 1–5 (2013).

250. Xia, F., Zuo, X., Yang, R., Xiao, Y., Kang, D., Vallée-Bélisle, A. *et al.* Colorimetric detection of DNA, small molecules, proteins, and ions using unmodified gold nanoparticles and conjugated polyelectrolytes. *Proc. Natl. Acad. Sci. U. S. A.* **107,** 10837–10841 (2010).

251. Zhu, Z., Wu, C., Liu, H., Zou, Y., Zhang, X., Kang, H. *et al.* An Aptamer Cross-Linked Hydrogel as a Colorimetric Platform for Visual Detection. *Angew. Chem. Int. Ed.* **49,** 1052–1056 (2010).

252. Zhang, J., Wang, L., Pan, D., Song, S., Boey, F. Y., Zhang, H. *et al.* Visual cocaine detection with gold nanoparticles and rationally engineered aptamer structures. *Small Weinh. Bergstr. Ger.* **4,** 1196–1200 (2008).

253. Tsoutsi, D., Montenegro, J. M., Dommershausen, F., Koert, U., Liz-Marzán, L. M., Parak, W. J. *et al.* Quantitative surface-enhanced Raman scattering ultradetection of atomic inorganic ions: the case of chloride. *ACS Nano* **5,** 7539–7546 (2011).

254. Wang, Y., Chen, J. T. & Yan, X. P. Fabrication of transferrin functionalized gold nanoclusters/graphene oxide nanocomposite for turn-on near-infrared fluorescent bioimaging of cancer cells and small animals. *Anal. Chem.* **85,** 2529–2535 (2013).

255. Kneipp, K., Haka, A. S., Kneipp, H., Badizadegan, K., Yoshizawa, N., Boone, C. *et al.* Surface-Enhanced Raman Spectroscopy in Single Living Cells Using Gold Nanoparticles. *Appl. Spectrosc.* **56,** 150–154 (2002).

256. Kong, L., Zhang, P., Yu, J., Setlow, P. & Li, Y. Rapid confocal Raman imaging using a synchro multifoci-scan scheme for dynamic monitoring of single living cells. *Appl. Phys. Lett.* **98,** 213703 (2011).

257. Yang, X., Stein, E. W., Ashkenazi, S. & Wang, L. V. Nanoparticles for photoacoustic imaging. *Wiley Interdiscip. Rev. Nanomed. Nanobiotechnol.* **1,** 360–368 (2009).

258. Kwon, S. P., Jeon, S., Lee, S. H., Yoon, H. Y., Ryu, J. H., Choi, D. *et al.* Thrombin-activatable fluorescent peptide incorporated gold nanoparticles for dual optical/computed tomography thrombus imaging. *Biomaterials* **150,** 125–136 (2018).

259. Lee, S. B., Yoon, G., Lee, S. W., Jeong, S.Y., Ahn, B. C., Lim, D. K. *et al.* Combined Positron Emission Tomography and Cerenkov Luminescence Imaging of Sentinel Lymph Nodes Using PEGylated Radionuclide-Embedded Gold Nanoparticles. *Small* **12,** 4894–4901 (2016).

260. Okuno, M. & Hamaguchi, H. Multifocus confocal Raman microspectroscopy for fast multimode vibrational imaging of living cells. *Opt. Lett.* **35,** 4096–4098 (2010).

261. Dorsey, J. F., Sun, L., Joh, D. Y., Witztum, A., Kao, G. D., Alonso-Basanta, M. *et al.* Gold nanoparticles in radiation research: potential applications for imaging and radiosensitization. *Transl. Cancer Res.* **2,** 280–291 (2013).

262. Hahn, M. A., Singh, A. K., Sharma, P., Brown, S. C. & Moudgil, B. M. Nanoparticles as contrast agents for in-vivo bioimaging: current status and future perspectives. *Anal. Bioanal. Chem.* **399,** 3–27 (2011).

263. Xie, H., Wang, Z. J., Bao, A., Goins, B. & Phillips, W. T. In vivo PET imaging and biodistribution of radiolabeled gold nanoshells in rats with tumor xenografts. *Int. J. Pharm.* **395,** 324–330 (2010).

264. Xie, H., Diagaradjane, P., Deorukhkar, A. A., Goins, B., Bao, A., Phillips, W. T. *et al.* Integrin αvβ3-targeted gold nanoshells augment tumor vasculature-specific imaging and therapy. *Int. J. Nanomedicine* **6,** 259–269 (2011).

265. Lu, W., Melancon, M. P., Xiong, C., Huang, Q., Elliott, A., Song, S. *et al.* Effects of photoacoustic imaging and photothermal ablation therapy mediated by targeted hollow gold nanospheres in an orthotopic mouse xenograft model of glioma. *Cancer Res.* **71,** 6116–6121 (2011).

266. You, J. , Zhang, R., Zhang, G., Zhong, M., Liu, Y., Van, C. S. *et al.* Photothermal-chemotherapy with doxorubicin-loaded hollow gold nanospheres: A platform for near-infrared light-trigged drug release. *J. Control. Release Off. J. Control. Release Soc.* **158,** 319–328 (2012).

267. Moses, W. W. Fundamental Limits of Spatial Resolution in PET. *Nucl. Instrum. Methods Phys. Res. Sect. Accel. Spectrometers Detect. Assoc. Equip.* **648 Supplement 1,** S236–S240 (2011).

268. Dhar, S., Daniel, W. L., Giljohann, D. A., Mirkin, C. A. & Lippard, S. J. Polyvalent oligonucleotide gold nanoparticle conjugates as delivery vehicles for platinum(IV) warheads. *J. Am. Chem. Soc.* **131,** 14652–14653 (2009).

269. Kim, D., Jeong, Y. Y. & Jon, S. A drug-loaded aptamer-gold nanoparticle bioconjugate for combined CT imaging and therapy of prostate cancer. *ACS Nano* **4,** 3689–3696 (2010).

270. Chakravarthy, K. V., Bonoiu, A. C., Davis, W. G., Ranjan, P., Ding, H., Hu, R. *et al.* Gold nanorod delivery of an ssRNA immune activator inhibits pandemic H1N1 influenza viral replication. *Proc. Natl. Acad. Sci. U. S. A.* **107,** 10172–10177 (2010).

271. Rosi, N. L., Giljohann, D. A., Thaxton, C. S., Lytton-Jean, A. K., Han, M. S. & Mirkin, C. A. Oligonucleotide-modified gold nanoparticles for intracellular gene regulation. *Science* **312,** 1027–1030 (2006).

272. Yavuz, M. S., Cheng, Y., Chen, J., Cobley, C. M., Zhang, Q., Rycenga, M. *et al.* Gold nanocages covered by smart polymers for controlled release with near-infrared light. *Nat. Mater.* **8,** 935–939 (2009).

273. Li, W., Cai, X., Kim, C., Sun, G., Zhang, Y., Deng, R. *et al.* Gold nanocages covered with thermally-responsive polymers for controlled release by high-intensity focused ultrasound. *Nanoscale* **3,** 1724–1730 (2011).

274. Agasti, S. S., Chompoosor, A., You, C. C., Ghosh, P., Kim, C. K. & Rotello, V. M. Photoregulated release of caged anticancer drugs from gold nanoparticles. *J. Am. Chem. Soc.* **131,** 5728–5729 (2009).

275. Takahashi, H., Niidome, Y. & Yamada, S. Controlled release of plasmid DNA from gold nanorods induced by pulsed near-infrared light. *Chem. Commun. Camb. Engl.* 2247–2249 (2005). doi:10.1039/b500337g

276. Sun, T., Zhang, Y. S., Pang, B., Hyun, D. C., Yang, M. & Xia, Y. Engineered nanoparticles for drug delivery in cancer therapy. *Angew. Chem. Int. Ed Engl.* **53,**

12320–12364 (2014).

277.   He, Q. & Shi, J. MSN anti-cancer nanomedicines: chemotherapy enhancement, overcoming of drug resistance, and metastasis inhibition. *Adv. Mater. Deerfield Beach Fla* **26,** 391–411 (2014).

278.   He, Q., Gao, Y., Zhang, L., Zhang, Z., Gao, F., Ji, X. *et al.* A pH-responsive mesoporous silica nanoparticles-based multi-drug delivery system for overcoming multi-drug resistance. *Biomaterials* **32,** 7711–7720 (2011).

279.   Wieder, M. E., Hone, D. C., Cook, M. J., Handsley, M. M., Gavrilovic, J. & Russell, D. A. Intracellular photodynamic therapy with photosensitizer-nanoparticle conjugates: cancer therapy using a 'Trojan horse'. *Photochem. Photobiol. Sci. Off. J. Eur. Photochem. Assoc. Eur. Soc. Photobiol.* **5,** 727–734 (2006).

280.   Camerin, M., Magaraggia, M., Soncin, M., Jori, G., Moreno, M., Chambrier, I. *et al.* The in vivo efficacy of phthalocyanine-nanoparticle conjugates for the photodynamic therapy of amelanotic melanoma. *Eur. J. Cancer Oxf. Engl. 1990* **46,** 1910–1918 (2010).

281.   Vankayala, R., Sagadevan, A., Vijayaraghavan, P., Kuo, C. L. & Hwang, K. C. Metal nanoparticles sensitize the formation of singlet oxygen. *Angew. Chem. Int. Ed Engl.* **50,** 10640–10644 (2011).

282.   Zhao, T., Shen, X., Li, L., Guan, Z., Gao, N., Yuan, P. *et al.* Gold nanorods as dual photo-sensitizing and imaging agents for two-photon photodynamic therapy. *Nanoscale* **4,** 7712–7719 (2012).

283.   Vankayala, R., Huang, Y. K., Kalluru, P., Chiang, C. S. & Hwang, K. C. First demonstration of gold nanorods-mediated photodynamic therapeutic destruction of tumors via near infra-red light activation. *Small Weinh. Bergstr. Ger.* **10,** 1612–1622 (2014).

284.   Gao, L., Liu, R., Gao, F., Wang, Y., Jiang, X. & Gao, X. Plasmon-mediated generation of reactive oxygen species from near-infrared light excited gold nanocages for photodynamic therapy in vitro. *ACS Nano* **8,** 7260–7271 (2014).

285.   Hainfeld, J. F., Slatkin, D. N. & Smilowitz, H. M. The use of gold nanoparticles to enhance radiotherapy in mice. *Phys. Med. Biol.* **49,** N309-315 (2004).

286.   Chang, M. Y., Shiau, A. L., Chen, Y. H., Chang, C. J., Chen, H. H. & Wu, C. L. Increased apoptotic potential and dose-enhancing effect of gold nanoparticles in combination with single-dose clinical electron beams on tumor-bearing mice. *Cancer Sci.* **99,** 1479–1484 (2008).

287.   Yasui, H., Takeuchi, R., Nagane, M., Meike, S., Nakamura, Y., Yamamori, T. *et al.* Radiosensitization of tumor cells through endoplasmic reticulum stress induced by PEGylated nanogel containing gold nanoparticles. *Cancer Lett.* **347,** 151–158 (2014).

288.   Connor, E. E., Mwamuka, J., Gole, A., Murphy, C. J. & Wyatt, M. D. Gold nanoparticles are taken up by human cells but do not cause acute cytotoxicity. *Small* **1,** 325–327 (2005).

289.   Li, J. J., Zou, L., Hartono, D., Ong, C. N., Bay, B. H. & Lanry, L. Y. Gold Nanoparticles Induce Oxidative Damage in Lung Fibroblasts In Vitro. *Adv. Mater.* **20,** 138–142 (2008).

290.   Nelson, B. C., Petersen, E. J., Marquis, B. J., Atha, D. H., Elliott, J. T., Cleveland, D. *et al.* NIST gold nanoparticle reference materials do not induce oxidative DNA damage. *Nanotoxicology* **7,** 21–29 (2013).

291.   Nativo, P., Prior, I. A. & Brust, M. Uptake and Intracellular Fate of Surface-Modified Gold Nanoparticles. *ACS Nano* **2,** 1639–1644 (2008).

292.   Thakor, A. S., Paulmurugan, R., Kempen, P., Zavaleta, C., Sinclair, R., Massoud, T. F. *et al.* Oxidative stress mediates the effects of Raman-active gold nanoparticles in human cells. *Small* **7,** 126–136 (2011).

293.   Li, J. J., Hartono, D., Ong, C. N., Bay, B. H. & Yung, L. Y. Autophagy and oxidative stress associated with gold nanoparticles. *Biomaterials* **31,** 5996–6003 (2010).

294.   Negahdary, M., Chelongar, R., Zadeh, S. K. & Ajdary, M. The antioxidant effects of silver, gold, and zinc oxide nanoparticles on male mice in in vivo condition. *Adv. Biomed. Res.* **4,** (2015).

295.   Xia, Q., Li, H., Liu, Y. & Xiao, K. The effect of particle size on the genotoxicity of gold nanoparticles. *J. Biomed. Mater. Res. A* n/a-n/a (2016). doi:10.1002/jbm.a.35944

296.   Yu, M. & Zheng, J. Clearance Pathways and Tumor Targeting of Imaging Nanoparticles. *ACS Nano* **9,** 6655–6674 (2015).

297.   Gratton, S. E., Ropp, P. A., Pohlhaus, P. D., Luft, J. C., Madden, V. J., Napier, M. E. *et al.* The effect of particle design on cellular internalization pathways. *Proc. Natl. Acad. Sci.* **105,** 11613–11618 (2008).

298.   Herd, H., Daum, N., Jones, A. T., Huwer, H., Ghandehari, H. & Lehr, C. M. Nanoparticle Geometry and Surface Orientation Influence Mode of Cellular Uptake. *ACS Nano* **7,** 1961–1973 (2013).

299.   Rancan, F., Gao, Q., Graf, C., Troppens, S., Hadam, S., Hackbarth, S. *et al.* Skin Penetration and Cellular Uptake of Amorphous Silica Nanoparticles with Variable Size, Surface Functionalization, and Colloidal Stability. *ACS Nano* **6,** 6829–6842 (2012).

300.   De Jong, W. H., Hagens, W. I., Krystek, P., Burger, M. C., Sips, A. J., Geertsma, R. E. Particle size-dependent organ distribution of gold nanoparticles after intravenous administration. *Biomaterials* **29,** 1912–1919 (2008).

301.   Sykes, E. A., Chen, J., Zheng, G. & Chan, W. C. Investigating the impact of nanoparticle size on active and passive tumor targeting efficiency. *ACS Nano* **8,** 5696–5706 (2014).

302.   Longmire, M., Choyke, P. L. & Kobayashi, H. Clearance properties of nano-sized particles and molecules as imaging agents: considerations and caveats. *Nanomed.* **3,** 703–717 (2008).

303.   De Crozals, G., Bonnet, R., Farre, C. & Chaix, C. Nanoparticles with multiple properties for biomedical applications: A strategic guide. *Nano Today* **11,** 435–463 (2016).

304.   Lundqvist, M., Stigler, J., Elia, G., Lynch, I., Cedervall, T. & Dawson, K. A. Nanoparticle size and surface properties determine the protein corona with possible implications for biological impacts. *Proc. Natl. Acad. Sci.* **105,** 14265–14270 (2008).

305.   Salvati, A., Pitek, A. S., Monopoli, M. P., Prapainop, K., Bombelli, F. B., Hristov, D. R. *et al.* Transferrin-functionalized nanoparticles lose their targeting capabilities when a biomolecule corona adsorbs on the surface. *Nat. Nanotechnol.* **8,** 137–143 (2013).

306.   Moghimi, S. M. & Szebeni, J. Stealth liposomes and long circulating nanoparticles: critical issues in pharmacokinetics, opsonization and protein-binding properties. *Prog. Lipid Res.* **42,** 463–478 (2003).

307.   Matsumura, Y. & Maeda, H. A new concept for macromolecular therapeutics in cancer chemotherapy: mechanism of tumoritropic accumulation of proteins and

the antitumor agent smancs. *Cancer Res.* **46,** 6387–6392 (1986).

308.   Jain, R. K. & Stylianopoulos, T. Delivering nanomedicine to solid tumors. *Nat. Rev. Clin. Oncol.* **7,** 653–664 (2010).

309.   You, J., Zhang, R., Xiong, C., Zhong, M., Melancon, M., Gupta, S. *et al.* Effective photothermal chemotherapy using doxorubicin-loaded gold nanospheres that target EphB4 receptors in tumors. *Cancer Res.* **72,** 4777–4786 (2012).

310.   Marega, R., Karmani, L., Flamant, L., Nageswaran, P. G., Valembois, V., Masereel, B. *et al.* Antibody-functionalized polymer-coated gold nanoparticles targeting cancer cells: an in vitro and in vivo study. *J. Mater. Chem.* **22,** 21305–21312 (2012).

311.   Dam, D. H., Culver, K. S., Kandela, I., Lee, R. C., Chandra, K., Lee, H. *et al.* Biodistribution and in vivo toxicity of aptamer-loaded gold nanostars. *Nanomedicine Nanotechnol. Biol. Med.* **11,** 671–679 (2015).

312.   Niidome, T., Yamagata, M., Okamoto, Y., Akiyama, Y., Takahashi, H., Kawano, T. *et al.* PEG-modified gold nanorods with a stealth character for in vivo applications. *J. Control. Release Off. J. Control. Release Soc.* **114,** 343–347 (2006).

313.   Sadauskas, E., Danscher, G., Stoltenberg, M., Vogel, U., Larsen, A. & Wallin, H. Protracted elimination of gold nanoparticles from mouse liver. *Nanomedicine Nanotechnol. Biol. Med.* **5,** 162–169 (2009).

314.   Deen, W. M., Lazzara, M. J. & Myers, B. D. Structural determinants of glomerular permeability. *Am. J. Physiol. Renal Physiol.* **281,** F579-596 (2001).

315.   Abdelhalim, M. A. Uptake of gold nanoparticles in several rat organs after intraperitoneal administration in vivo: a fluorescence study. *BioMed Res. Int.* **2013,** 353695 (2013).

316.   Ferreira, G. K., Cardoso, E., Vuolo, F. S., Michels, M., Zanoni, E. T., Carvalho-Silva, M. *et al.* Gold nanoparticles alter parameters of oxidative stress and energy metabolism in organs of adult rats. *Biochem. Cell Biol.* **93,** 548–557 (2015).

317.   Abdelhalim, M. A. Exposure to gold nanoparticles produces cardiac tissue damage that depends on the size and duration of exposure. *Lipids Health Dis.* **10,** 205 (2011).

318.   Cho, W. S., Cho, M., Jeong, J., Choi, M., Cho, H. Y., Han, B. S. *et al.* Acute toxicity and pharmacokinetics of 13 nm-sized PEG-coated gold nanoparticles. *Toxicol. Appl. Pharmacol.* **236,** 16–24 (2009).

319.   Khan, H. A., Abdelhalim, M. A., Alhomida, A. S. & Al-Ayed, M. S. Effects of naked gold nanoparticles on proinflammatory cytokines mRNA expression in rat liver and kidney. *BioMed Res. Int.* **2013,** 590730 (2013).

320.   Downs, T. R., Crosby, M. E., Hu, T., Kumar, S., Sullivan, A., Sarlo, K. *et al.* Silica nanoparticles administered at the maximum tolerated dose induce genotoxic effects through an inflammatory reaction while gold nanoparticles do not. *Mutat. Res. Toxicol. Environ. Mutagen.* **745,** 38–50 (2012).

321.   Yang, C., Yang, H., Wu, J., Meng, Z., Xing, R., Tian, A. *et al.* No overt structural or functional changes associated with PEG-coated gold nanoparticles accumulation with acute exposure in the mouse heart. *Toxicol. Lett.* **222,** 197–203 (2013).

322.   Sousa, A. A., Hassan, S. A., Knittel, L. L., Balbo, A., Aronova, M. A., Brown, P. H. *et al.* Biointeractions of ultrasmall glutathione-coated gold nanoparticles: effect of small size variations. *Nanoscale* **8,** 6577–6588 (2016).

323.   Siddiqi, N. J., Abdelhalim, M. A., El-Ansary, A. K., Alhomida, A. S. & Ong, W. Y. Identification of potential biomarkers of gold nanoparticle toxicity in rat brains. *J. Neuroinflammation* **9,** 123 (2012).

324. Pokharkar, V., Dhar, S., Bhumkar, D., Mali, V., Bodhankar, S. & Prasad, B. L. Acute and subacute toxicity studies of chitosan reduced gold nanoparticles: a novel carrier for therapeutic agents. *J. Biomed. Nanotechnol.* **5,** 233–239 (2009).

325. Uchiyama, M. K., Deda, D. K., Rodrigues, S. F., Drewes, C. C., Bolonheis, S. M., Kiyohara, P. K. *et al.* In vivo and in vitro toxicity and anti-inflammatory properties of gold nanoparticle bioconjugates to the vascular system. *Toxicol. Sci. Off. J. Soc. Toxicol.* **142,** 497–507 (2014).

326. Katsnelson, B. A., Privalova, L. I., Gurvich, V. B., Makeyev, O. H., Shur, V. Y., Beikin, Y. B. *et al.* Comparative in vivo assessment of some adverse bioeffects of equidimensional gold and silver nanoparticles and the attenuation of nanosilver's effects with a complex of innocuous bioprotectors. *Int. J. Mol. Sci.* **14,** 2449–2483 (2013).

327. Reeves, P. G., Nielsen, F. H. & Fahey, G. C. AIN-93 purified diets for laboratory rodents: final report of the American Institute of Nutrition ad hoc writing committee on the reformulation of the AIN-76A rodent diet. *J. Nutr.* **123,** 1939–1951 (1993).

328. Ohkawa, H., Ohishi, N. & Yagi, K. Assay for lipid peroxides in animal tissues by thiobarbituric acid reaction. *Anal. Biochem.* **95,** 351–358 (1979).

329. Sonia, S., Linda, J. K., Ruckmani, K. & Sivakumar, M. Antimicrobial and antioxidant potentials of biosynthesized colloidal zinc oxide nanoparticles for a fortified cold cream formulation: A potent nanocosmeceutical application. *Mater. Sci. Eng. C* **79,** 581–589 (2017).

330. Mousavi, S. Z., Nafisi, S. & Maibach, H. I. Fullerene nanoparticle in dermatological and cosmetic applications. *Nanomedicine Nanotechnol. Biol. Med.* **13,** 1071–1087 (2017).

331. Duhan, J. S., Kumar, R, Kumar, N., Kaur, P., Nehra, K. & Duhan, S. Nanotechnology: The new perspective in precision agriculture. *Biotechnol. Rep.* **15,** 11–23 (2017).

332. Ballottin, D., Fulaz, S., Cabrini, F., Tsukamoto, J., Durán, N., Alves, O. L. *et al.* Antimicrobial textiles: Biogenic silver nanoparticles against Candida and Xanthomonas. *Mater. Sci. Eng. C* **75,** 582–589 (2017).

333. Fei, J., Sun, L., Zhou, C., Ling, H., Yan, F., Zhong, X. *et al.* Tuning the Synthesis of Manganese Oxides Nanoparticles for Efficient Oxidation of Benzyl Alcohol. *Nanoscale Res. Lett.* **12,** (2017).

334. Kim, D. Y., Shinde, S. & Ghodake, G. Colorimetric detection of magnesium (II) ions using tryptophan functionalized gold nanoparticles. *Sci. Rep.* **7,** 3966 (2017).

335. Han, K. N., Choi, J. S. & Kwon, J. Gold nanozyme-based paper chip for colorimetric detection of mercury ions. *Sci. Rep.* **7,** 2806 (2017).

336. Lorenzo, T., Restuccia, N. & Paterniti, I. Gold Nanoparticles By Laser Ablation For X-Ray Imaging And Protontherapy Improvements. *Recent Pat. Nanotechnol.* doi:10.2174/1872210511666170609093433 (2017).

337. Meir, R. & Popovtzer, R. Cell tracking using gold nanoparticles and computed tomography imaging. *Wiley Interdiscip. Rev. Nanomed. Nanobiotechnol.* doi:10.1002/wnan.1480 (2017).

338. Neshastehriz, A., Tabei, M., Maleki, S., Eynali, S. & Shakeri-Zadeh, A. Photothermal therapy using folate conjugated gold nanoparticles enhances the effects of 6MV X-ray on mouth epidermal carcinoma cells. *J. Photochem. Photobiol. B* **172,** 52–60 (2017).

339. Zhang, M., Kim, H. S., Jin, T. & Moon, W. K. Near-infrared photothermal

therapy using EGFR-targeted gold nanoparticles increases autophagic cell death in breast cancer. *J. Photochem. Photobiol. B* **170,** 58–64 (2017).

340.   Lin, W., Yao, N., Qian, L., Zhang, X., Chen, Q., Wang, J. *et al.* pH-responsive unimolecular micelle-gold nanoparticles-drug nanohybrid system for cancer theranostics. *Acta Biomater.* doi:10.1016/j.actbio.2017.06.003 (2017).

341.   Yilmaz, G., Demir, B., Timur, S. & Becer, C. R. Poly(methacrylic acid)-Coated Gold Nanoparticles: Functional Platforms for Theranostic Applications. *Biomacromolecules* **17,** 2901–2911 (2016).

342.   Suvarna, S., Das, U., Kc, S., Mishra, S., Sudarshan, M., Saha, K. D. *et al.* Synthesis of a novel glucose capped gold nanoparticle as a better theranostic candidate. *PLoS ONE* **12,** e0178202 (2017).

343.   Scheinberg, D. A., Grimm, J., Heller, D. A., Stater, E. P., Bradbury, M. & McDevitt, M. R. Advances in the clinical translation of nanotechnology. *Curr. Opin. Biotechnol.* **46,** 66–73 (2017).

344.   Talamini, L., Violatto, M. B., Cai, Q., Monopoli, M. P., Kantner, K., Krpetic, Z. *et al.* Influence of Size and Shape on the Anatomical Distribution of Endotoxin-Free Gold Nanoparticles. *ACS Nano.* doi:10.1021/acsnano.7b00497 (2017).

345.   Schneider, T., Westermann, M. & Glei, M. In vitro uptake and toxicity studies of metal nanoparticles and metal oxide nanoparticles in human HT29 cells. *Arch. Toxicol*. doi:10.1007/s00204-017-1976-z (2017).

346.   Ortega, M. T., Riviere, J. E., Choi, K. & Monteiro-Riviere, N. A. Biocorona formation on gold nanoparticles modulates human proximal tubule kidney cell uptake, cytotoxicity and gene expression. *Toxicol. Vitro Int. J. Publ. Assoc. BIBRA* **42,** 150–160 (2017).

347.   Coradeghini, R., Gioria, S., García, C. P., Nativo, P., Franchini, F., Gilliland, D. *et al.* Size-dependent toxicity and cell interaction mechanisms of gold nanoparticles on mouse fibroblasts. *Toxicol. Lett.* **217,** 205–216 (2013).

348.   Freese, C., Uboldi, C., Gibson, M. I., Unger, R. E., Weksler, B. B., Romero, I. A. *et al.* Uptake and cytotoxicity of citrate-coated gold nanospheres: Comparative studies on human endothelial and epithelial cells. *Part. Fibre Toxicol.* **9,** 23 (2012).

349.   Leite, P. E., Pereira, M. R., do Nascimento, C., Campos, A. P., Esteves, T. M. & Granjeiro, J. M. Gold nanoparticles do not induce myotube cytotoxicity but increase the susceptibility to cell death. *Toxicol. Vitro Int. J. Publ. Assoc. BIBRA* **29,** 819–827 (2015).

350.   Piryazev, A. P., Azizova, O. A., Aseichev, A. V., Dudnik, L. B. & Sergienko, V. I. Effect of gold nanoparticles on production of reactive oxygen species by human peripheral blood leukocytes stimulated with opsonized zymosan. *Bull. Exp. Biol. Med.* **156,** 101–103 (2013).

351.   Mateo, D., Morales, P., Ávalos, A. & Haza, A. I. Oxidative stress contributes to gold nanoparticle-induced cytotoxicity in human tumor cells. *Toxicol. Mech. Methods* **24,** 161–172 (2014).

352.   George, J. M., Magogotya, M., Vetten, M. A., Buys, A. V. & Gulumian, M. From the Cover: An Investigation of the Genotoxicity and Interference of Gold Nanoparticles in Commonly Used In Vitro Mutagenicity and Genotoxicity Assays. *Toxicol. Sci. Off. J. Soc. Toxicol.* **156,** 149–166 (2017).

353.   Paino, I. M., Marangoni, V. S., de Oliveira, R., Antunes, L. M. & Zucolotto, V. Cyto and genotoxicity of gold nanoparticles in human hepatocellular carcinoma and peripheral blood mononuclear cells. *Toxicol. Lett.* **215,** 119–125 (2012).

354.   Xia, Q., Li, H., Liu, Y., Zhang, S., Feng, Q. & Xiao, K. The effect of particle size

on the genotoxicity of gold nanoparticles. *J. Biomed. Mater. Res. A* **105,** 710–719 (2017).

355.   Chueh, P. J., Liang, R. Y., Lee, Y. H., Zeng, Z. M. & Chuang, S. M. Differential cytotoxic effects of gold nanoparticles in different mammalian cell lines. *J. Hazard. Mater.* **264,** 303–312 (2014).

356.   Cardoso, E., Rezin, G. T., Zanoni, E. T., de Souza, F., Leffa, D. D., Damiani, A. P. *et al.* Acute and chronic administration of gold nanoparticles cause DNA damage in the cerebral cortex of adult rats. *Mutat. Res.* **766–767,** 25–30 (2014).

357.   Lee, E., Oh, E., Lee, J., Sul, D. & Lee, J. Use of the tail moment of the lymphocytes to evaluate DNA damage in human biomonitoring studies. *Toxicol. Sci. Off. J. Soc. Toxicol.* **81,** 121–132 (2004).

358.   Wente, S. R. & Rout, M. P. The Nuclear Pore Complex and Nuclear Transport. *Cold Spring Harb. Perspect. Biol.* **2,** (2010).

359.   Naz, F., Koul, V., Srivastava, A., Gupta, Y. K. & Dinda, A. K. Biokinetics of ultrafine gold nanoparticles (AuNPs) relating to redistribution and urinary excretion: a long-term in vivo study. *J. Drug Target.* **24,** 720–729 (2016).

360.   Sung, J. H., Ji, J. H., Park, J. D., Song, M. Y., Song, K. S., Ryu, H. R. *et al.* Subchronic inhalation toxicity of gold nanoparticles. *Part. Fibre Toxicol.* **8,** 16 (2011).

361.   Chen, H., Dorrigan, A., Saad, S., Hare, D. J., Cortie, M. B. & Valenzuela, S. M. In vivo study of spherical gold nanoparticles: inflammatory effects and distribution in mice. *PloS One* **8,** e58208 (2013).

362.   Chen, Y. S., Hung, Y. C., Liau, I. & Huang, G. S. Assessment of the In Vivo Toxicity of Gold Nanoparticles. *Nanoscale Res. Lett.* **4,** 858 (2009).

363.   Abdelhalim, M. A., Al-Ayed, M. S. & Moussa, S. A. The effects of intraperitoneal administration of gold nanoparticles size and exposure duration on oxidative and antioxidants levels in various rat organs. *Pak. J. Pharm. Sci.* **28,** 705–712 (2015).

364.   Tedesco, S., Doyle, H., Redmond, G. & Sheehan, D. Gold nanoparticles and oxidative stress in Mytilus edulis. *Mar. Environ. Res.* **66,** 131–133 (2008).

365.   Zhang, Q., Ma, Y., Yang, S., Xu, B. & Fei, X. Small-sized gold nanoparticles inhibit the proliferation and invasion of SW579 cells. *Mol. Med. Rep.* doi:10.3892/mmr.2015.4433 (2015).

366.   Tlotleng, N., Vetten, M. A., Keter, F. K., Skepu, A., Tshikhudo, R., Gulumian, M. Cytotoxicity, intracellular localization and exocytosis of citrate capped and PEG functionalized gold nanoparticles in human hepatocyte and kidney cells. *Cell Biol. Toxicol.* **32,** 305–321 (2016).

367.   Cho, W. S., Cho, M., Jeong, J., Choi, M., Han, B. S., Shin, H. S. *et al.* Size-dependent tissue kinetics of PEG-coated gold nanoparticles. *Toxicol. Appl. Pharmacol.* **245,** 116–123 (2010).

368.   Morais, T., Soares, M. E., Duarte, J. A., Soares, L., Maia, S., Gomes, P. *et al.* Effect of surface coating on the biodistribution profile of gold nanoparticles in the rat. *Eur. J. Pharm. Biopharm.* **80,** 185–193 (2012).

369.   Elci, S. G., Jiang, Y., Yan, B., Kim, S. T., Saha, K., Moyano, D. F. *et al.* Surface Charge Controls the Suborgan Biodistributions of Gold Nanoparticles. *ACS Nano* **10,** 5536–5542 (2016).

370.   Cai, H., Ma, Y., Wu, Z., Ding, Y., Zhang, P., He, X. *et al.* Protein corona influences liver accumulation and hepatotoxicity of gold nanorods. *NanoImpact* **3–4,** 40–46 (2016).

371.   Dragoni, S., Franco, G., Regoli, M., Bracciali, M., Morandi, V., Sgaragli, G. *et al.* Gold nanoparticles uptake and cytotoxicity assessed on rat liver precision-cut slices. *Toxicol. Sci.* **128,** 186–197 (2012).

372.   Lopez-Chaves, C., Soto-Alvaredo, J., Montes-Bayon, M., Bettmer, J., Llopis, J. & Sanchez-Gonzalez, C. Gold nanoparticles: Distribution, bioaccumulation and toxicity. In vitro and in vivo studies. *Nanomedicine Nanotechnol. Biol. Med.* doi:10.1016/j.nano.2017.08.011 (2017).

373.   Sun, Y. N., Wang, C. D., Zhang, X. M., Ren, L. & Tian, X. H. Shape dependence of gold nanoparticles on in vivo acute toxicological effects and biodistribution. *J. Nanosci. Nanotechnol.* **11,** 1210–1216 (2011).

374.   Yang, L., Kuang, H., Zhang, W., Aguilar, Z. P., Wei, H. & Xu, H. Comparisons of the biodistribution and toxicological examinations after repeated intravenous administration of silver and gold nanoparticles in mice. *Sci. Rep.* **7,** 3303 (2017).

375.   Oh, N. & Park, J. H. Surface chemistry of gold nanoparticles mediates their exocytosis in macrophages. *ACS Nano* **8,** 6232–6241 (2014).

376.   Balasubramanian, S. K., Jittiwat, J., Manikandan, J., Ong, C. N., Yu, L. E. & Ong, W. Y. Biodistribution of gold nanoparticles and gene expression changes in the liver and spleen after intravenous administration in rats. *Biomaterials* **31,** 2034–2042 (2010).

377.   Abdelhalim, M. A. & Abdelmottaleb, S. A. The gold nanoparticle size and exposure duration effect on the liver and kidney function of rats: In vivo. *Saudi J. Biol. Sci.* **20,** 177–181 (2013).

378.   Bednarski, M., Dudek, M., Knutelska, J., Nowinski, L., Sapa, J., Zygmunt, M. *et al.* The influence of the route of administration of gold nanoparticles on their tissue distribution and basic biochemical parameters: In vivo studies. *Pharmacol. Rep. PR* **67,** 405–409 (2015).

379.   Keene, A. M., Peters, D., Rouse, R., Stewart, S., Rosen, E. T. & Tyner, K. M. Tissue and cellular distribution of gold nanoparticles varies based on aggregation/agglomeration status. *Nanomed.* **7,** 199–209 (2012).

380.   Koyama, Y., Matsui, Y., Shimada, Y. & Yoneda, M. Biodistribution of gold nanoparticles in mice and investigation of their possible translocation by nerve uptake around the alveolus. *J. Toxicol. Sci.* **40,** 243–249 (2015).

381.   Zhu, Z. J., Carboni, R., Quercio, J., Yan, B., Miranda, O. R., Anderton, D. L. *et al.* Surface properties dictate uptake, distribution, excretion, and toxicity of nanoparticles in fish. *Small* **6,** 2261–2265 (2010).

382.   Lee, J. K., Kim, T. S., Bae, J. Y., Jung, A. Y., Lee, S. M., Seok, J. H. *et al.* Organ-specific distribution of gold nanoparticles by their surface functionalization. *J. Appl. Toxicol.* **35,** 573–580 (2015).

383.   Takeuchi, I., Nobata, S., Oiri, N., Tomoda, K. & Makino, K. Biodistribution and excretion of colloidal gold nanoparticles after intravenous injection: Effects of particle size. *Biomed. Mater. Eng.* **28,** 315–323 (2017).

384.   Zagainova, E. V., Bugrova, M. L., Snopova, L. B., Elagin, V. V., Sirotkina, M. A., Shirmanova, M. V. *et al.* Investigation of biodistribution of gold nanoparticles in healthy animals. *Nanotechnologies Russ.* **5,** 409–416 (2010).

385.   Simpson, C. A., Salleng, K. J., Cliffel, D. E. & Feldheim, D. L. In vivo toxicity, biodistribution, and clearance of glutathione-coated gold nanoparticles. *Nanomedicine Nanotechnol. Biol. Med.* **9,** 257–263 (2013).

386.   Lipka, J., Semmler-Behnke, M., Sperling, R. A., Wenk, A., Takenaka, S., Schleh, C. *et al.* Biodistribution of PEG-modified gold nanoparticles following intratracheal

instillation and intravenous injection. *Biomaterials* **31,** 6574–6581 (2010).

387.   Semmler-Behnke, M., Kreyling, W. G., Lipka, J., Fertsch, S., Wenk, A., Takenaka, S. *et al.* Biodistribution of 1.4- and 18-nm Gold Particles in Rats. *Small* **4,** 2108–2111 (2008).

388.   Yang, R. S., Chang, L. W., Wu, J. P., Tsai, M. H., Wang, H. J., Kuo, Y. C. *et al.* Persistent tissue kinetics and redistribution of nanoparticles, quantum dot 705, in mice: ICP-MS quantitative assessment. *Environ. Health Perspect.* **115,** 1339–1343 (2007).

389.   You, J., Zhou, J., Zhou, M., Liu, J., Robertson, J. D., Liang, D. *et al.* Pharmacokinetics, clearance, and biosafety of polyethylene glycol-coated hollow gold nanospheres. *Part. Fibre Toxicol.* **11,** 26 (2014).

390.   Zhang, X. D., Luo, Z., Chen, J., Wang, H., Song, S. S., Shen, X. *et al.* Storage of gold nanoclusters in muscle leads to their biphasic in vivo clearance. *Small* **11,** 1683–1690 (2015).

391.   Bastos, V., Ferreira, J. M., Brown, D., Jonhston, H., Malheiro, E., Daniel, A. L. *et al.* The influence of Citrate or PEG coating on silver nanoparticle toxicity to a human keratinocyte cell line. *Toxicol. Lett.* **249,** 29–41 (2016).

392.   Sonavane, G., Tomoda, K. & Makino, K. Biodistribution of colloidal gold nanoparticles after intravenous administration: Effect of particle size. *Colloids Surf. B Biointerfaces* **66,** 274–280 (2008).

393.   Wang, Y., Seebald, J. L., Szeto, D. P. & Irudayaraj, J. Biocompatibility and Biodistribution of Surface-Enhanced Raman Scattering Nanoprobes in Zebrafish Embryos: In vivo and Multiplex Imaging. *ACS Nano* **4,** 4039–4053 (2010).

394.   Wang, J. Y., Chen, J., Yang, J., Wang, H., Shen, X., Sun, Y. M. *et al.* Effects of surface charges of gold nanoclusters on long-term in vivo biodistribution, toxicity, and cancer radiation therapy. *Int. J. Nanomedicine* **11,** 3475–3485 (2016).

395.   Han, S. G., Lee, J. S., Ahn, K., Kim, Y. S., Kim, J. K., Lee, J. H. *et al.* Size-dependent clearance of gold nanoparticles from lungs of Sprague-Dawley rats after short-term inhalation exposure. *Arch. Toxicol.* **89,** 1083–1094 (2015).

396.   Balasubramanian, S. K., Poh, K. W., Ong, C. N., Kreyling, W. G., Ong, W. Y., Yu, L. E. *et al.* The effect of primary particle size on biodistribution of inhaled gold nano-agglomerates. *Biomaterials* **34,** 5439–5452 (2013).

397.   Betzer, O., Shilo, M., Opochinsky, R., Barnoy, E., Motiei, M., Okun, E. *et al.* The effect of nanoparticle size on the ability to cross the blood-brain barrier: An in vivo study. *Nanomed.* **12,** 1533–1546 (2017).

398.   Escudero-Francos, M. A., Cepas, V., González-Menéndez, P., Badía-Laíño, R., Díaz-García, M. E., Sainz, R. M. *et al.* Cellular uptake and tissue biodistribution of functionalized gold nanoparticles and nanoclusters. *J. Biomed. Nanotechnol.* **13,** 167–179 (2017).

399.   Sadauskas, E., Wallin, H., Stoltenberg, M., Vogel, U., Doering, P., Larsen, A. *et al.* Kupffer cells are central in the removal of nanoparticles from the organism. *Part. Fibre Toxicol.* **4,** 10 (2007).

400.   Hillyer, J. F. & Albrecht, R. M. Gastrointestinal persorption and tissue distribution of differently sized colloidal gold nanoparticles. *J. Pharm. Sci.* **90,** 1927–1936 (2001).

401.   Schleh, C., Semmler-Behnke, M., Lipka, J., Wenk, A., Hirn, S., Schäffler, M. *et al.* Size and surface charge of gold nanoparticles determine absorption across intestinal barriers and accumulation in secondary target organs after oral administration. *Nanotoxicology* **6,** 36–46 (2012).

402. Shah, N. B., Vercelloti, G. M., White, J. G., Fegan, A., Wagner, C. R. & Bischof, J. C. Blood-nanoparticle interactions and in vivo biodistribution: impact of surface PEG and ligand properties. *Mol. Pharm.* **9,** 2146–2155 (2012).

403. Abdelhalim, M. A. Alterations in gold nanoparticle levels are size dependent, with the smaller ones inducing the most toxic effects and related to the time of exposure of the gold nanoparticles. *West Indian Med. J.* **65,** 87–92 (2016).

404. Terentyuk, G. S., Maslyakova, G. N., Suleymanova, L. V., Khlebtsov, B. N., Kogan, B. Y., Akchurin, G. G. *et al.* Circulation and distribution of gold nanoparticles and induced alterations of tissue morphology at intravenous particle delivery. *J. Biophotonics* **2,** 292–302 (2009).

405. Simpson, C. A., Huffman, B. J. & Cliffel, D. E. In Vivo Testing for Gold Nanoparticle Toxicity. *Methods Mol. Biol.* **1026,** 175-186 (2013).

406. Lasagna-Reeves, C., Gonzalez-Romero, D., Barria, M. A., Olmedo, I., Clos, A., Sadagopa, V. M. *et al.* Bioaccumulation and toxicity of gold nanoparticles after repeated administration in mice. *Biochem. Biophys. Res. Commun.* **393,** 649–655 (2010).

407. Sengupta, J., Datta, P., Patra, H. K., Dasgupta, A. K. & Gomes, A. In vivo interaction of gold nanoparticles after acute and chronic exposures in experimental animal models. *J. Nanosci. Nanotechnol.* **13,** 1660–1670 (2013).

408. Chen, J., Wang, H., Long, W., Shen, X., Wu, D., Song, S. S. *et al.* Sex differences in the toxicity of polyethylene glycol-coated gold nanoparticles in mice. *Int. J. Nanomedicine* **8,** 2409-2419 (2013).

409. Zhang, X. D., Wu, H. Y., Wu, D., Wang, Y. Y., Chang, J. H., Zhai, Z. B. *et al.* Toxicologic effects of gold nanoparticles in vivo by different administration routes. *Int. J. Nanomedicine* **5,** 771–781 (2010).

410. Zhang, X. D., Wu, D., Shen, X., Liu, P. X., Fan, F. Y. & Fan, S. J. In vivo renal clearance, biodistribution, toxicity of gold nanoclusters. *Biomaterials* **33,** 4628–4638 (2012).

411. Saleh, H. M., Soliman, O. A., Elshazly, M. O., Raafat, A., Gohar, A. K. & Salaheldin, T. A. Acute hematologic, hepatologic, and nephrologic changes after intraperitoneal injections of 18 nm gold nanoparticles in hamsters. *Int. J. Nanomedicine* **11,** 2505–2513 (2016).

412. Khan, H. A., Ibrahim, K. E., Khan, A., Alrokayan, S. H., Alhomida, A. S. & Lee, Y. K. Comparative evaluation of immunohistochemistry and real-time PCR for measuring proinflammatory cytokines gene expression in livers of rats treated with gold nanoparticles. *Exp. Toxicol. Pathol.* **68,** 381–390 (2016).

413. Durocher, I., Noël, C., Lavastre, V. & Girard, D. Evaluation of the in vitro and in vivo proinflammatory activities of gold (+) and gold (−) nanoparticles. *Inflamm. Res.* 1–12 (2017). doi:10.1007/s00011-017-1078-7

414. Zhang, X. D., Wu, D., Shen, X., Liu, P. X., Yang, N., Zhao, B. *et al.* Size-dependent in vivo toxicity of PEG-coated gold nanoparticles. *Int. J. Nanomedicine* **6,** 2071–2081 (2011).